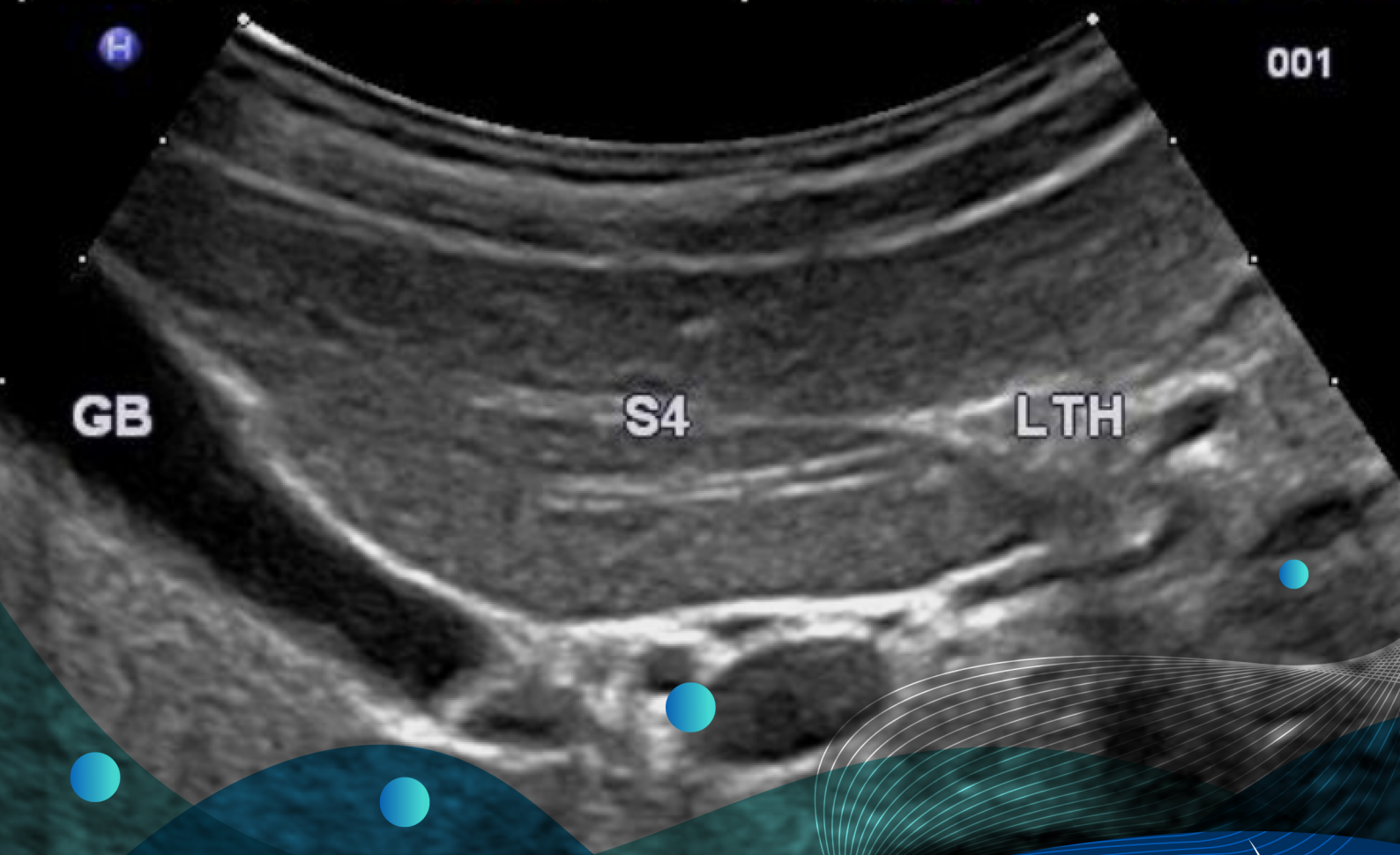

EFSUMB
European Federation of Societies for Ultrasound in Medicine and Biology

EFSUMB Course Book

2nd Edition

Editor: Christoph F. Dietrich

Ch02: Ultrasound of the liver

Christoph F. Dietrich[1], Carla Serra[2], Maciej Jedrzejczyk[3]

1. Caritas-Krankenhaus Bad Mergentheim, Germany
2. University of Bologna
3. Department of Diagnostic Imaging, 2nd Medical Faculty of Warsaw Medical University

Corresponding author: Prof. Dr. Christoph F. Dietrich
Medizinische Klinik 2, Caritas-Krankenhaus Bad Mergentheim, Uhlandstr. 7, 97980 Bad Mergentheim
Tel.: (+) 49 - 7931 – 58 – 2201
Fax: (+) 49 - 7931 – 58 – 2290
Email: christoph.dietrich@ckbm.de

Acknowledgment:
The authors thank Lucas Greiner, Julie Walton, Ioan Sporea, Christian Nolsoe, XinWu Cui, Norbert Gritzmann and Yi Dong for peer review of the manuscript.

Content

Inhalt

Topographic remarks

The liver is located inside the intraperitoneal cavity and under the right hemidiaphragm, but can also extend across the midline reach to the left hemidiaphragm and to the spleen in some cases. The liver is fixed to the diaphragm by the *pars affixa* and to the ventral abdominal wall by the ligamentum falciforme (falciform ligament) and its strong margin, the

ligamentum teres hepatis. The minor omentum consists of the ligamentum hepatogastricum and the ligamentum hepatoduodenale. The hepatoduodenal ligament carries three vessels – two containing blood (the portal vein and hepatic artery) and one carrying bile (common bile duct (CBD)). The further course of these three vessels (known as Glisson's triad) is mainly parallel.

The structures of the liver hilum are accompanied by a number of ventrally and dorsally (in relation to the portal vein) located lymph nodes, which can be routinely demonstrated by ultrasound [(1-6)]; however, lymphatic vessels are too small to be visualised on ultrasound.

The liver has three main (hepatic) veins – left, middle and right – that drain the liver blood to the inferior vena cava (IVC) located in the retroperitoneum. The IVC is variably surrounded by liver parenchyma.

The organs and structures of the peritoneal cavity surround the liver, as well as pleural and pericardial structures. Neighbouring structures adjacent to the liver are numerous and include (clockwise) basal lung portions separated by the muscular layers of the right diaphragm (and more or less the left diaphragm as well), heart, stomach, intestine (*e.g.* upper duodenal loop and right colonic flexure), abdominal aorta, IVC, right adrenal gland and right kidney.

The interposition of the colon between the liver and the anterior abdominal wall can prevent sonographic approach to the right liver lobe in cases of Chilaiditi's syndrome. Finally, in the case of complete or incomplete situs inversus, topographic relations are inverted.

Liver anatomy

Anatomical orientation

Liver anatomy is defined by ligaments and fissures as well as by vascular architecture *i.e.* the branches of the hepatic artery, portal vein and bile ducts define the centers of liver segment anatomy by their parallel course [(7)].

Liver segment anatomy

A simplified anatomy divides the liver into the larger right lobe (including segment V, VI, VII and VIII) [http://media.falkfoundation.de/index.php?id=122&L=1]; the left lobe with its

medial (IVa,b) and lateral segments (II, III) [http://media.falkfoundation.de/index.php?id=119&L=1 and http://media.falkfoundation.de/index.php?id=120&L=1]; and the caudate lobe (I).

Couinaud classification

The widely accepted Couinaud [(8, 9)] system describes liver segment anatomy. This classification, modified by Bismuth (segment IVa, b), is based on eight segments, each of which has its own arterial and portal venous vessel architecture (Glisson's triad) for vascular inflow, outflow and biliary drainage [(10, 11)]. As a result of this division into self-contained units, each can be resected (alone or in groups) without damaging the remaining segments because the vascular inflow, outflow and biliary drainage is preserved. Depending on the three-dimensional volume orientation of the liver (longitudinal or oblique), the interpretation of the Couinaud classification can be inconsistent in the literature. While the portal vein plane has often been described as transverse, it may also be oblique because the left branch runs superiorly and the right runs inferiorly. In addition to forming an oblique transverse plane between segments, the left and right portal veins branch superiorly and inferiorly to project into the centre of each segment.

Liver segment nomenclature

In a clockwise fashion starting with the caudate lobe as segment I, the left posterolateral segment is number II, followed by the left anterolateral, segment III; left superomedial, segment IVa; left inferomedial, segment IVb; right anteroinferior, segment V; right posteroinferior, segment VI; right posterosuperior, segment VII; and right anterosuperior, segment VIII. This appears more complicated than it actually is. For more details see "EFSUMB examination technique videos", http://www.efsumb.org/blog/?page_id=1750.

Right liver lobe

Anterior segments V and VI are separated from the posterior segments VII and VIII in the plane of the right hepatic and portal veins. The anterior and posterior divisions are further sub-divided by a plane defined by the right main branch of the portal vein.

Segments IVa (superior) and IVb (inferior) are situated to the left of the plane separating the right and left liver lobes. Segments V and VIII are to the right and segment VIII is more superior and dorsal to segment V.

In the Couinaud classification, the plane defined by the middle hepatic vein sub-divides the liver into the true right and left lobes. A standard right or left lobectomy requires division along the plane of the middle hepatic vein. Segments IVa and IVb are located to the left of the plane, while segments V and VIII are located to the right; segment VIII being more superior to V. In Couinaud nomenclature, the plane defined by the right branch of the portal vein divides the anterior and posterior portions of the right liver superiorly and inferiorly, thus dividing the right lobe into four segments (V-VIII) [(9)].

Left liver lobe

The “umbilical level” separates segments IVa and IVb from the lateral segments II and III. Remarkably, this level is the only plane with a vertical orientation not defined by a hepatic vein. The left liver lobe can be defined on the surface of the liver by its associated landmarks. It extends from the umbilical fissure anteriorly through the ligamentum venosum along the lateral aspect of the caudate lobe. Structures within the plane of the umbilical fissure include the falciform ligament, ligamentum venosum (remnant of the ductus venosus) and the ligamentum teres (remnant of the umbilical vein).

The left hepatic vein plane is somewhat controversial. The left hepatic vein courses laterally to the umbilical fissure. Most investigators believe that the plane defined by the left hepatic vein is a true intersegmental boundary and is not the same as the plane of the umbilical fissure. However, others claim the true division between segments II and III is formed by the transverse plane of the left portal vein. We will define the plane of the left hepatic vein as the boundary between segments II and III. The medial segment of the left lobe can be divided into two segments by the plane of the portal vein (IVa and IVb).

Caudate lobe (segment I)

The most unique of the Couinaud segments is segment I, which is part of the caudate lobe (sometimes called the Spiegel lobe). This segment is located posteriorly and adjacent to segment IV. Its medial and lateral boundaries are defined by the IVC and ligamentum venosum, respectively. The caudate lobe has a variable vessel anatomy that differs from the

rest of the liver; its portal inflow is derived from both the left and right branches of the portal vein, and it has its own short (and usually small) hepatic veins that connect directly to the IVC. Owing to the variable and extensive crossing of vessels, and its position relative to the liver hilum and IVC, segment I is frequently not resected, unless absolutely necessary.

Surgical resection

Surgical resections proceed along the vessels that define the peripheries of the segments. In general, this means resection lines are parallel to the hepatic veins to preserve the hepatic arteries, portal veins and bile ducts that provide vascular inflow and biliary drainage through the centre of the segment. When a lesion occurs within the lateral segment of the left lobe, usually both Couinaud segments II and III are removed together based on the plane formed by the umbilical fissure (known as left lateral segmentectomy). Note that because the plane of the left hepatic vein is oblique, it forms a division between segments III anteriorly and segment II posteriorly.

Additional anatomical structures

The falciforme ligament runs between the ventral abdominal wall and the liver, ending with its free caudal margin as the ligamentum teres containing the obliterated umbilical vein. It can be identified at the left lateral border of segment IVb (in the quadrate lobe), and it is often mistaken to form the anatomical border between the left and right liver lobe, which is not the case. This border follows a plane along the middle hepatic vein between the IVC and the longitudinal gallbladder axis. It is identified by ultrasound only in patients with one-sided biliary obstruction and a subsequent different fluid content between the right and left liver lobes in cholangiocellular carcinoma (CCC) in the Klatskin's position.

The ventral border of segment I is delineated by the ligamentum venosum (remnant of duct of Arantii in the foetus), which runs caudally to the hepatic artery and can be identified in this way.

Ultrasound examination technique

Patient preparation

It is recommended that patients undergo a period of fasting prior to upper abdominal imaging to maximise the distension of the gall bladder and reduce food residue and gas in the upper gastrointestinal (GI) tract, which may reduce image quality or preclude liver imaging [(12-14)]. This is essential for full imaging of the liver and related biliary tree, but may not be required in an acute situation, such as trauma where immediate imaging of the gall bladder is not essential. A patient may have small amounts of still water by mouth prior to the scan, *e.g.* for medication. There is some evidence that smoking can reduce image quality when scanning the upper abdominal structures and it is good practice to encourage the patient not to smoke for 6-8h prior to an ultrasound scan. This is because smoking increases the gas intake into the upper GI tract, which can reduce image quality, and some chemicals in tobacco are known to cause contraction of the smooth muscle of the GI tract, which can cause contraction of the gall bladder, even after fasting.

Examination

The liver is a large, pyramidal shaped organ and liver sectional anatomy may be best described, imaged and defined using real-time ultrasound imaging (see "Liver segment anatomy" [http://www.efsumb.org/blog/?page_id=1750]). Conventional real-time ultrasound produces images of thin slices of the liver on screen, therefore it is essential that the operator always scans the entire organ systematically in at least two anatomical planes to ensure the entire volume of the liver tissue and structures have been imaged. The operator must then use this two-dimensional information to visualise a three-dimensional map of the individual patient's liver anatomy and pathology. This requires good hand-eye-brain coordination [(15)].

For orientation, the central portion of the liver can be differentiated into three levels:

- Level of the confluences of the hepatic veins (Figure 1).
- Level of the pars umbilicalis of the (left) portal vein branch (Figure 2).
- Level of the gall bladder (Figure 3).

Figure 1 **First level, confluences of the hepatic veins. This "junction" level is the first in ultrasound examination of the right liver lobe by sub-costal scanning sections steeply "looking" upwards, preferably in deep inspiration [http://media.falkfoundation.de/index.php?id=121&L=1]. VCI, inferior vena cava; LLV, left liver vein; MLV, middle liver vein; C, confluens of the LLV and MLV; RLV, right liver vein. The RLV often separately joins the inferior vena cava, whereas the LLV and MLV often reveal a common trunk (c).**

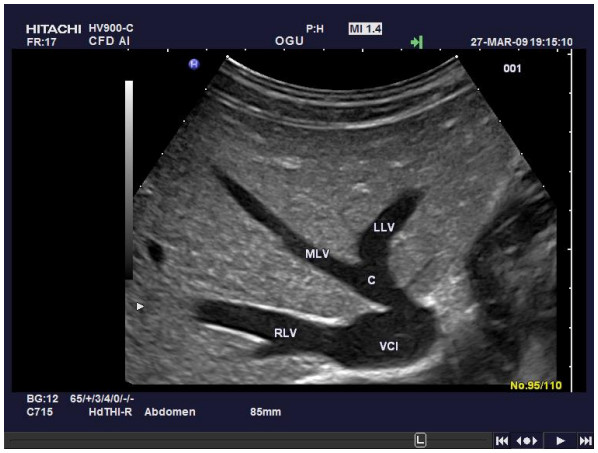

Figure 2 **Second level, pars umbilicalis of the portal vein [http://media.falkfoundation.de/index.php?id=121&L=1]. Scanning planes display the left and right liver lobes in a more downwards orientated view into the right liver lobe as compared with the level of the confluens of the hepatic veins. PA, portal vein; PU, pars umbilicalis of the portal vein; VCI, inferior vena cava.**

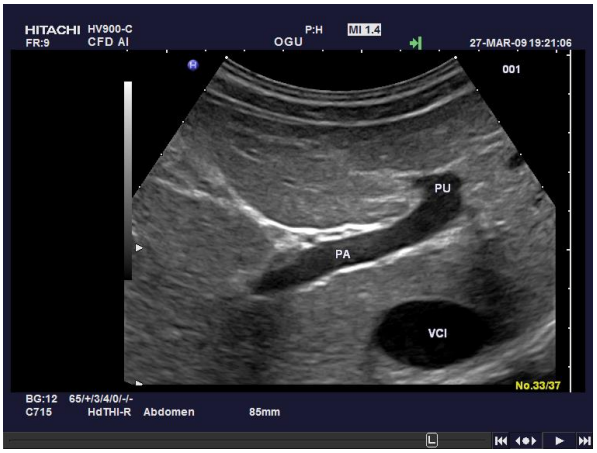

Figure 3 **Third level, gallbladder level as the most caudate scanning plane [[http://media.falkfoundation.de/index.php?id=121&L=1]]. GB, gallbladder; LTH, ligamentum teres hepatis; S4, segment IV of the liver (quadrate lobe).**

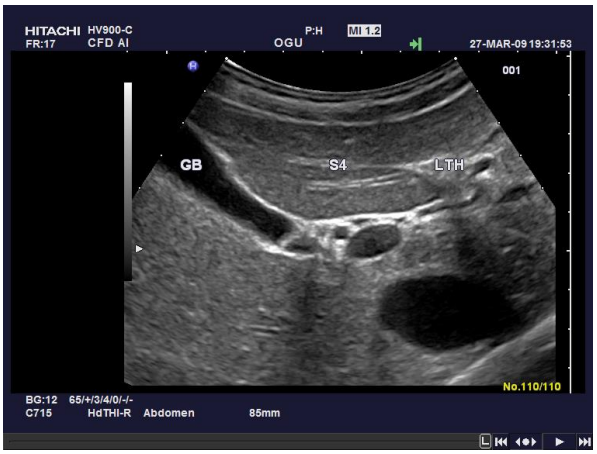

Using these levels as, more or less, parallel scanning sections allows the examiner to visualise a real-time three-dimensional (some call it “4D”) image of the patient’s individual

anatomy and pathology. Standardised scanning in a systematic sequence of probe and patient positions, and of scanning planes is mandatory to cover all segments and the complete liver surface.

The patient should be examined from the sub- to the intercostals in the decubitus position as well in the modified, slightly oblique, positions with the right arm above the head and the right leg stretched during all respiration cycles to identify the best approach and to avoid artefacts caused by the thorax.

Examination in the standing position is also helpful owing the liver moving caudally with gravity [http://media.falkfoundation.de/index.php?id=133&L=1]. Scanning from the sub- or intercostal probe positions (depending on the individual anatomy) avoids interposed lung, which can occur in the right posterolateral (superficial) parts of the liver when using the intercostal approach. There are other examination techniques that can also be used, but these will not be mentioned here in detail.

There are a number of variations from the norm that will be encountered (*e.g.* with respect to accessory lobules, vascular branching, shape and configuration).

The anatomy and examination technique are explained in the videos available online [http://www.efsumb.org/blog/?page_id=1750)].

Examination criteria

The acronym SSOTM (**S**ize, **S**hape, **O**utline, **T**exture and **M**easurement) is a useful way to recall the examination criteria.

Size

The size of the liver has had many methods of measurement, including three-dimensional-reconstructions. However, liver size measurement does not form part of current clinical practice because there is no established reliable or reproducible ultrasound method at present [(16, 17)].

Shape and Outline

The shape is normally described as pyramidal. The normal liver surface should be smooth with no protruding lumps or indentations. The inferior liver border in the normal patient

should have an acute angled edge [http://media.falkfoundation.de/index.php?id=132&L=1]. Liver surface border delineation and other ultrasound criteria are described in the respective chapters including the costodiaphragmatic recessus [http://media.falkfoundation.de/index.php?id=131&L=1].

Texture and echogenicity

The normal liver parenchyma is of medium homogenous echogenicity [(16, 18-20)]. It is usually slightly darker than the spleen and slightly brighter than the renal cortex, independent of age except in childhood [(20, 21)]. It is essential when comparing the liver with the spleen and renal cortex that comparison is done at the same depth. Liver surface and vessel borders are smooth and vascular architecture with its classic branching dichotomy is perceived as a harmonic and detailed aspect. The normal parenchyma image varies very little between individuals.

Hepatic veins

The three hepatic veins are positioned in between the liver segments. Their course, in addition to the Glisson's triad, is helpful in defining liver lobes and liver segments [http://www.efsumb.org/blog/?page_id=1750)]. The number and course of the hepatic veins are somewhat variable (Figure 1) [(22)].
The normal and pathological flow patterns are described in the Doppler chapter and examination technique videos [http://media.falkfoundation.de/index.php?id=127&L=1].

Portal vein

Formed by the confluens of the splenic and superior mesenteric vein, the portal vein can be displayed sonographically by scanning more or less perpendicular to the lower costal margin (orientation can be achieved by reference to the right shoulder to the umbilicus), preferably in a left decubitus position and on variably deep inspiration [(2, 22)]. Intrahepatically, the portal vein bifurcates into a main left and right branch. The first (right) portal vein branch splits into an anterior and a posterior branch, which itself leads to the segments V to VIII. The latter (left) main portal branch bifurcates into segments II and III and, into the left medial branches for segments I (caudate lobe), IVa and IVb (Figure 2).

The normal and pathological flow patterns are described in the Doppler chapter and examination technique videos [http://media.falkfoundation.de/index.php?id=123&L=1, http://media.falkfoundation.de/index.php?id=124&L=1, http://media.falkfoundation.de/index.php?id=125&L=1, http://media.falkfoundation.de/index.php?id=126&L=1].

Hepatic artery

The common hepatic artery originates from the coeliac axis, branching into the gastroduodenal artery and the proper hepatic artery (arteria hepatica propria). Anatomical variations are frequent (in up to 50% of the population), and include the origin of the left proper hepatic artery from the left gastric artery, as well as the variable arterial supply to the liver by superior mesenteric arterial branches. The hepatic artery runs with the portal vein, the right main arterial branch frequently meanders around the portal vein and is displayed sonographically as short segments medially (or less often laterally) of the portal vein. The normal and pathological flow patterns are described in the Doppler chapter and examination technique videos [http://media.falkfoundation.de/index.php?id=128&L=1].

Bile ducts (liver hilum)

Bile ducts accompany the portal vein and hepatic artery branches from the liver hilum into the liver lobules. Intrahepatically, they form the ductus principalis dexter and the ductus principalis sinister, which join as the CBD (Figure 4). The extrahepatic course of the CBD is cranially (prepancreatic), often ventral to the portal vein and caudally (intrapancreatic) more dorsolateral. The respective course of the hepatic artery is more variable [http://media.falkfoundation.de/index.php?id=113&L=1].

Figure 4 **Common bile duct (CBD), and therefore the liver hilum, is often best examined in a left lateral decubitus position using a sub-costal approach in slight inspiration [video]. The image is shown with (a) and without (b) labeling. In a typical view the CBD (in between markers (+)), portal vein (PV), hepatic artery**

(HA), inferior vena cava (IVC) and right renal artery (RRA) (sometimes the aorta (AO)) can also be seen; the papilla region (PAP) is indicated.

a

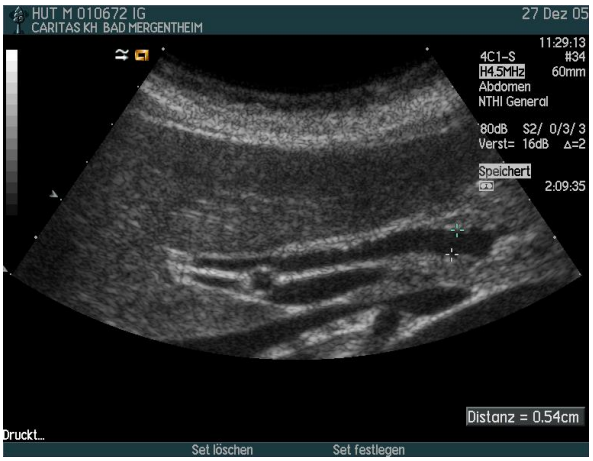

b

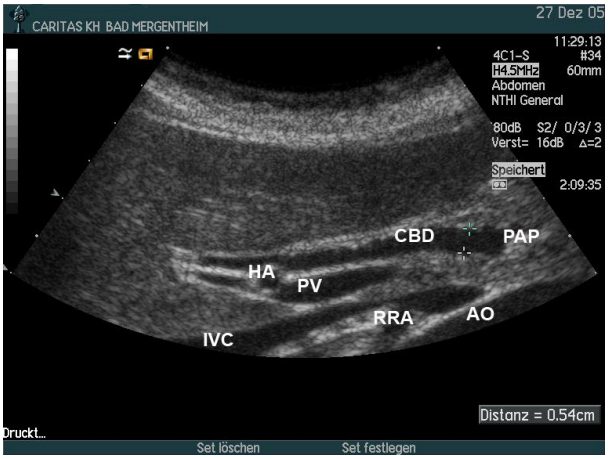

Perihepatic lymph nodes

Perihepatic lymph nodes in the hepatoduodenal ligament are commonly found next to the cystic duct and are therefore called cystic duct lymph nodes (Figure 5). They are enlarged in inflammatory [(1-6)] and neoplastic liver diseases [http://media.falkfoundation.de/index.php?id=115&L=1].

Figure 5 Perihepatic lymph nodes in the hepatoduodenal ligament (LK) are commonly found next to the cystic duct and are therefore known as cystic duct lymph node. They are shown here in a post-mortem examination on (a) ultrasound and (b) macroscopically. VCI, inferior vena cava [(23)].

a

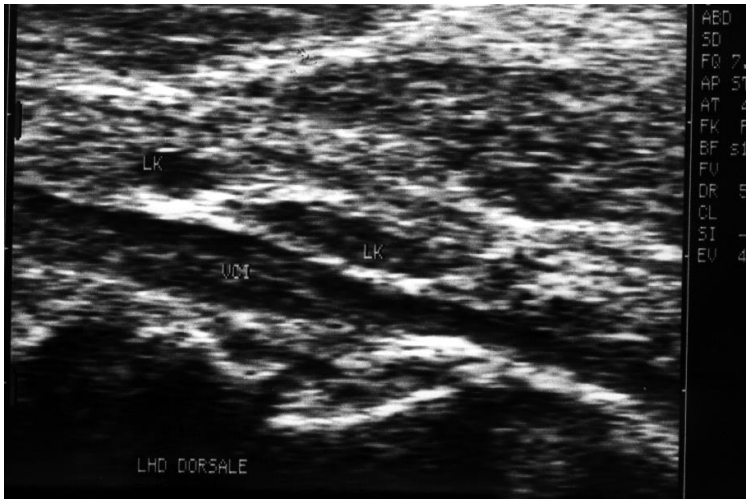

b

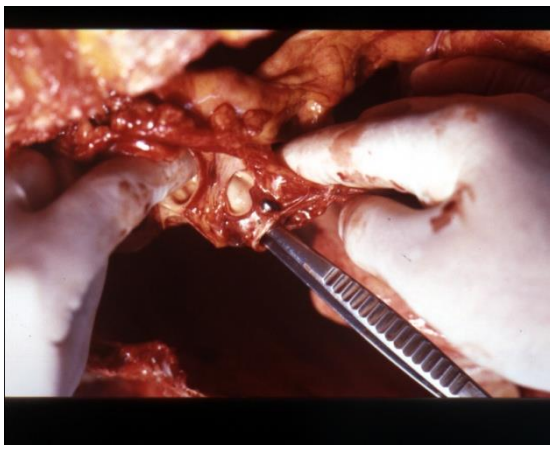

Liver pathology: diffuse liver disease

Criteria for analysing diffuse liver disease include the evaluation of:

- liver parenchyma (echo-texture, ultrasound attenuation, vascular architecture, etc.) as well as the liver surface (a high frequency transducer can be helpful to detect

details of superficially located structures) [(24-27)] [http://media.falkfoundation.de/index.php?id=130&L=1];

- liver hilum structures including perihepatic lymph nodes in the hepatoduodenal ligament, lymph nodes in inflammatory liver disease [(1-6)] or neoplastic infiltration;
- hepatic vessel flow patterns using colour and pulsed wave Doppler imaging (CDI) [(22, 28-39)].

Ultrasound contrast agents (USCA) have improved the detection/exclusion rate of focal liver lesions (FLL) in diffuse liver disease.

Hepatic steatosis

Hepatic steatosis (fatty liver) is the most common liver pathology. Sensitivity and specificity of the detection of hepatic steatosis by B-mode ultrasound examination can be very high in the hands of an expert investigator, who consistently applies specific criteria in patients with significant fatty liver disease. In transabdominal ultrasound, hepatic steatosis is characterised by increased echogenicity, which is often compared with spleen or kidney parenchyma at the same depth [(37, 40-43)] (Figure 6); supporting findings include ultrasound attenuation (the decrease in intensity as sound travels through a material, caused by absorption, scattering and beam divergence). Attenuation decreases the detail of vascular architecture, and it can cause a loss of visibility deeper within the liver and impeded imaging of the diaphragm [(16, 20, 37, 44)].

Figure 6 Sonographic signs of hepatic steatosis (fatty liver) include hepatomegaly with rounded borders, increased echogenicity, ultrasound attenuation caused by absorption, scattering and beam divergence, and decreased detail display of intrahepatic vascular architecture. There is an exaggeration of the difference between the kidney parenchyma and liver echogenicity. The right kidney is shown between callipers (+).

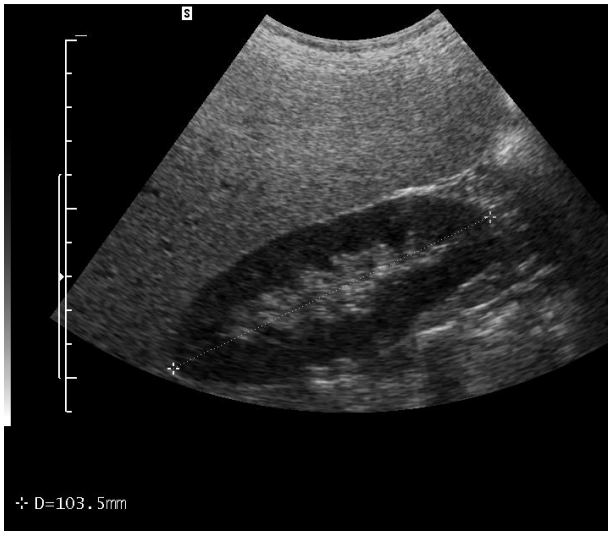

In the majority of patients with hepatic steatosis, distinctive hypoechoic areas in the liver hilum can be demonstrated by ultrasound examination (Figure 7) [(37, 40, 43, 45)]. It is believed that the presence of focal hypoechoeic areas (FHA) within the liver hilum (and elsewhere in the liver) corresponds to parenchymal islands, with, or close to, normal fat content (owing to a locally different blood supply), which are surrounded and contrasted by bright echogenic parenchyma with fatty infiltration. Sub-capsular FHA and FHA close to hepatic veins are other typical locations, these “pseudolesions” are polycyclic and non-round in shape. The FHAs are relatively specific to hepatic steatosis and may be helpful in differentiating fatty from fibrotic liver disease.

Similar FHA were demonstrated in patients with liver steatosis owing to systemic corticosteroid therapy [(45)], even though the more important focal lesions in this condition are hyperechoic (Figure 8). Pathophysiologically, areas of different fat content might be caused by the different arterial and portal venous blood supply in comparison with the surrounding liver parenchyma, which is mainly portal venous and therefore contains a higher

fat and insulin concentration in focal fatty infiltration a similar phenomenon in the surrounding of arterial shunts [(46)].

Figure 7 **Hepatic steatosis. Perhaps the most objective, and therefore the most important, sign of hepatic steatosis is the circumscribed focal hypoechoic areas in the liver hilum examined in a left posterior oblique position. (a) B-mode ultrasound demonstrates a focal liver lesion in between callipers (+). (b) Colour Doppler imaging indicates a centrally located vessel of undetermined origin. (c) Contrast enhanced ultrasound shows the typical enhancement pattern. Typically a centrally located arterial vessel can be displayed in the arterial phase (arrow) and (d) a portal vein branch in the portal venous phase (arrow) and homogenous enhancement in the late phase [EFSUMB cases of the month 2009, www.efsumb.org].**

a

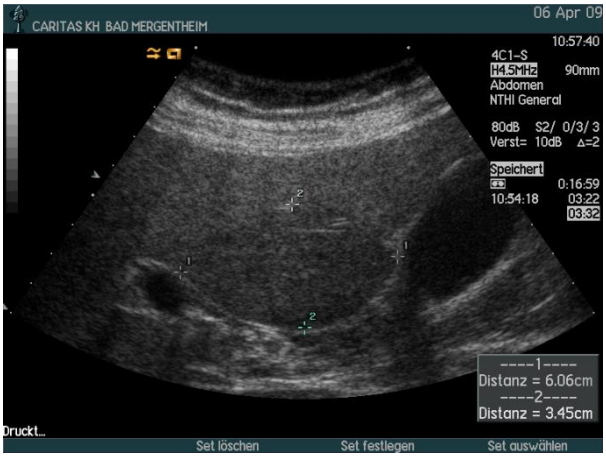

b

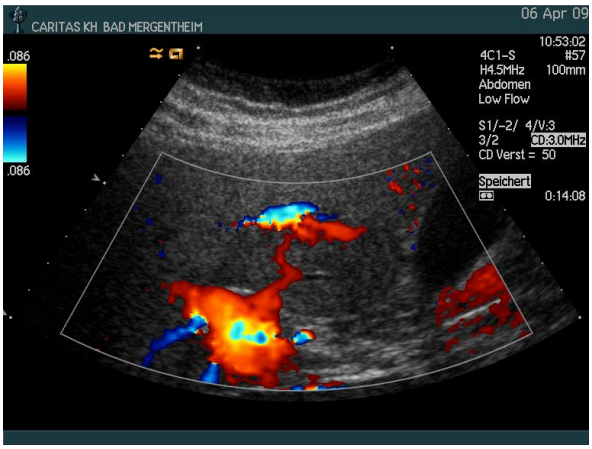

c

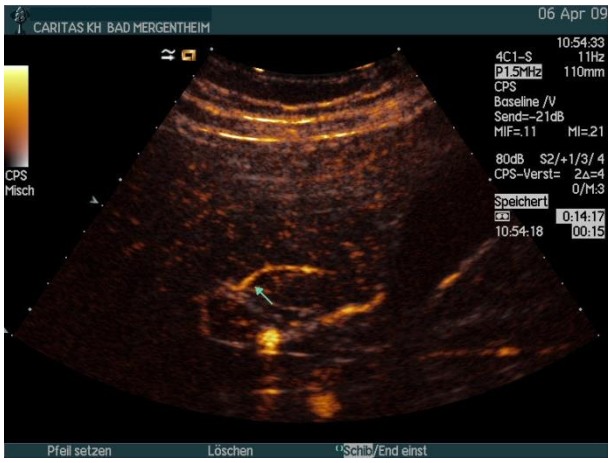

d

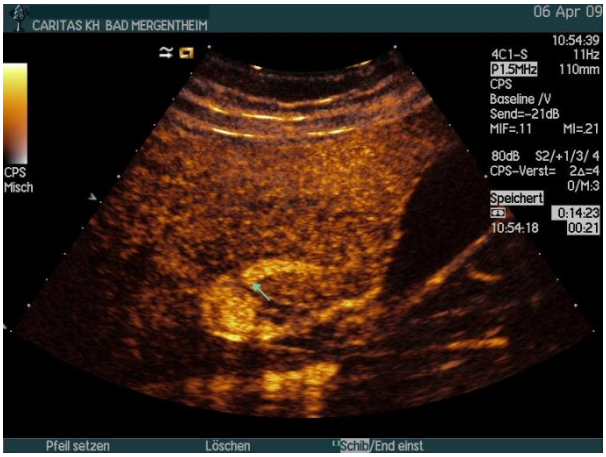

Figure 8 **Hepatic steatosis indicated by focal hyperechoic areas in the liver hilum. They are characterised by centrally located (portal) vein branches identified by colour Doppler imaging (a), spectral analysis (b) and contrast enhanced ultrasound (c). Such lesions are typically found sub-capsular next to the teres ligament [(17, 37, 45)] [EFSUMB cases of the month 2009, www.efsumb.org].**

a

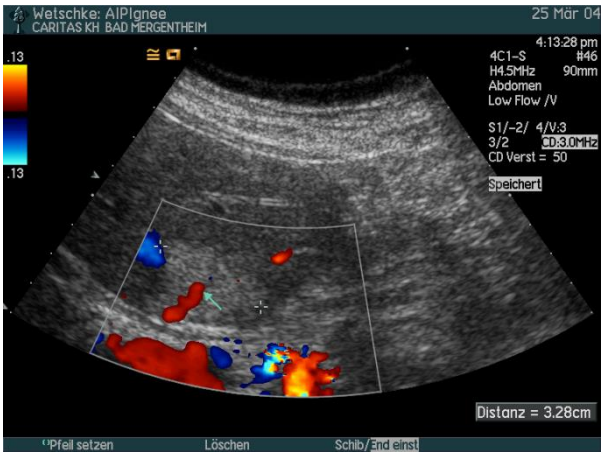
Welschke: AIPIgnee
CARITAS KH BAD MERGENTHEIM
25 Mär 04
4:13:28 pm
4C1-S #46
H4.5MHz 90mm
Abdomen
Low Flow /V
S1/-2/ 4/V:3
3/2 CD:3.0MHz
CD Verst = 50
Speichert
Distanz = 3.28cm
Pfeil setzen
Löschen
Schlb/2nd einst

b

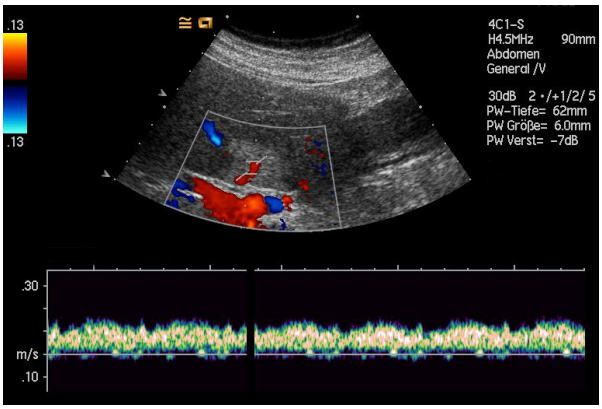
4C1-S
H4.5MHz 90mm
Abdomen
General /V
30dB 2 •/+1/2/ 5
PW-Tiefe= 62mm
PW Größe= 6.0mm
PW Verst= -7dB
.30
m/s
.10

c

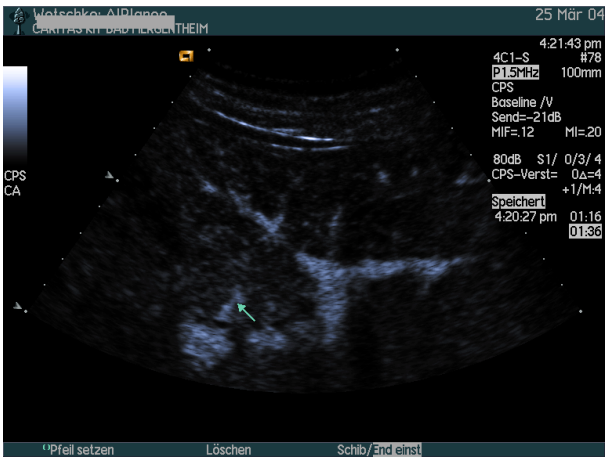
25 Mär 04
4:21:43 pm
4C1-S #78
P1.5MHz 100mm
CPS
Baseline /V
Send=-21dB
MIF=.12 MI=.20
80dB S1/ 0/3/ 4
CPS-Verst= 0Δ=4
+1/M:4
Speichert
4:20:27 pm 01:16
01:36
CPS
CA
Pfeil setzen
Löschen
Schlb/2nd einst

Liver cirrhosis

The accuracy of ultrasound in the correct diagnosis of liver cirrhosis in patients with complications (ascites, splenomegaly and collaterals) is high (>90%). In the initial stages and in micronodular cirrhosis, it may be overlooked in up to 30% of cases [(20, 47-49)]. Sonographic signs of liver cirrhosis include inhomogenous echo-texture and irregular-nodular liver surface delineation, and a variety of other possible findings, including destroyed vascular architecture, dependent on the aetiology of the disease (Figure 9). Disproportional segment atrophy (and hypertrophy) has also been observed (Figure 10).

Figure 9 **Typical signs of liver cirrhosis include (a) inhomogenous echo-texture and irregular liver surface delineation (arrow); (b) distinctive nodules are also suggestive. Sometimes it may be difficult to identify the liver parenchyma, in these cases the organ is indicated as well: Leber: liver.**

a

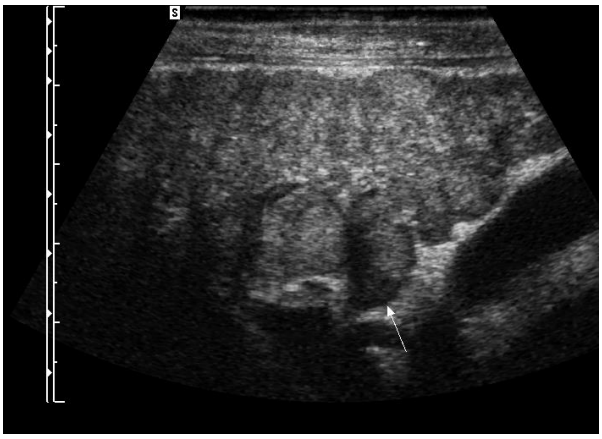

b

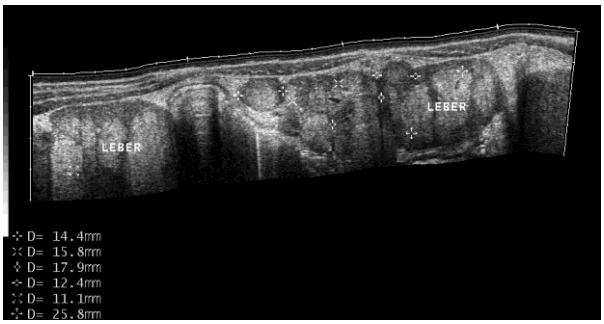

Nodular liver surface (especially when using high frequency transducers) has an excellent positive predictive value (close to 100%) for cirrhosis. A disproportional volume enlargement of the caudate lobe in relation to the right and left lobe can be indicative of liver cirrhosis, but this sign is of limited value in daily clinical practice.

Coarse liver parenchyma and a disturbed or destroyed vascular architecture as a sign of portal hypertension, such as reversed portal flow and collateral vessels, are other indicators of liver cirrhosis. In Doppler studies, a rise in the arterioportal peak velocity ratio (maximum velocity of the hepatic artery divided by the maximum velocity of the vena portae) of more than 3.5 is predictive of cirrhosis. The positive predictive value for the detection of portal hypertension is excellent [(50-52)], the signs include reversed portal flow and the detection of collateral vessels. The negative predictive value is not as high; the overall accuracy is only 60%. An enlarged portal vein diameter greater than 12.5 mm or a reduced portal vein flow velocity indicates cirrhosis with a sensitivity and specificity of approximately 80%. However, all these parameters are of limited value in daily clinical practice.

Figure 10 Liver lobes and segments may behave differently during the course of a disease, as shown in this patient with systemic sclerodermy and gradual shrinkage of the right liver lobe (between +). The changes to the liver evolved gradually over 10 years.

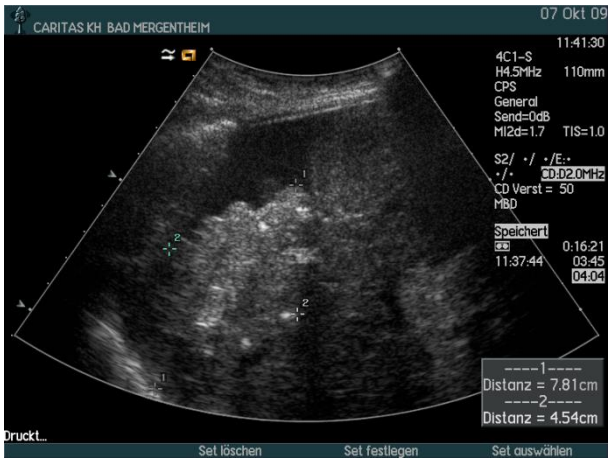

Detection of lymph nodes in the hepatoduodenal ligament (perihepatic lymphadenopathy)

Improvement of sonographic technology, techniques [(53)] and knowledge of well-defined anatomical sites of perihepatic lymph nodes (between the inferior cava and portal vein next to the right renal artery) have led to improved identification of, not only, enlarged, but also normal sized lymph nodes in the liver hilum by ultrasound. Normal lymph node size is up to 19 mm [(1, 2, 21, 54, 55)]. Two groups of lymph nodes can normally be detected: the dorsal in the hepatoduodenal ligament adjacent to the cystic duct (”cystic duct nodes”) and ventral in the hepatoduodenal ligament adjacent to the orifice of the foramen epiploicum next to the common hepatic artery (Figure 11). The liver hilum should be examined in a slight left lateral oblique patient position (15-30°) with the right arm elevated, thus improving the detection rate from 25% to 75% compared with the decubitus position (http://media.falkfoundation.de/index.php?id=113&L=1) [(2)].

Figure 11 **Two groups of lymph nodes can normally be detected in anatomical examinations: the dorsal group in the hepatoduodenal ligament adjacent to the common hepatic bile duct and cystic duct (“cystic duct nodes”, seen in (a) and (b) between markers (+). VCI, inferior vena cava; VP, portal vein; and (c) ventral in the hepatoduodenal ligament adjacent to the orifice of the foramen epiploicum next to the common hepatic artery (between markers).**

a

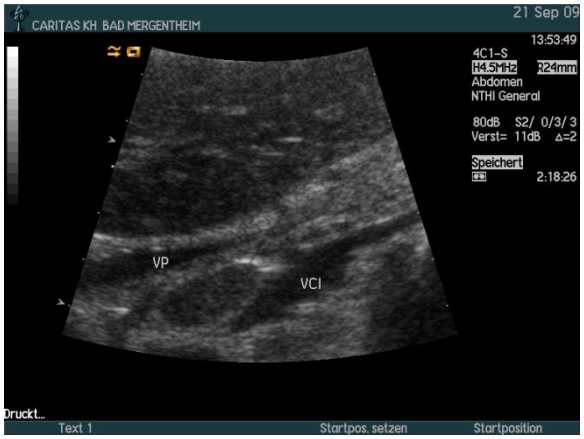

b

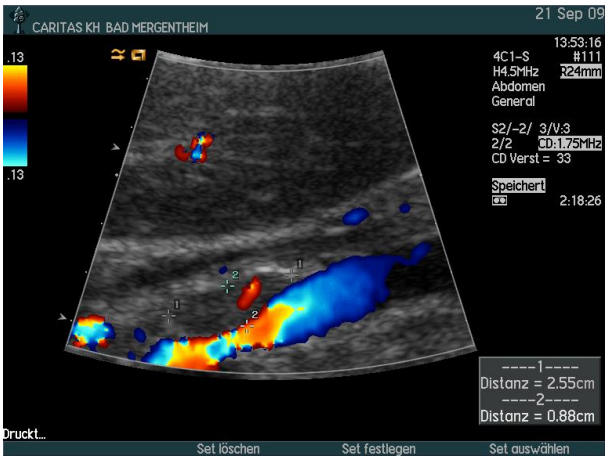

c

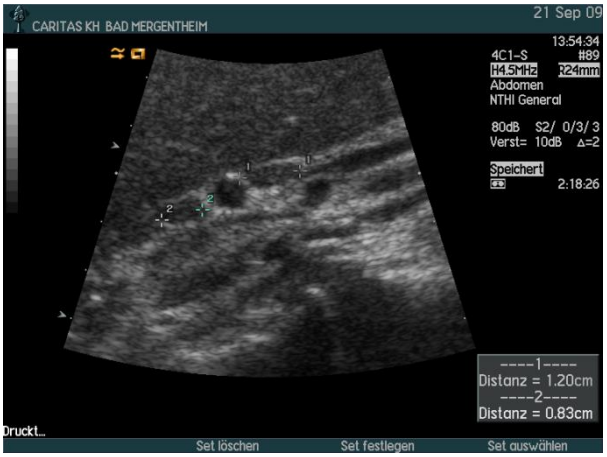

Acute viral hepatitis

There are no significant changes in liver echo-texture in acute viral hepatitis. However, enlarged perihepatic lymph nodes are a fairly constant feature, which is also present in chronic hepatitis, conditions such as viral and autoimmune hepatitis (AIH) (including primary sclerosing cholangitis (PSC)) [(47, 56)], but not in toxic inflammatory liver disease or haemochromatosis. One study of 40 patients with acute hepatitis found enlarged perihepatic lymph nodes could be identified by transabdominal ultrasound in all patients with adequate visualisation of the liver hilum (a sensitivity of 100%), which is helpful to differentiate between toxic and viral genesis [(6)] (Figure 12).

Figure 12 Sonographic presentation of enlarged perihepatic lymph nodes ventral and dorsal in the hepatoduodenal ligament (in between markers) in a patient with acute virus hepatitis B. See also cases of the month [http://www.efsumb-archive.org/asp/detail06.asp?ref=304&url=/case-month/cm-archive.asp?ref=1].

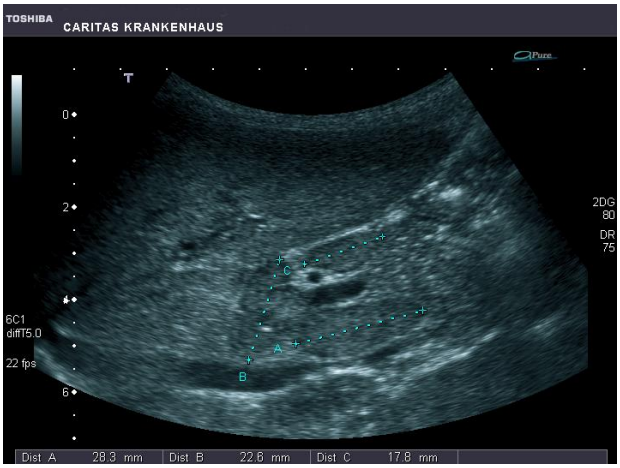

Additionally, in chronic liver disease, perihepatic lymphadenopathy was present in 86% of patients with viral hepatitis, in 90% with AIH, in 100% with PSC, in 97% with primary biliary cirrhosis (PBC) [(3)], but in only 6% with haemochromatosis, in 1% with fatty liver disease and in 4% with cholecystolithiasis [(23)].

Doppler techniques can be used to exclude complications (*e.g.* portal vein thrombosis) and reveal an unspecific hyperdynamic state in hepatic vessels with a higher diastolic arterial blood flow when compared with healthy individuals. Portal venous blood flow is increased and, perhaps owing to oedema and narrowing of the hepatic veins, the flow pattern is often non-triphasic [(57)].

Gallbladder wall thickening (Figure 13) is a short-life sonographic phenomenon of early phase acute hepatitis in approximately 50% of patients [(6)]. This must not be confused with acute cholecystitis where there is no circumscribed pain under ultrasound visualized palpation.

Figure 13 Gallbladder wall thickening in acute hepatitis is a short-life sonographic phenomenon of early phase acute hepatitis in approximately 50% of patients, which can be confused with acute cholecystitis.

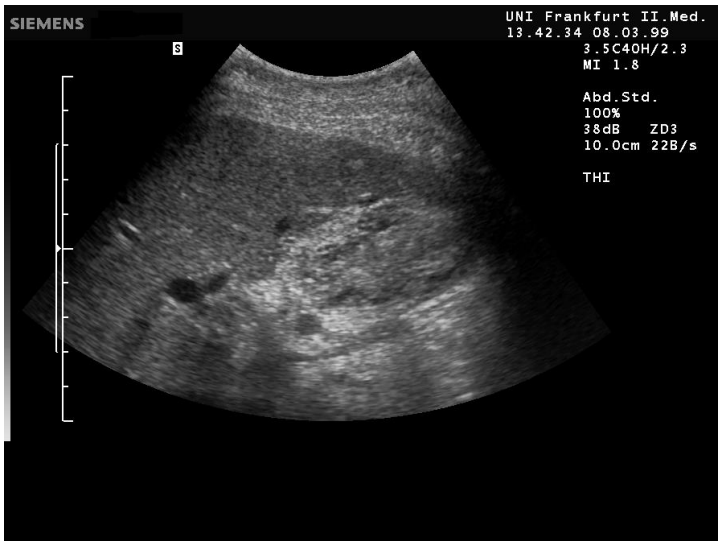

Chronic viral hepatitis C

In patients with chronic viral hepatitis C (HCV) infection, hepatic steatosis is a frequent histological finding and occurs in more than 50% of cases [(20)]. The reason for this remains poorly understood; even when the most common causes of steatosis are excluded, a significant proportion of patients with chronic HCV infection show signs of liver steatosis.

Perihepatic lymphadenopathy

Lymph nodes are detectable within the hepatoduodenal ligament in almost all patients with chronic HCV [(1)]. The total perihepatic lymph node volume changes according to the antiviral response and leads to progressive normalisation of the perihepatic lymph node volume in those patients with a sustained virological response [(5)]. A decrease in perihepatic lymph node volume is associated with an improvement in liver histology. Mediastinal lymphadenopathy has also been described in patients with chronic HCV using mediastinal ultrasound, whereas other abdominal lymph node locations are not significantly altered in patients with the infection [(4)].

Primary biliary cirrhosis

The echo-texture of the liver parenchyma in patients with PBC in Stage I and II is often unremarkable. In Stage IV typical signs of liver cirrhosis are detectable. The liver parenchyma of patients with Stage III PBC show advanced sonomorphological modifications such as inhomogenous parenchyma, but no indicative signs of liver cirrhosis. The extent of perihepatic lymphadenopathy reflects the progression of the disease with a larger lymph node size in more advanced stages [(3, 58)].

Primary sclerosing cholangitis

Neither the clinical symptoms nor the biochemical evidence of cholestasis are specific to PSC and they lack sensitivity, particularly in the early course of the disease. Ultrasound is useful in the detection and follow-up of extrahepatic bile duct lesions, but it should be noted that alterations of the intrahepatic duct system are not displayed under all circumstances. Asymmetric mural thickening is a typical ultrasound finding in advanced PSC (Figure 14), but it is important to mention that symmetric mural thickening by itself is a rather unspecific marker for cholangitis. Finally, enlarged hilum lymph nodes are detectable in almost all patients with PSC [(47, 56)].

Figure 14 Asymmetrical mural thickening of the common bile duct (between markers, +) is a sensitive sign of primary sclerosing cholangitis.

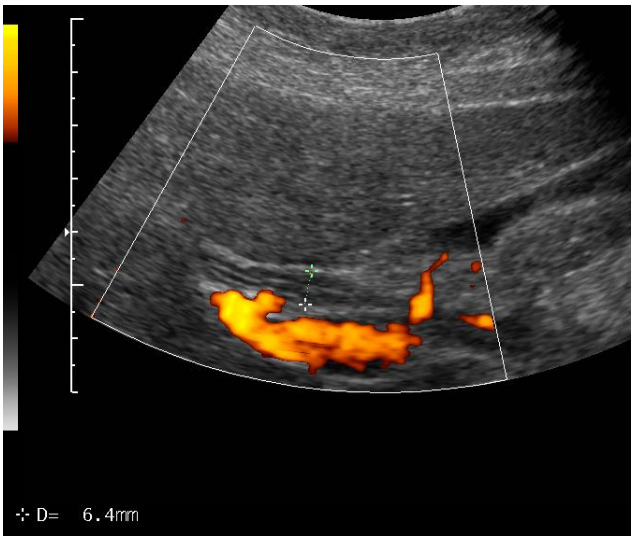

Other diffuse liver diseases

Patients with autoimmune hepatitis (AIH) generally show perihepatic lymphadenopathy with lymph nodes over 19 mm in size. There are no other typical ultrasound features of liver texture or the hepatobiliary tract in patients with AIH [(47)].

Changes in the liver parenchyma and echo-texture in patients with sarcoidosis are unspecific, but occasionally circumscribed (isoechoic) sarcoid infiltrations can be observed, which mimic malignancies even with contrast enhanced techniques. Perihepatic lymphadenopathy in these patients is sometimes impressive with lymph nodes of up to 60 mm noted. Perihepatic lymphadenopathy is indicative of hepatic involvement. In patients with advanced disease, signs of liver cirrhosis and portal hypertension are common with the respective flow changes of the hepatic vessels [(59-62)]. Similar to PBC, the flow pattern in the portal and hepatic veins is increased in contrast with other forms of liver cirrhosis.

In the recently published literature none of the cystic fibrosis patients showed enlarged perihepatic lymph nodes (with the exception of patients with CBD stones and cholangitis). There are no typical liver echo-texture sonographic findings. One study reported a micro-gallbladder as a typical sign of cystic fibrosis. The authors found a frequency of 18 in 72 (25%) patients compared with 0 in the control group [(63, 64)].

In patients with alcoholic steatohepatitis (ASH) and non-alcoholic steatohepatitis (NASH) the attenuation of the ultrasound beam makes it difficult to examine the liver hilum. Adequate visualization is possible in only 80% of patients. In a series of 60 patients no enlarged perihepatic lymph nodes could be found (unpublished data by the author). Toxic liver disease is frequently encountered, but sonographic features in patients are unspecific. In a currently unpublished series of 100 patients, no enlarged perihepatic lymph nodes could be found (unpublished data, personal communication).

Changes to liver parenchyma in patients with human immunodeficiency virus infection are dependent on opportunistic infections or neoplastic infiltration [see respective chapters of the EFSUMB Course Book]. Many causes have to be considered [*e.g*. bacillary angiomatosis] [(65)]. In a consecutive series, 82 of 100 patients with acquired immune deficiency syndrome showed enlarged perihepatic lymph nodes (unpublished data, personal communication). Co-

infection with hepatitis B and C virus and mycobacteriosis is common. There was no significant correlation with viraemia. Hepatobiliary infection as a cause of perihepatic lymphadenopathy should also be considered, *e.g.* cytomegaly virus infection. Enlarged perihepatic lymph nodes have been found in almost all patients with end-stage liver disease.

Wilson's disease is a rare autosomal-recessive inherited disorder of copper metabolism, which results in the accumulation of copper in the liver and many other organs. Liver disease varies depending on the severity of the disease at time of diagnosis. Histopathological findings include (focal) fatty changes, signs of acute (including hepatic necrosis) or chronic hepatitis, fibrosis and cirrhosis. Liver imaging findings reflect a wide range of physiopathological processes of the disease and demonstrate the associated findings of cirrhosis in cases with advanced disease [(47)] [EFSUMB cases of the month, www.efsumb.org].

Ultrasound findings in end-stage Wilson’s disease resemble liver cirrhosis caused by other aetiologies. In early stages multiple intrahepatic small (<20 mm) hypoechoic nodules were observed in 8 out of 10 consecutive patients with Wilson’s disease (unpublished data). In these lesions biopsy and histological examination revealed prominent copper accumulation in comparison with the surrounding liver parenchyma (Figure 15). In two patients additional dysplastic nodules were observed.

Figure 15 Wilson's disease. The parenchymal echo pattern has typical increased echogenicity with abundant round or oval foci of decreased echogenicity (shown between the callipers) resembling metastatic liver disease. Biopsy and histology revealed prominent copper accumulation [EFSUMB cases of the month 2008, www.efsumb.org].

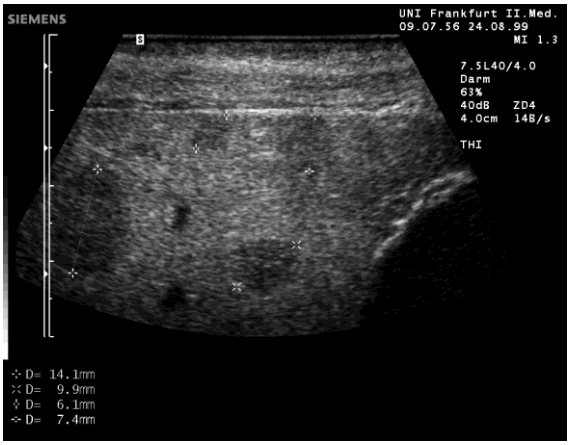

There are many liver diseases with specific and unspecific ultrasound changes that are not described here. We have focused on the common diseases of the Western world; however, examples with striking ultrasound features from elsewhere in the world include patients with ascariasis [(66)], fasciolosis [(67)], hepatobiliary schistosomiasis [(68, 69)] in association with portal hypertension who show typical fibrotic strands as sequelae of fibrous portal venous obliteration (Figure 16). For further reading we refer to the mentioned literature.

Figure 16 Schistosomiasis shows hyperechoic typical fibrotic strands as sequelae of fibrous portal venous obliteration.

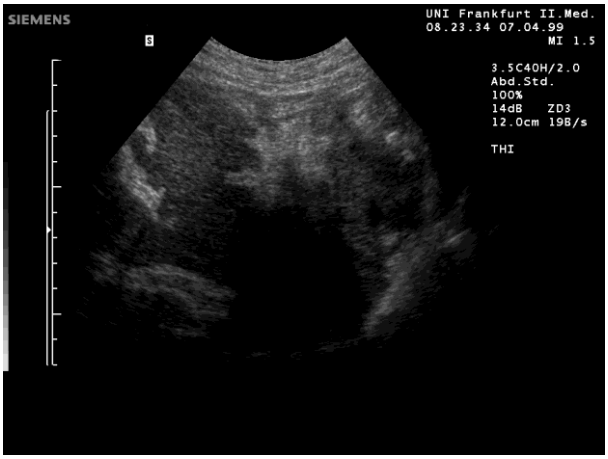

Vascular liver diseases

Anatomy and blood supply

Hepatic vascularisation is characterised by two vascular systems with completely different haemodynamics and one outflow system which have been characterized by ultrasound techniques [(13, 22, 28-32, 35, 36, 39, 51, 70-82)]:

- Arterial inflow (high pressure, low flow resistance) (Figures 17 and 18) [http://media.falkfoundation.de/index.php?id=128&L=1 and http://media.falkfoundation.de/index.php?id=129&L=1].

Portal-venous inflow (low pressure, low flow resistance) (Figure 19 and 20) [http://media.falkfoundation.de/index.php?id=123&L=1; http://media.falkfoundation.de/index.php?id=124&L=1; http://media.falkfoundation.de/index.php?id=125&L=1 and http://media.falkfoundation.de/index.php?id=126&L=1]

- Venous outflow (low pressure and low flow resistance) (Figure 21) [http://media.falkfoundation.de/index.php?id=127&L=1].

Vascular hepatopathies include the abnormal vascular course, aneurysms, stenoses and occlusions of the vessels in these systems.

Arterial flow

Arterial liver disorders are rare. A diminished arterial blood flow can be caused by congenital malformations as well as by acquired embolic, thrombotic, inflammatory, vascular-tumourous, vasculitic or arteriosclerotic-degenerative changes, or, in acute myocardial, by forward failure and shock [(32, 34, 78, 83, 84)]. Hypervascularity is observed even less frequently and is due to arteriovenous shunts, of congenital (*e.g.* Osler's disease) [(85-87)], traumatic or septic-embolic origin. Pathological sonographic findings of arterial vessels are summarised, examples include:

- Hypoplasia and aplasia of the common hepatic artery and/or its branches with atrophy of related liver segments,
- Aneurysms of the common hepatic artery and its branches,
- Atypical vascular courses (*e.g.* with impression of the hepatic choledochal duct),
- Arteriovenous and arterioportovenous shunts (*e.g.* Osler's disease)
- Abnormal hepatic vascular malformations occur more frequently in connection with vascular changes in other organs (heart, lungs, brain and kidneys), which tend to determine the clinical course and prognosis.

Figure 17 Extrahepatic hepatic arterial vessels. B-mode ultrasound (a), colour Doppler imaging (b) of the coeliac trunk, which supplies the arterial blood for the liver and the perihepatic structures. The liver hilum is often best examined in a left lateral decubitus position.

a

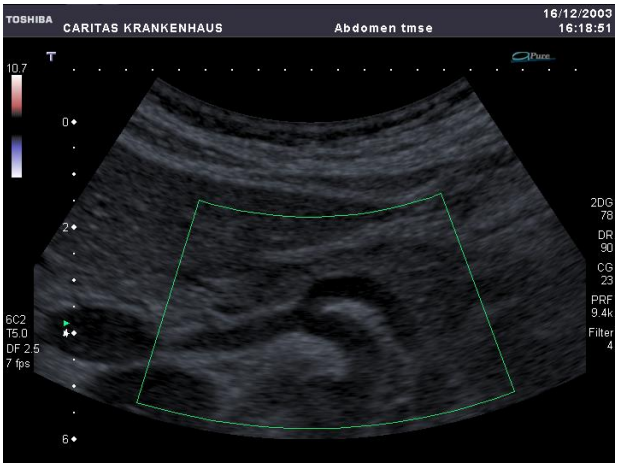

b

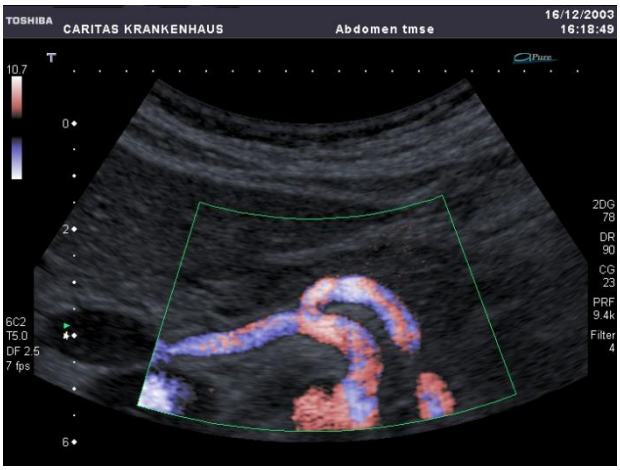

Portal venous system

Signs of portal hypertension (splenomegaly, ascites and collateral vessels) with continued liver function impairment can be shown on ultrasound [(13, 30, 33-35, 39, 57, 72, 73, 78, 88-96)]. The most important disorder to identify is portal vein thrombosis.

Venous outflow

In disorders of venous outflow, firstly liver function is substantially restricted and secondly, signs of high portal vein pressure are detected. Right-ventricular heart failure is the most common venous outflow disorder. The increase in post-hepatic resistance reduces portal hepatic perfusion and can lead to a pendular or retrograde flow in the portal vein, especially in cases with an additional intra-hepatic increase in resistance [(34, 38, 71, 75-77, 83, 97)].

Colour Doppler imaging for analysis of hepatic vessel flow pattern – an introduction

Colour Doppler imaging (CDI) is an accurate and well-established technique in evaluating portal hypertension, portal vein thrombosis, Budd-Chiari syndrome and other forms of sinusoidal obstruction syndrome (SOS) respective veno-occlusive disease (VOD) [(98-100)]. CDI is routinely used to evaluate patients prior to liver transplantation to determine portal vein patency, signs of portal hypertension and hepatic artery patency post-operatively. CDI is

also important to monitor flow direction and patency of spontaneous and artificial portosystemic shunts, *e.g.* transjugular intrahepatic portosystemic shunts (TIPSS) [(88, 90, 91, 101)]. Post-liver transplantation patients are monitored by analysing the hepatic artery profile; stenosis and rejection are indicated by changes in the resistance flow pattern (*e.g. pulsus parvus et tardus*) [(102-104)].

Chronic heart failure reveals tetra-phasic flow in the right liver vein and highly undulating flow patterns in the portal vein, which reverses during intensified therapy. Analysis of the flow pattern in the hepatic veins is helpful to characterise diffuse parenchymal liver disease [(38, 71, 76)].

Vascular (Doppler) indices

Vascular indices, (*e.g.* Doppler perfusion index (DPI)), hepatic transit time and various ratios analysing different vessels have been used for liver tumour detection and characterisation, but are currently only used in experimental settings. The portal vein congestive index (PVCI) is defined as the ratio of cross-sectional area of the extra-hepatic portal vein to the time averaged mean velocity of blood flow in the portal vein. The PVCI is elevated in liver cirrhosis at an early stage with a constant portal vein blood flow (cross-sectional area multiplied by the time averaged mean velocity), which can be reached by an increased portal vein pressure with consecutive dilatation of the latter vessel. The method, which, after some training, is more difficult in its wording than in its application, has still not achieved general acceptance.

The DPI is the ratio of hepatic arterial blood flow (normally below 20%) to the total liver blood flow (hepatic arterial and portal venous blood flow). DPI is reported to be elevated in the presence of intra-hepatic tumours as well as in patients with liver cirrhosis, and has been used to screen patients with suspected metastases; however, the promising data could not be reproduced [(79, 105, 106)].

Examination of the hepatic artery in patients with diffuse liver disease

Examination technique

There are only limited data analysing hepatic arterial vessels in diffuse hepatic disease compared with portal venous studies. The reason for this is clear: the common anatomical variations of the coeliac trunk in up to 50% of the population do not allow reproducible and standardised examinations. Resistance and pulsatility indices represent the parenchymal influence distal to the measurement point. These indices can therefore represent hepatic parenchymal influence with a certain degree of confidence. Interobserver variability when analysing hepatic arterial blood flow at this measurement point is less than 12%, but much higher for peak systolic, end diastolic and time averaged mean velocity, and for blood flow volume (approximately 30%) [(36, 39)]. Hepatic blood flow can also depend on food intake, posture, activity and is influenced by drugs. The examination technique is described in the EFSUMB examination technique videos [http://media.falkfoundation.de/index.php?id=128&L=1].

Figure 18 The hepatic artery in its typical topographic next to the common bile duct and portal vein [video 4]. A low resistance flow pattern is typical with significant diastolic flow [(36, 39)].

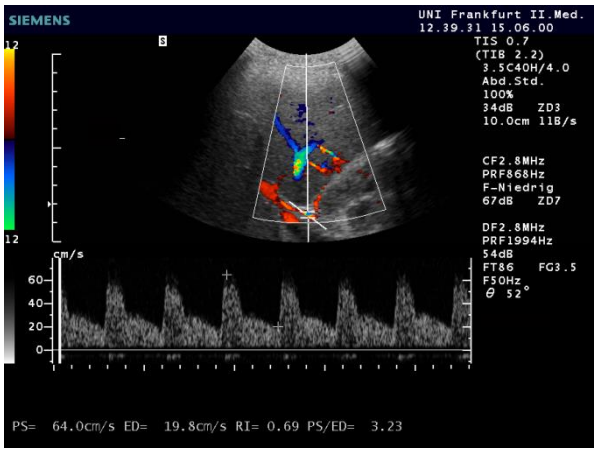

Table 1 Table of normal flow parameters analysed in 47 healthy probands.

Vessel	TC	AMS	AHC	AHP
PSV (cm/s)	137±45 (53-260)	145±42 (47-228)	102±46 (31-202)	58±34 (23-193)
EDV (cm/s)	39±15 (17-90)	18±9 (5-40)	27±11 (10-56)	20±12 (8-60)
RI	0.7±0.06 (0.59-0.88)	0.87±0.05 (0.74-0.96)	0.71±0.09 (0.5-0.83)	0.65±0.07 (0.52-0.78)
PI	1.86±0.9 (1.03-4.77)	3.74±1.39 (177-7.75)	1.68±0.59 (0.72-2.93)	1.16±0.25 (0.73-1.75)
TAV_{max} (cm/s)	59±21 (22-115)	37±15 (15.6-73)	45±20 (15-108)	34±20 (13-102)
TAV_{mean} (cm/s)	33±12 (10-70)	22±9 (9-40.66)	25±13 (10–72)	20±12 (9-68)
D (mm)	6±1 (4.2-8.8)	6±1 (4-10)	4±1 (3-7)	3±1 2-6)
BF (ml/min)	630±250 (184-1239)	395±206 (159-1061)	250±220 (88-1163)	105±89 (24-503)
Angle (°)	26±19 (1-60)	42±16 (7-63)	59±14 (22-81)	42±19 (7-73)

TC, celiac trunk; AMS, mesenteric superior artery; AHC, common hepatic artery; AHP, proper hepatic artery; PSV, peak systolic velocity; EDV, end diastolic velocity; RI, resistance index; PI, pulsatility index; $TAV_{max,}$ time averaged maximum velocity; $TAV_{mean,}$ time averaged mean velocity; D, diameter; BF, blood flow volume. Values are mean±standard deviation (range)

Examination of the portal vein in patients with diffuse liver disease

Examination technique

Portal vein diameter and flow pattern is measured using an intercostal approach at an angle close to 0^{o}, just before the portal vein splits into the right and left branches. Biphasic fast Fourier transformation (FFT) Doppler spectrum of the portal vein should be documented during a 5-8 s suspended respiration at a mid-respiration level, avoiding respiratory and thoracic pressure influences. The sample gate is adjusted to the inner diameter of the vessel and the FFT spectral analysis is recorded. The maximum (V_{max}) and minimum (V_{min}) velocity in centimetres per second of an undulational circle are set automatically or manually. The differences in V_{max} and V_{min} are calculated as a parameter of biphasic oscillations as well as the portal vein resistance index ((V_{max}–V_{min})/V_{max}) in a similar way to the resistance index of arterial vessels. The reproducibility of the method was investigated by repeated sonographic examinations of the portal vein flow in 10 healthy individuals over 7 consecutive days. The mean coefficient of variation for intra-individual assessment of the flow velocity (V_{max} and V_{min}) was 12% and 10%, respectively [(22)].

The examination technique is described in the EFSUMB examination technique videos [http://media.falkfoundation.de/index.php?id=123&L=1, http://media.falkfoundation.de/index.php?id=124&L=1, http://media.falkfoundation.de/index.php?id=125&L=1, http://media.falkfoundation.de/index.php?id=126&L=1].

Normal and pathological portal venous blood flow

Normal portal venous blood flow undulates slightly (normal values, 12–24cm/s using the intercostal approach with a mean resistance index of 0.36). Different pathological flow patterns of the portal venous system have also been described [(34, 36, 76, 102)].

Figure 19 The portal vein (arrows) is scanned using a transcostal approach on (a) colour Doppler imaging and (b) continuous duplex scanning with a normal flow pattern range of 12–24 cm/s [(22)].

a

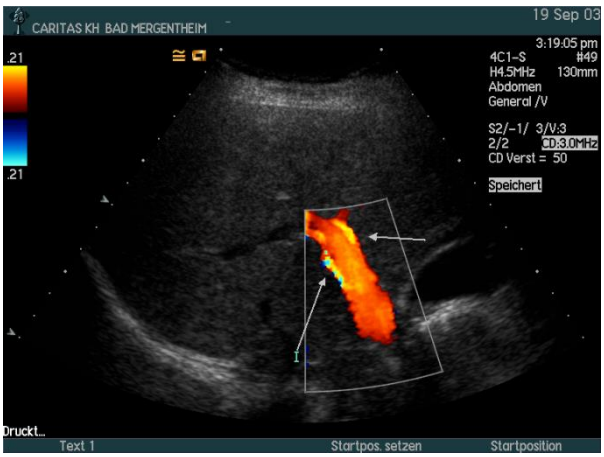

b

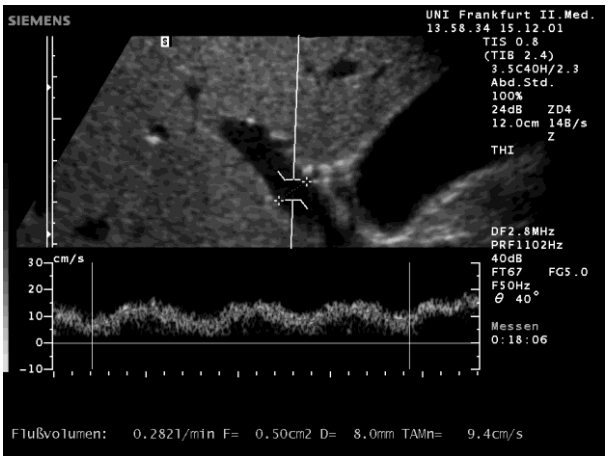

Portal hypertension

Colour Doppler ultrasound examination is recommended in patients with suspected portal hypertension because CDI is helpful in the detection of the presence and direction of blood flow within the portal venous system [(22, 30, 50, 63, 92, 107, 108)]. Hepatofugal flow in the portal vein is found in approximately 10% of patients with liver cirrhosis. Prevalence does not differ in relation to the aetiology of liver cirrhosis, but it is stage dependent and is often found more frequently in Child B and C cirrhosis compared with Child A cirrhosis. The clinical significance of this Doppler phenomenon is still unclear, especially in relation to repeat variceal bleeding.

Increased pulsatile flow (high resistance index) in the portal vein has predominantly been found in patients with severe right heart failure, demonstrating that right atrial pressure is negatively correlated with portal vein pulsatility ratio (Figure 20) [(78, 89, 92)]. In patients with steatosis the flow is flattened and is demonstrated by a low resistance index.

Figure 20 Increased pulsatile flow in the portal vein, which is predominantly found in patients with severe right heart failure and demonstrates that right atrial pressure is negatively correlated with the portal vein pulsatility ratio.

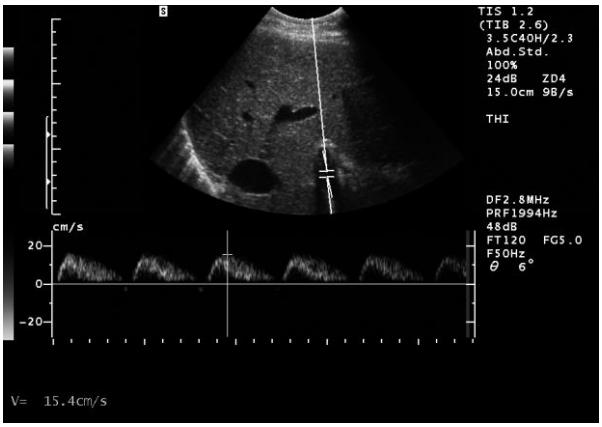

No portal venous blood flow

Very slow portal vein velocities of less than 2 cm/s are difficult to detect because the Doppler signal is lower than the threshold of the ultrasound equipment and additional respiratory modulation of the patient. A stagnant or portal venous "0" flow is seen mainly in patients with advanced liver cirrhosis. In patients with stagnant portal vein flow the use of ultrasound contrast enhancing agents may be helpful in the exclusion of portal vein (appositional) thrombosis.

Retrograde portal venous blood flow

Reversed portal venous blood flow can be observed when intrahepatic resistance is greater than the resistance of portosystemic collaterals (Figure 21). An association has been found between portal venous flow patterns (*e.g.* abnormal flow direction) and the presence of, mainly spontaneous, portosystemic shunts as well as oesophageal varices and ascites. The increase of intrahepatic resistance may be explained by structural abnormalities, *e.g.* hepatocyte enlargement, space of Disse collagenisation and hepatic vein sclerosis. Retrograde portal venous flow has mainly been observed in patients with portal hypertension. Respiration dependent hepatofugal portal flow is a rare finding associated

with periodic portal hypertension in patients with right heart insufficiency and/or liver disease; the clinical significance is unclear.

Pulmonary hypertension, pericardial effusion, constrictive pericarditis, pericardial tumours, right atrial tumour and other causes that lead to an increased right atrial pressure are responsible for pressure-related hepatic venous out-flow block with subsequent trans-sinusoidal hepatoportal shunting, similar to the mechanical outflow block that causes reversed pulsatile flow in liver cirrhosis. Portal vein–hepatic vein shunts and portocaval (portosystemic) shunts may also cause pulsatile portal flow.

Figure 21 Retrograde portal venous blood flow as a typical sign of severe portal hypertension.

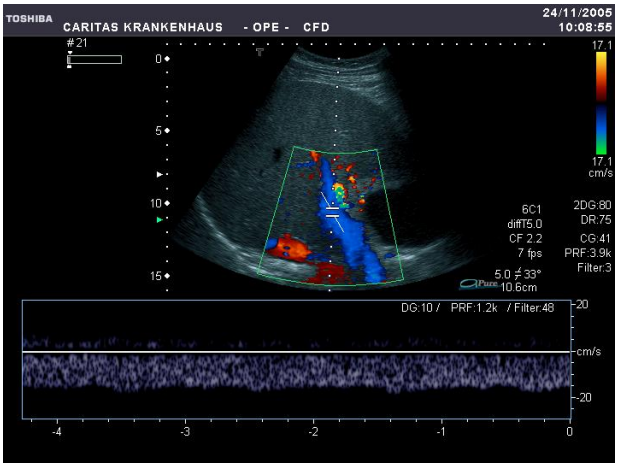

Portal vein thrombosis

Portal vein occlusion with an increase in pre-hepatic portal vein pressure may have a variety of causes including coagulation defects with thrombocystosis, and an increase in fibrinogen concentration owing to inflammation. Periportal venous collaterals, as a cavernous transformation, may at least partially compensate the portal venous hepatic inflow. Reduced portal venous blood supply may be compensated by an increased arterial perfusion so that liver function appears only slightly impaired. However, portosystemic collaterals lead to a reduced “first-pass” deteriorating effect (*e.g.* encephalopathy). This is especially important

when portal vein thrombosis is caused by cirrhosis with a reduction of flow, because of this, encephalopathy may manifest and liver-dependent medication metabolism may be disturbed. Colour-coded duplex sonography was the method of choice for detection of PVT but today contrast enhanced ultrasound is preferred [(109-113)]. It has a high degree of sensitivity (>90%) for the detection of localised segmental or complete portal venous thrombosis (Figure 22).

Figure 22 Portal vein thrombosis. (a) hyperechoic total portal vein thrombosis intrahepatically and (b) extrahepatically. Circumscript portal vein thrombosis is shown in (c) B-mode ultrasound and (d) using contrast enhanced ultrasound.

a

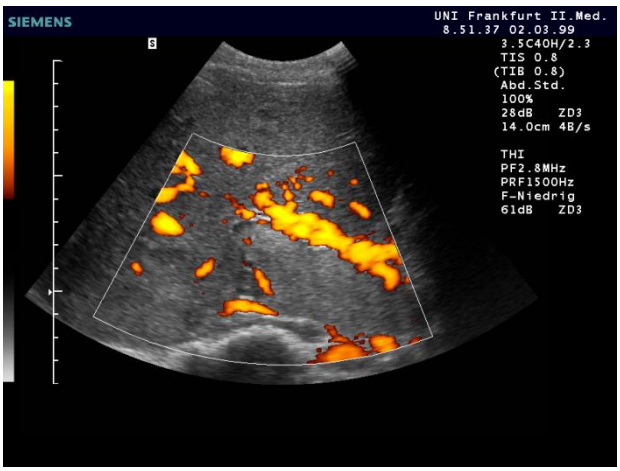

b

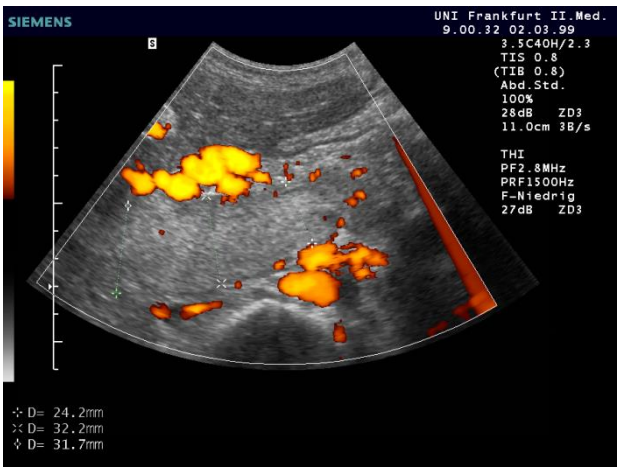

c

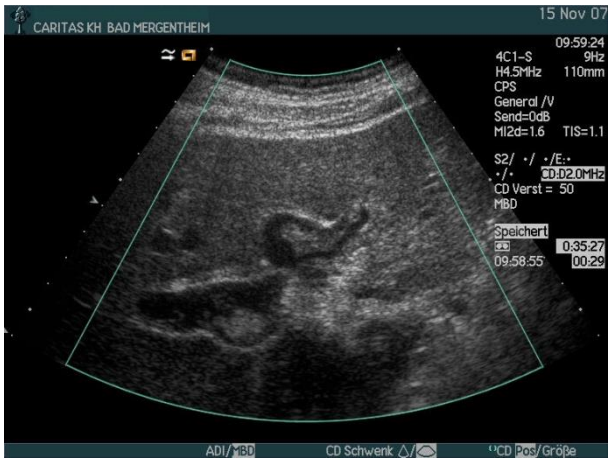

d

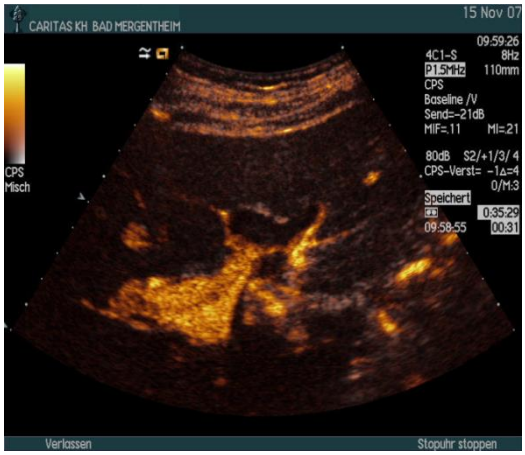

Contrast enhanced CT and MRI are alternatives in the diagnosis of portal vein thrombosis, especially in obese patients.

Before operations or interventions it is often desirable to perform angiography of the visceral vessels. Ultrasound is specific for the exclusion of infiltration of hepatic vessels (*e.g.* portal and hepatic veins). Portal vein thrombosis is a common sign of tumour angiogenesis, especially in extensive tumour stages. To differentiate between benign and malignant portal and hepatic vein thrombosis it is useful to use CDI or contrast enhanced techniques. Using CDI malignant infiltration can be assumed, if pulsatile flow is derived from inside of the thrombus. If this is not conclusive, CEUS is more sensitive in depicting arterial enhancement of the thrombus [(109, 110)].

Examination of the hepatic veins in patients with diffuse liver disease

The normal flow pattern in the right hepatic vein is triphasic [(22)] (Figure 23). The FFT-Doppler ultrasound spectrum of the right hepatic vein next to the IVC reflects mainly cardiovascular and respiratory changes in pressure and flow pattern. In contrast, the FFT-Doppler ultrasound spectrum of the right hepatic vein, 6-8 cm distal to the confluence of the hepatic veins, reflects histological changes of the liver parenchyma and can be classified into a triphasic waveform with a short-reversed flow, a biphasic waveform with no reversed flow with a fluttering of more than 10% of the mean phasic amplitude, or a monophasic flat waveform with a fluttering of less than 10% of the mean phasic amplitude. In patients with heart insufficiency the flow can be tetraphasic, which means there is a significant amount of hepatopetal flow showing a pendular flow (backward and forward). The maximum, medium and minimum (reversed flow) velocity in centimetres per second could also be recorded. Owing to changes in the vessel diameter of up to 2 mm per cycle during systole and diastole, and different directions of the normal triphasic hepatic vein flow, it is not useful to calculate the blood flow (in millilitres per minute) in the hepatic veins [(22)].

Examination technique

The right hepatic vein is identified via the right intercostal approach, displayed longitudinally by a counter-clockwise turn, the sample gate is positioned 6-8 cm distal to the confluence of hepatic veins and adjusted according to the inner diameter of the vessel (typically 3-7 mm). FFT spectral analysis is recorded for at least 5 s. The Doppler ultrasound spectrum can be recorded within a short breathing pause of 5-8 s without relevant intra-abdominal or intra-thoracic pressure related artefacts. To avoid artefacts as a result of different respiratory positions and different abdominal and intra-thoracic pressures, the evaluation of the right hepatic vein via the 10th or 11th intercostal space 6-8 cm distal to the confluence of the hepatic veins offers a standardised procedure and provided reproducible results with an acceptable insonation angle in all patients and healthy individuals [(22)].

Which hepatic vein should be examined?

The close anatomical relationship between the left liver lobe and the heart frequently leads to Doppler signal artefacts in any signal obtained from the left hepatic vein. Owing to these artefacts, which are mainly due to heart movements, the left hepatic vein cannot always be reliably evaluated. Adequate sonographic visualisation of the middle hepatic vein and evaluation of the FFT-spectrum is best accomplished during slight inspiration and via the sub-costal route. However, in 35 out of 135 patients evaluation of the middle hepatic vein this was only possible during deep inspiration with respiration related artefacts of the Doppler ultrasound spectrum with an initial monophasic waveform changing to a bi- and triphasic waveform during the examination. The most reproducible Doppler ultrasound spectrum can be obtained from the right hepatic vein via the right intercostal approach [(22)].

The reproducibility of the method was investigated by repeated sonographic examinations of the flow pattern in the right hepatic vein in 10 healthy individuals over 7 consecutive days. The mean coefficient of variation for intra-individual assessment of flow velocity was 13% for the hepatofugal flow and 19% for the reversed flow. The flow pattern in the 10 individuals investigated was always triphasic. The reproducibility for the middle hepatic vein was less favourable with a mean coefficient of variation for intra-individual assessment of the flow velocity of 25% for the hepatofugal flow and of 76% for the reversed flow [(22)].

Clinical application

It has been previously shown that a non-triphasic hepatic vein flow (HVF) is mainly associated with the degree of fat deposition within the liver and less related to inflammatory parameters and the extent of liver fibrosis. Recently, a large scale study on patients with chronic HCV infection confirmed that hepatic steatosis can be excluded by normal liver haemodynamics; however, some operative characteristics (specificity and positive predictive values) were rated insufficient. Non-triphasic HVF and FHA within the liver hilum are both parameters that can be easily measured and quantified by ultrasound. The recorded values are reproducible and less dependent on the investigators interpretation than conventional grey scale imaging [(22, 31, 77)].

In general more than 90% of healthy probands have a triphasic flow pattern, whereas only 60–70% of patients with a hepatopathy show a non-triphasic pattern. So, for non-triphasic flow and the diagnosis “liver disease”, the positive predictive value is high but the negative predictive value is low.

Figure 23 Hepatic vein blood profile. The normal hepatic flow profile is triphasic in the right liver vein (RLV); the portal vein is also indicated (PV) (a,b). Monophasic flow deformation is mainly due to hepatic fat infiltration, as shown in this patient with steatohepatitis (c) [(22)].

a

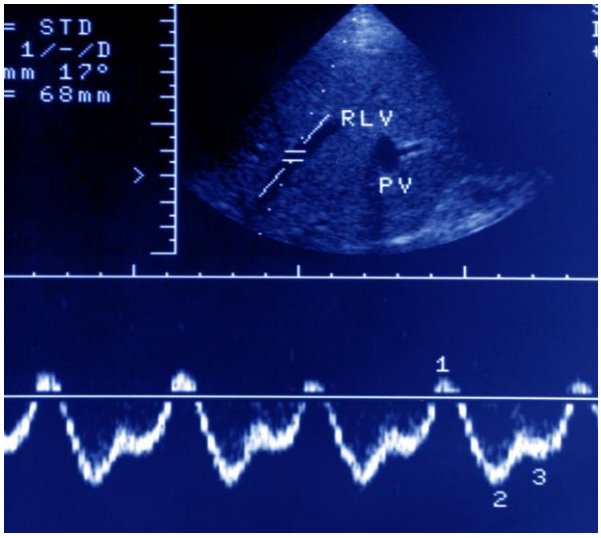

b

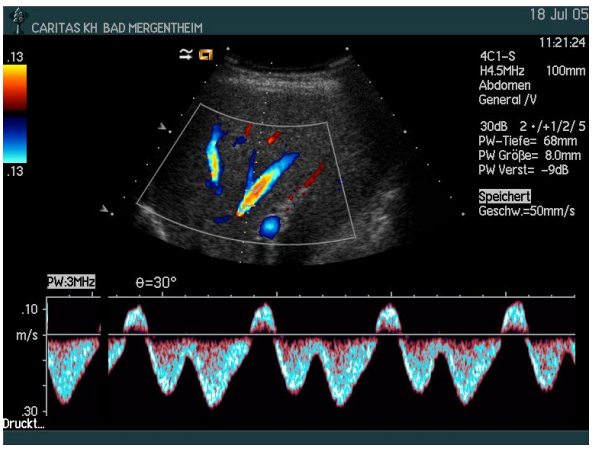

c

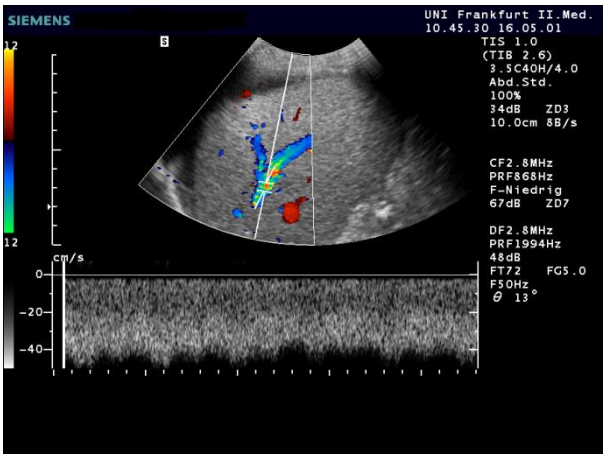

Hepatic venous outflow obstruction (Budd-Chiari syndrome)

Budd-Chiari syndrome is a rare cause of liver disease with or without signs of portal hypertension. Approximately, one-third of patients present with acute disease with sonographically detectable thrombosis. Approximately, two-thirds have chronic presentation sonographically with occluded hepatic veins and intrahepatic collaterals (Figure 24) [(114-116)].

Figure 24 Budd-Chiari syndrome. Approximately, one-third of patients present with acute disease with sonographically detectable thrombosis. Approximately, two-thirds have chronic presentation songraphically with (a) occluded hepatic veins (between markers), (b) retrograde portal venous outflow, and intrahepatic collaterals with or without extrahepatic shunts. PV, portal vein.

a

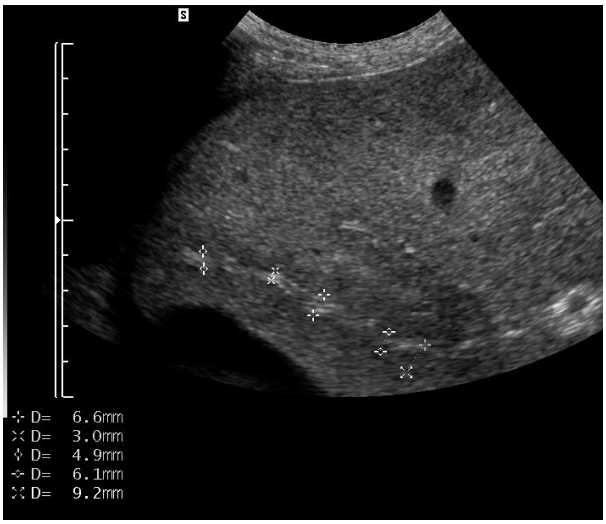

b

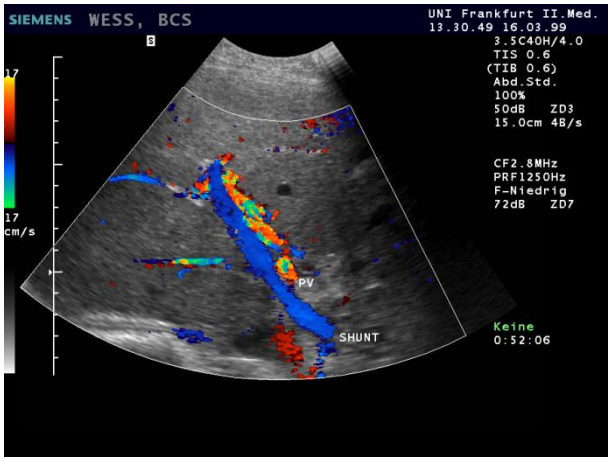

The hepatic vein, in this stage, can be occluded appearing as a fibrous strand or spontaneously, partially or completely recanalised depending on the aetiology. CDI is helpful in the diagnosis of BCS. Doppler ultrasound accurately detected the site of the block in most patients with newly diagnosed Budd-Chiari syndrome [own data, not yet published]. HCC has to be ruled out by CEUS or other imaging methods.

Veno-occlusive disease

Duplex sonography of the portal vein system and the hepatic veins may show typical changes, but may display only a relatively low sensitivity and specificity. Sonographic signs of VOD are ascites, thickening of the gall bladder wall, increase of the resistance index in the hepatic artery as well as retrograde flow in the portal vein and changes in the portal vein

flow profile. CDI in the diagnosis of 12 patients with VOD after bone marrow (or stem-cell) transplantation reveals low (<10 cm/s) or reversed portal venous flow, high resistance arterial flow pattern (resistance index >0.85) and flattened monophasic flow pattern in the right hepatic vein of less than 8 cm/s. Published data are sparse in patients with VOD [(98-100)].

Osler's disease

Liver involvement occurs in 30–70% of cases and can lead to a specific form of liver cirrhosis, as a result of sclerosis formed around the multiple vascular malformations that can be easily detected on ultrasound [(86)]. Doppler ultrasound helps to identify the nature of shunts (arterio-portal, arterio-systemic, arterio-porto-systemic) (Figure 25). When using conventional B-mode ultrasound, especially in the supply area of the superior mesenteric artery dense network of vessels, oval cystic lesions with corresponding malformations are found to represent shunts [(85-87)].

Figure 25 Osler's disease showing intrahepatic arterio-porto-venous shunts with typical Doppler spectrum for shunts.

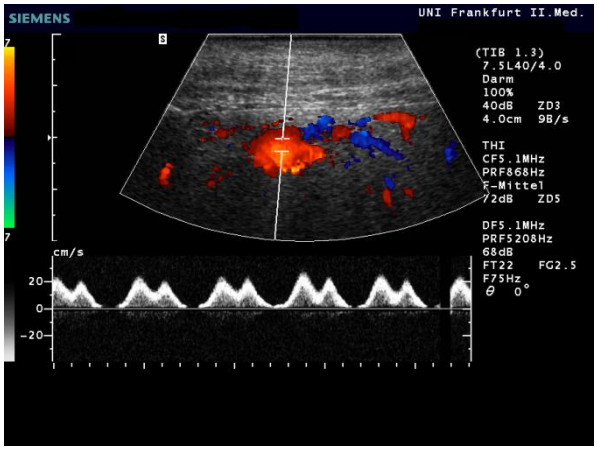

Cirrhosis, as well as a number of porto-systemic shunts caused by vascular malformations, contributes to the development of encephalopathy. Liver cirrhosis owing to the basic disease flow pattern must be distinguished from the effects of, the often, multiple transfusions (*i.e.* post-transfusion hepatitis).

In the case of arterio-venous shunt formation in the liver with systemic effects (which frequently occur at a later age, the selective arterial embolisation of the supply vessels has proven successful. Depending on the general health of the patient, surgery (ligature of the supplying vessel and partial resection of the liver) is not always possible.

Transjugular intrahepatic portosystemic shunts

A high percentage of patients with TIPSS have post-procedural shunt complications, including thrombosis of the stent, stenosis of the stent, or stenosis of the hepatic vein draining the stent [(50, 51, 88, 90, 91, 101, 116)]. Doppler ultrasound is an excellent non-invasive screening technique for the detection of complications of TIPSS. Complications can be detected using different criteria, including no flow for thrombosis, a temporal change in peak stent velocity greater than 50 cm/s for stent and/or hepatic vein stenosis, and reversed flow in the hepatic vein draining the stent and, rarely, stent stenosis. In 55 patients the change (increase or decrease) in peak stent velocity of greater than 50 cm/s from the post-TIPSS baseline sonogram as the diagnostic criterion for the detection of shunt stenoses resulted in 91% sensitivity and 80% specificity [own data, not yet published].

Liver pathology - detection and characterisation of focal liver lesions (FLL)

The definition of a FLL is the difference in echogenicity between a circumscribed area and the surrounding liver tissue. Differences in ultrasound echogenicity usually, although not necessarily, show a pronounced difference in X-ray attenuation and MR as well. Consequently, most FLL are visualised by all three sectional imaging modalities, whereas a few are shown by only one or two of these modalities.

FLL are detected and characterised sonographically by echogenicity differences from the surrounding liver tissue, as well as by the detection of hyper- or hypovascularisation (on colour Doppler ultrasound). Conventional B-mode ultrasound makes it possible to unequivocally detect the frequently of typical liver cysts and calcifications. However, detection and characterisation of liver tumours still represents a challenge to all imaging modalities despite the advances in imaging techniques (*i.e.* ultrasound, CT and MRI scanning).

More recently, CEUS has been able to provide important additional information on FLL enhancement characteristics and vascularisation pattern. Circumscribed lesions of foreign-liver-tissue (*e.g.* metastases) can be detected by the absence of uptake of contrast media Such lesions appear in the post-vascular late-phase image as storage defects, although this late-phase effect is neither absolutely specific nor absolutely sensitive. As a result of their doubled blood supply via the portal vein and the hepatic artery, focal lesions in the liver often exhibit no general hyper- or hypoenhancement, but depending on the flow phase and the histology, present a complex temporal and spatial picture of increased and reduced contrast. Certain lesions can give a characteristic vascular picture (*e.g.* the wheel-spoke phenomenon) or a distinctive enhancement pattern (*e.g.* halo contrasting or iris diaphragm phenomenon), allowing the lesions to be characterised, but contrast patterns do not always take this typical form. Similar arterial, parenchymatous and venous characteristics are exhibited by the spleen and lymph nodes.

The technique of CEUS is described in the technical chapter of this book. Contrast agents are used in the liver for different purposes [(109-113, 117)] including:

- detection of liver tumours [(118-120)];
- characterisation of liver tumours [(121-127)] (benign *vs* malignant [(26, 128, 129)]);
- monitoring of local ablative treatment [(130-137)];
- imaging hepatic vessels;
- describing diffuse liver disease by demonstrating intrahepatic microscopic shunts and measuring the hepatic transit time (time interval between appearance in the hepatic artery to in the hepatic veins);
- analysing time intensity curves [(138, 139)].

Liver tumour detection

CEUS increases the detection rate of metastases as compared with conventional B-mode ultrasound, which has been demonstrated by multicentre trials. Comparative studies have shown that the detection rate has the same accuracy as the detection rate for contrast-enhanced CT and MRI scans. CEUS allows the same detection rate for benign FLL compared

with the occurrence in normal liver parenchyma (10% of all livers), which is important for differential diagnosis [(118-120)].

Differentiation of benign and malignant lesions

Characterisation of a liver lesion begins once an abnormality is found. An imaging procedure used to detect liver masses should also enable the examiner to differentiate between benign and malignant lesions. CEUS in the portal venous and late phase after injection of SonoVue® (Bracco, Italy) considerably improves the characterisation of liver tumours compared with conventional B-mode ultrasound, leading to differentiation of benign and malignant liver lesions in most patients, if cysts and calcifications are excluded by conventional B-mode ultrasound [(26, 128, 129)]. CEUS facilitates the clinical decision regarding whether a sonographically detected liver lesion will need further investigation or not. This new technique may help to reduce unnecessary or invasive examinations in certain cases (*e.g.* invasive liver biopsy, CT scan and MRI). Only a few false positive findings have been observed so far, mainly owing to abscesses or necrosis, old fibrous focal nodular hyperplasia (FNH) predominantly with scar tissue, sarcoidosis lesions, and inflammatory pseudotumours of the liver [(26, 140)].

Focal liver lesion characterisation

Liver cyst

Liver cysts are a frequent finding (Figure 26-28) and are easily diagnosed using conventional B-mode ultrasound. Liver cysts are characterised, as are other cysts, as typically round, anechoic, smoothly delineated structures with refraction shadows at the edges; a strong posterior wall echo and post-cystic enhancement owing to an intensity difference between the beam intensity deep to the cyst and in the cysts. Cysts displaying all these sonographic signs are defined as typical (Figure 26), whereas cysts showing only some of the signs are defined as atypical (Figure 27). Very early echinococcosis can be confused with atypical liver cysts. Cystadenoma can also be another differential diagnosis (Figure 28).

Figure 26 **Typical liver cyst. The exophytic liver cyst is next to the spleen. Typical liver cysts display all the morphological criteria (echo-free, round-oval, well-defined borders with lateral shadowing and transducer distal (posterior) echo enhancement), while atypical liver cysts do not. Leber: liver.**

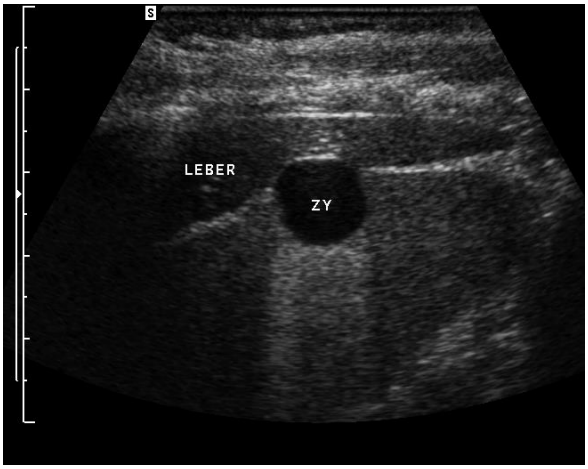

Figure 27 **Atypical liver cyst. These cysts do not display all the morphological criteria of typical liver cysts (echo-free, round-oval, thin-walled, well-defined borders with lateral refraction shadowing and post-cystic echo enhancement). (a) Owing to the small diameter and slice thickness artefacts the cyst is not echo-free, but (b) contrast enhanced ultrasound shows the cyst. (c,d) In another example the cyst-like structure is a hepatic vessel, which can be difficult to recognise using conventional B-mode ultrasound.**

a

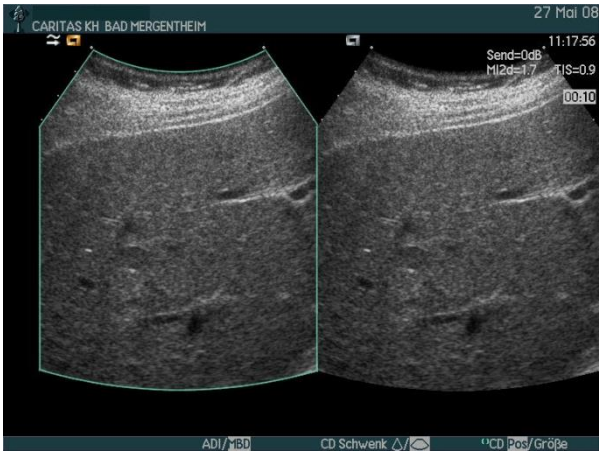

b

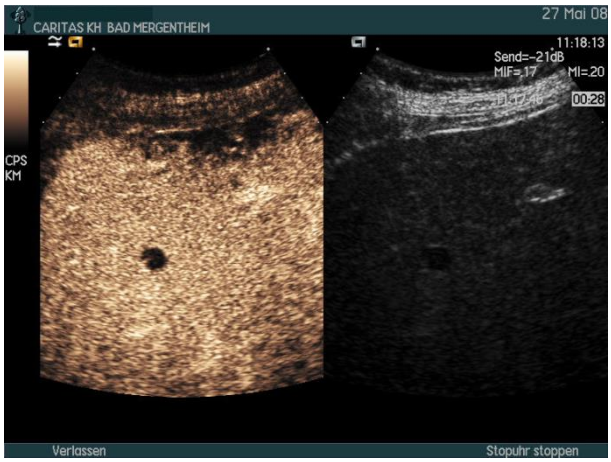

c

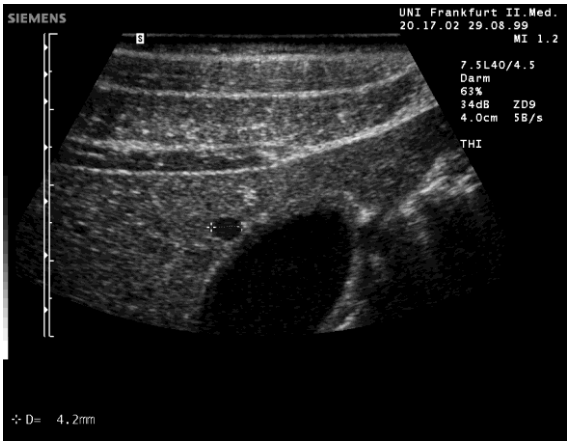

d

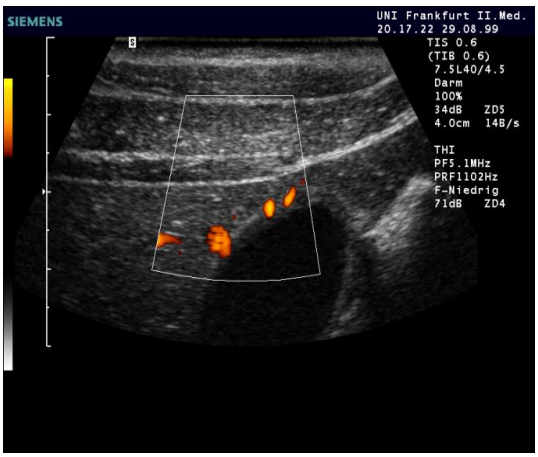

Blood vessels mimicking a simple cyst have to be excluded by CDI to rule out arterioportal venous malformations (Figure 27). On CEUS, cysts show no contrast enhancement at all. As small cysts may be confused with metastases on CEUS, conventional B-mode ultrasound has

to precede CEUS. Cystadenoma are rare neoplastic differential diagnoses of atypical cysts. (Figure 28) [(141)].

Figure 28 Cystadenoma are rare neoplastic differential diagnoses of atypical cysts. Contrast enhancing nodules are indicative for this diagnosis.

a

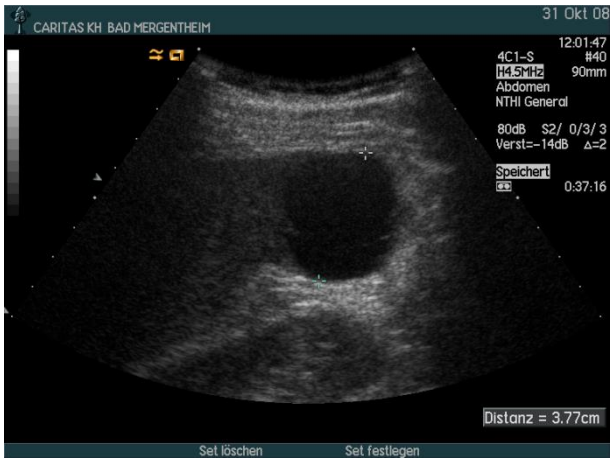

b

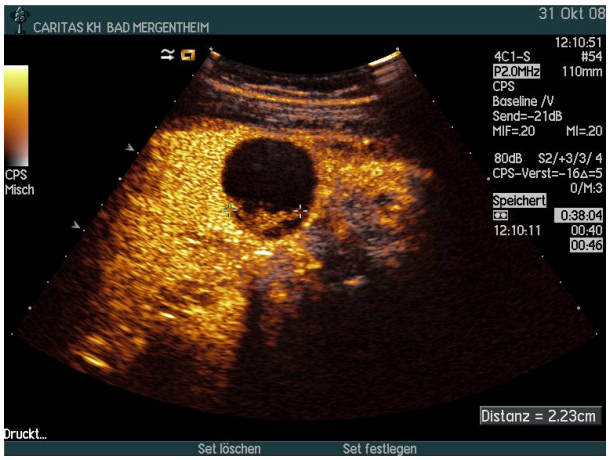

Echinococcosis, Echinococcus cysticus

Gharbi et al (1981) first introduced the widely used and most cited classification of hydatid disease, which has been modified many times. Gharbi Type I cysts consist of pure fluid; Type II have a fluid collection with a split wall; Type III cysts contain daughter cysts (with or

without degenerated solid material); Type IV have a heterogeneous echo pattern; and Type V have a calcified wall. It is important to note that lesions may show different stages of hydatid evolution [(142-145)].

Ultrasound and CEUS are helpful in recognising echinococcosis in all stages. Most useful is the combination of morphological criteria and biological behaviour *e.g.* fertile cysts with viable protoscoleces (Gharbi Type I, II), transitional phase (Gharbi Type III) and inactive cysts that have lost their fertility (Gharbi Type IV, V). Characteristics on ultrasound that are suggestive of an inactive lesion include a collapsing, flattened elliptical cyst (corresponds to low pressure within the cyst), detachment of the germinal layer from the cyst wall ("water lily sign"), coarse echoes within the cyst and calcification of the cyst wall.

The use of a combined classification including imaging criteria and biological evidence of viable parasites will enable clinicians to perform the correct clinical procedures for the different cyst types [(132, 133, 144, 145)].

Type I The most common Type I lesion (50–80%) represents an anechoic smooth, round pure fluid collection without hydatid sand and septa. Containing usually fertile cysts with viable protoscoleces, which can be difficult to distinguish from a benign cyst. The roundish lesion with well-defined borders is characterised by an irregular localised thickened wall (the initial stage of splitting the wall), which should be carefully sought by high frequency, and therefore high resolution probes (7–15MHz), and CEUS, which delineates the nodular appearance very early in the course of the disease.

Type II: Splitting of the wall (infolding of the inner cyst wall resulting in floating membrane, the so-called water lily sign) is typical for Type II fluid-filled lesions also containing fertile cysts, and appears to be the most important and pathognomonic sign of echinococcosis. It is of interest that splitting of the wall to the outer margin (outfolding) is the typical fine nodular appearance with contrast enhancement. When the liver cyst contains membranes and “hydatid sand” mixed echoes will appear, which can be confused with a neoplasm or abscess. The term "hydatid sand" reflects a complex image that consists predominantly of parts of protoscolices (hooklets and scolexes). The finding of mobile sand may be overt and visible when the patient's position is turned, *e.g.* into the standing position.

Type III: When daughter cysts are present, characteristic internal septation is the result. Type III lesions are characterised by septa, which result in a honeycomb appearance with infolding membranes. This stage has been described as transitional, when the integrity of

the cyst has been compromised either by the host or by medical treatment. The “cyst in the cyst sign” occurs by separation of the hydatid membrane from the wall and the hydatid sand in combination with a fine nodular appearance of contrast enhancement are both pathognomonic of echinococcosis. Neoplasia can be ruled out by the exclusion of contrast enhancement within the lesion. In the very early stages of echinococcosis, without calcifications, ultrasound can depict the specific intralesional morphology in detail much earlier than any other imaging modality (Figure 29).

Type IV: Type IV lesions are characterised by a heterogenous echo pattern. The echogenicity of the lesion may be more hypoechoic, but it can also be hyperechoic owing to regressive changes. This stage is unspecific compared with the pathognomonic Stages II and III.

Type V: The Type V pattern reflects a solid heterogeneous mass that is difficult to differentiate from a tumour. An identifiable thickened hyperechoic calcified wall suggests an echinococcal cyst. Cysts with a calcified rim may have a typical "eggshell" appearance. Type IV and V lesions represent inactive cysts with degeneration, which have lost their fertility. Calcification, which usually takes 5 to 10 years to develop, usually occurs with hepatic cysts. Calcifications in pulmonary or bone cysts are more rarely encountered. Total calcification of the cyst wall suggests that the cyst is non-viable [see also the chapter on tropical disease in which the more recently WHO-classification is described].

Figure 29 Echinococcosis stage in this patient is characterised by multiloculated cysts in a honeycomb appearance with infolding membranes (a). Calcifications are difficult to recognise. The contrast enhanced image (b) does not show any enhancement [(143)]. See also cases of the month [http://www.efsumb-archive.org/asp/detail06.asp?ref=347&url=/case-month/cm-archive.asp?ref=1].

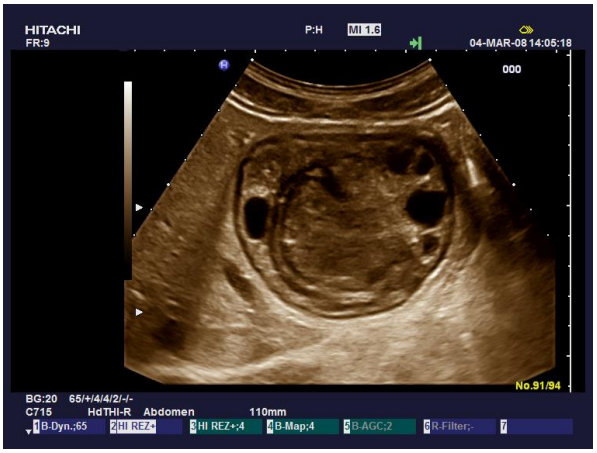

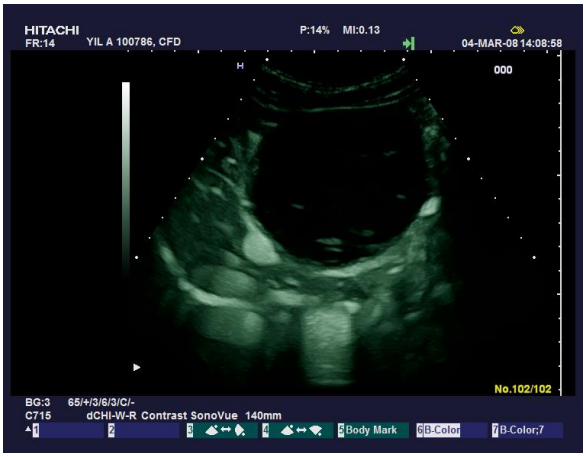

Calcification

Calcifications are characterised as hyperechoic structures, which normally show acoustic shadowing distally owing to reflection/attenuation of the ultrasound (Figure 30).

Figure 30 **Calcifications within the liver. The mirror artefact owing to the acoustic impedance characteristics of the lower lung surface is also shown [(82, 146-150)]. Distinct changes of the transducer position show a different kind of mirror artefact (a-c).**

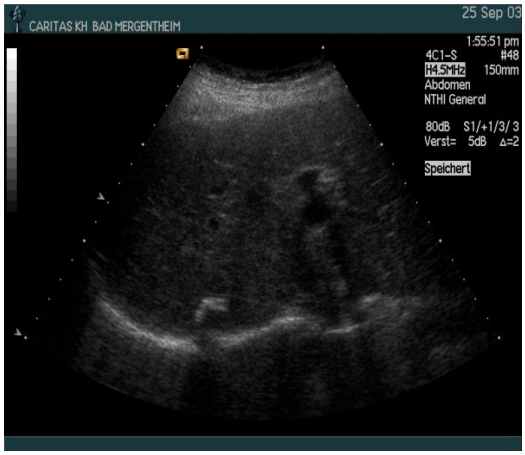

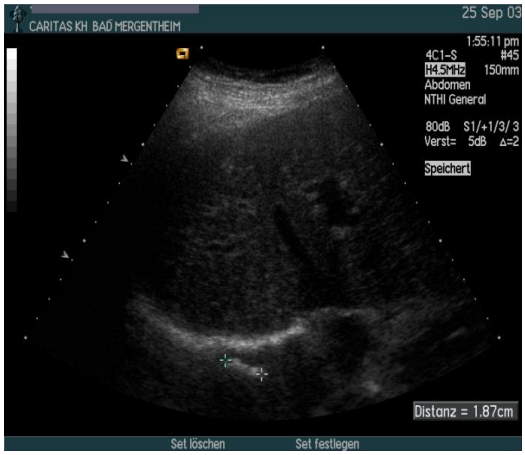

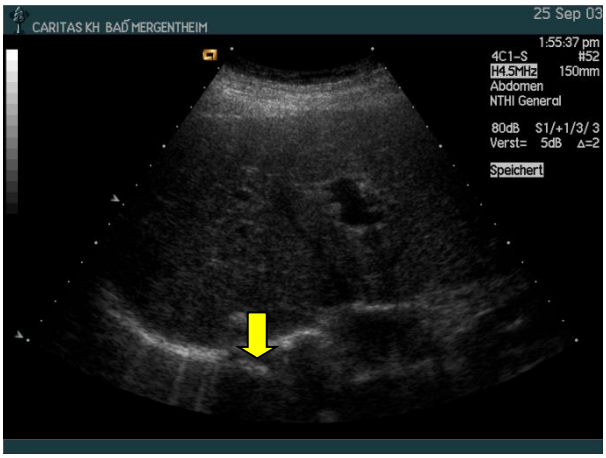

Haemangioma

Hepatic haemangiomas are known to be the most common benign liver tumour, with an incidence at autopsy and imaging studies of up to 7% (Figure 31-33). Up to 10% of patients with haemangiomas cannot be reliably diagnosed using imaging methods. In these patients only ultrasound guided liver biopsy and examination of the specimen is required for a final diagnosis usually in patients with malignant underlying disease. A retrospective study, of percutaneous biopsies of 38 patients (1 cm to 13.5 cm; mean 3 cm) with suspected haemangioma using 20 gauge needles, reported that it is safe and effective for establishing a diagnosis of haemangioma.

Conventional B-mode ultrasound

Most haemangiomas demonstrate typical sonomorphological features in conventional B-mode ultrasound. They are characterised as less than 3 cm in diameter, lobulated with a well-defined outline, located adjacent to liver vessels, demonstrate an hyperechoic texture and occasionally posterior acoustic enhancement owing to blood filled capillaries (Table 2).

Table 2 Typical haemangioma: diagnostic criteria

B-mode criteria
Less than 3 cm in diameter
Hyperechoic structure
Homogeneous inside
Round or slightly oval shape
Smooth outline
Absence of any halo sign
Possible detection of feeding and draining vessel
Absence of any signs of invasive growth
Posterior acoustic enhancement

Colour Doppler imaging

Although haemangiomas are highly vascularised masses, from a histopathological perspective, they essentially consist of a large number of capillary-sized vessels and so, even with the use of high-end ultrasound systems, conventional colour Doppler ultrasound often detects little or no blood flow inside the haemangioma because the blood flow velocity in the capillary haemangioma is too slow. The supplying and draining vessels ("feedings vessels") may be visualised (depending on the ultrasound systems performance) at the edge of the lesion.

Contrast enhanced ultrasound

CEUS has markedly improved the correct diagnosis of haemangioma, which is now possible in approximately 95% of patients. CEUS demonstrates typical haemangioma imaging characteristics, *i.e.* peripheral nodular contrast enhancement and the iris diaphragm sign in a high percentage of patients with an undetermined lesion. Difficult differential diagnoses include shunt haemangioma (synonymous high-flow haemangioma, which might be confused with FNH when small); HCA; or HCC. A thrombosed haemangioma might be confused with a metastasis by demonstrating a contrast sparing in the arterial and portal venous phase.

Arterioportal shunts

Arterioportal shunts associated with hepatic tumours have been reported primarily in patients with malignant tumours, especially in advanced HCC with portal vein invasion. However, arterioportal shunts have been observed in hepatic haemangiomas not only using CEUS but also on multiphase helical CT and MRI. One possible explanation for rapidly enhancing small haemangiomas is a hyperdynamic status with large arterial inflow, rapid tumoural enhancement, and consequently, large and rapid outflow, which seems to result in early opacification of the draining portal vein via shunts. Shunt haemangiomas are typically surrounded by focal hypoechoic areas representative of less fat content in comparison with the surrounding liver parenchyma [(46)]. The metabolic changes are explained by a mainly

arterial blood supply of the hypoechoic areas, whereas blood supply of the surrounding liver parenchyma is mainly by portal venous vessels, which contain more lipids possibly due to a higher concentration of insulin (Figure 33). See also cases of the month [http://www.efsumb-archive.org/asp/detail06.asp?ref=289&url=/case-month/cm-archive.asp?ref=1].

Figure 31 Haemangioma. Haemangioma in B-mode between markers (a). The typical contrast enhanced ultrasound findings are peripheral nodular contrast enhancement and centripetal fill-in ("iris diaphragm phenomenon") with the exception of thrombosed areas and calcifications (shown between callipers (+)) [b-d] (see also cases of the month, www.EFSUMB.org).

a

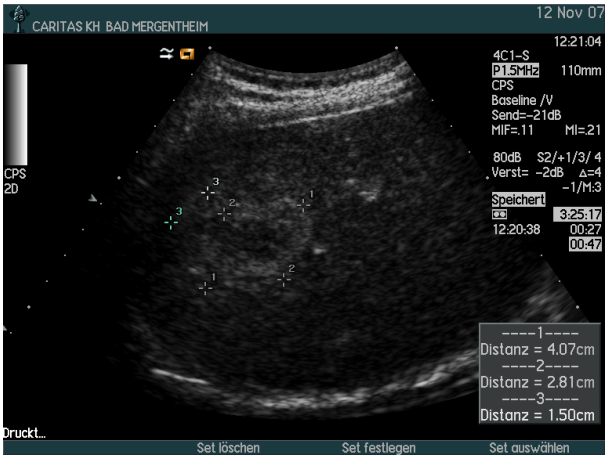

b

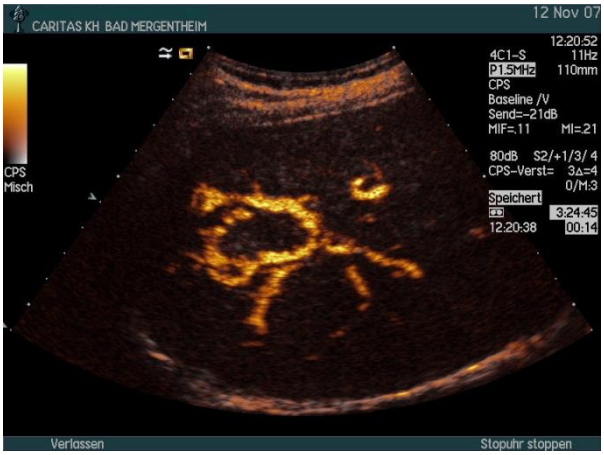

c

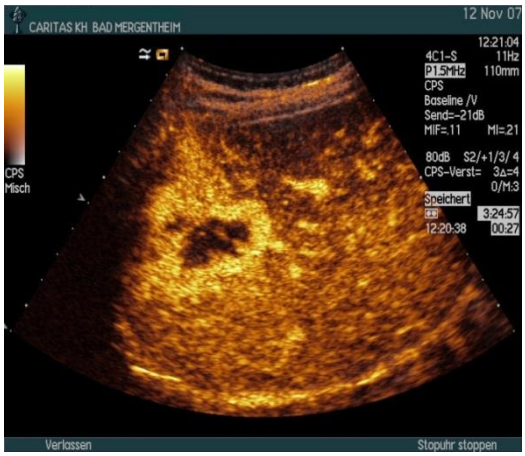

d

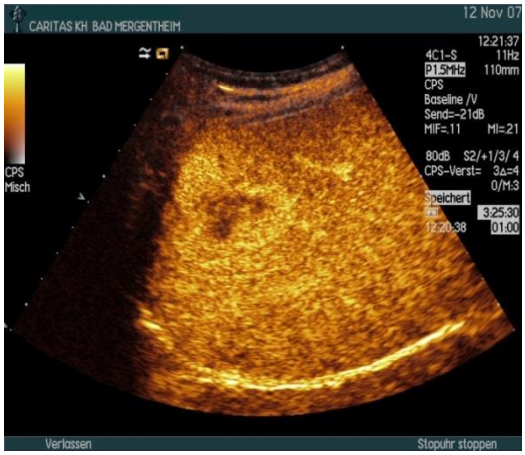

Figure 32 Haemangioma. (a) The typical B-mode appearance is hyperechoic, which is also seen in liver cirrhosis. Contrast enhanced ultrasound findings are peripheral nodular contrast enhancement and centripetal fill in with the exception of thrombosed areas and calcifications (iris diaphragm phenomenon) (b,c) (see also cases of the month, www.EFSUMB.org).

a

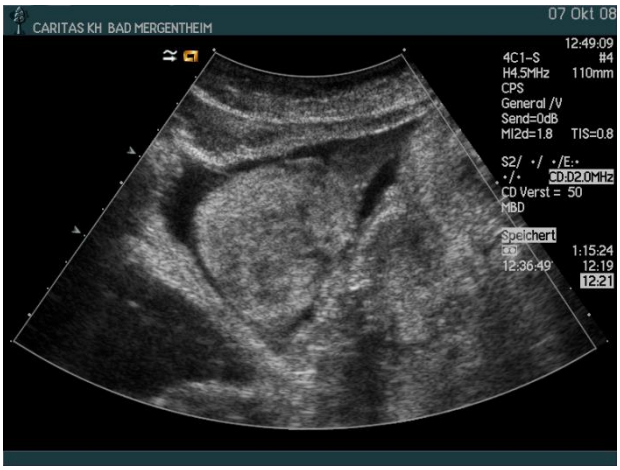

b

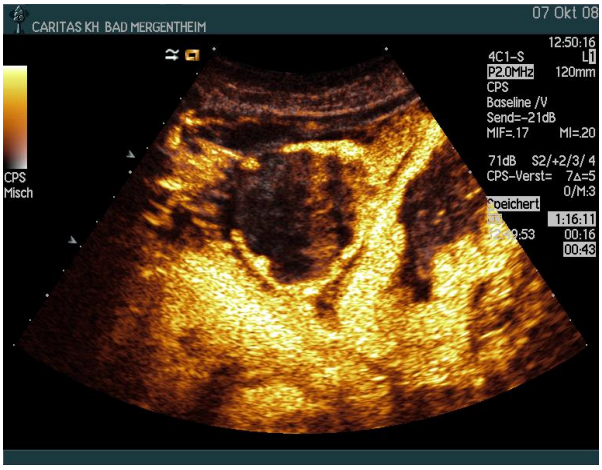

c

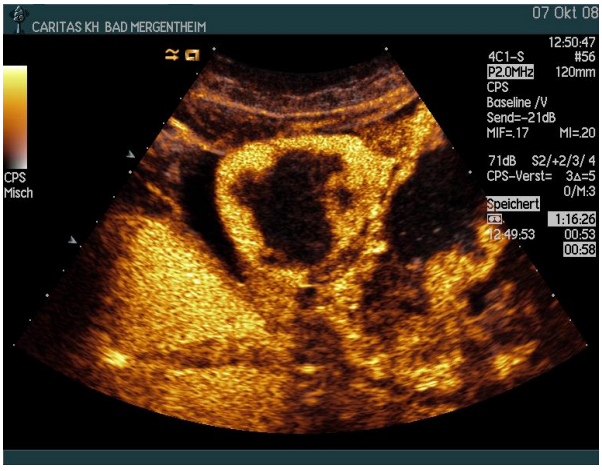

Figure 33 **Shunt haemangioma. (a) Focal hypoechoic and hyperechoic lesions are sub-capsular with inhomogenous echogenicity. Colour and power Doppler imaging were not helpful. The real lesion is shunt haemangioma (shown between**

callipers (+)) with arterioportal venous shunts (shunt haemangioma) leading to regional inhomogeneous fat content. (b,c) The typical contrast enhanced ultrasound finding is centripetal fill-in within seconds and bright appearance in the portal venous phase. The lesions are often missed by CT and MRI because of their small size (typically less than 15 mm) and differences in the arterial enhancement pattern in comparison with the surrounding parenchyma for only 1-2 s. The final diagnosis is made by histology in patients with malignant underlying disease [(46)] (see also cases of the month, www.EFSUMB.org).

a

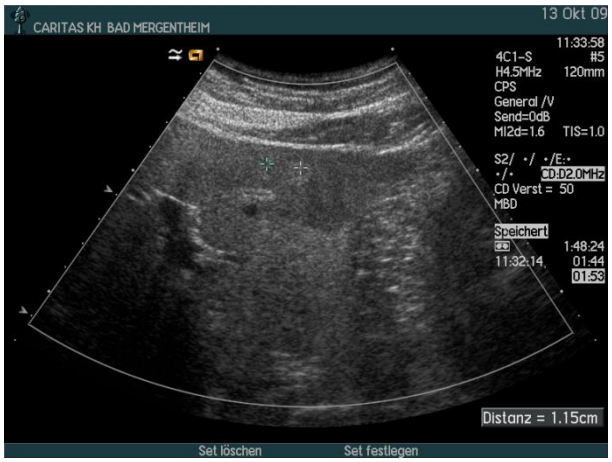

b

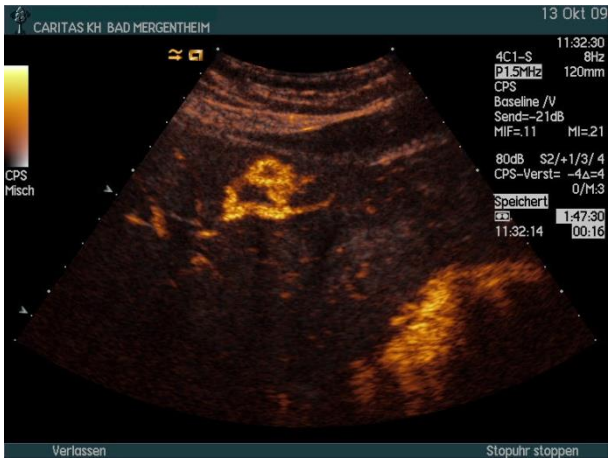

c

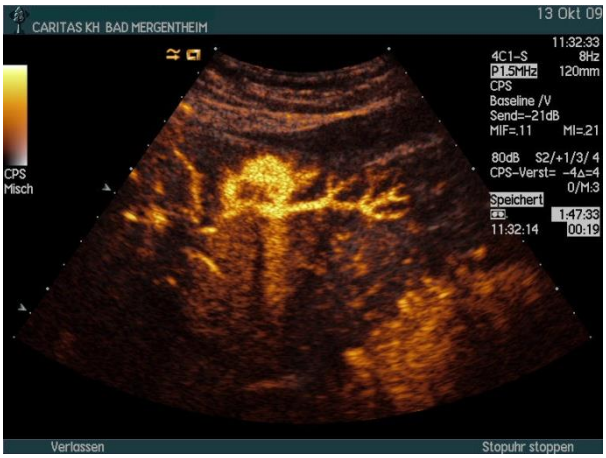

Focal nodular hyperplasia

FNH and the important differential diagnosis of HCA are two benign, mostly incidental, hepatic neoplasias, which occur predominantly in young and middle-aged women. Differentiation is essential because of the different therapeutic approaches; HCA is an indication for surgery because of the risk of haemorrhage and potential malignant transformation, in contrast FNH can be managed conservatively. Until recently non-invasive differentiation of, especially, atypical FNH from HCA and other benign or malignant neoplasia has remained challenging; there have been no satisfactory tests apart from histological examination of a liver biopsy sample. Histological features of FNH are controversial in the literature. Congenital absence of portal veins has been reported in a few patients, mainly children.

Helical CT and MRI do provide some useful information in the diagnosis of FNH, especially when the lesion depicts typical features, such as a central scar and uniform hypervascularity. Typical features are only reported in approximately 50% of patients. In a series of 305 macroscopically studied FNH, a central scar was found in only approximately 50% [(151)].

Conventional B-mode ultrasound

FNH is typically an isoechoic tumour of variable size, with a central scar and calcifications (in 50–80%).

Colour Doppler imaging

Typically, CDI reveals an arterially hypervascularised tumour (in >90%) with characteristic (para-) central arterial blood supply. In many patients, increased blood flow compared with the surrounding liver tissue can be detected even in colour Doppler mode, which causes a so-called wheel-spoke phenomenon. Inter-observer reliability in recognising the wheel-spoke appearance is low.

Contrast-enhanced ultrasound

The examination of the hepatic arterial and portal venous/sinusoidal phase by contrast-enhanced phase inversion ultrasound allows for a reliable differentiation between FNH and HCA. This important finding can be explained by the lack of portal veins in contrast with FNH, which presents (atypical) portal veins in many but not all patients.

In contrast enhanced examination, FNH typically appears as a hyperperfused tumour-like lesion relative to the surrounding liver tissue in the early arterial phase. The lesion's hyperenhancement is easily visible with contrast enhancement during continuous scanning, compared with the surrounding hepatic arteries. Depending on the patient's cardiac output, some 8 to 20 s after injection of the echo-signal enhancer into the cubital vein there is a rapid take-up of the substance with demonstration of the arterial vascular pattern and enhancement from the centre outwards. During the portal venous phase FNH is isoechogenic with the portal vein, and, therefore, slightly hyperenhancing in comparison with the surrounding liver parenchyma [(140)] (Figure 34). See also the EFSUMB cases of the month [http://www.efsumb-archive.org/asp/detail06.asp?ref=291&url=/case-month/cm-archive.asp?ref=1].

Figure 34 (a) Focal nodular hyperplasia (FNH) using B-mode ultrasound often appears as isoechoic in comparison with the surrounding liver parenchyma and cannot be differentiated from malignant tumours such as hepatocellular carcinoma. (b-e) FNH in the arterial phase typically appears as a hypervascular and hyperperfused structure relative to the surrounding liver tissue demonstrating the typical central artery in up to 70% of cases, whereas in larger FNH more

than one supply artery can be displayed (indicated by numbers). During the portal venous phase FNH is slightly hyperechoic in comparison with the surrounding liver parenchyma in more than 90% of lesions. The typical central scar (arrow, f) can be found in up to 70% of patients with FNH, which has been proven in autopsy studies [(26, 140, 151)] (see also cases of the month, www.EFSUMB.org).

a

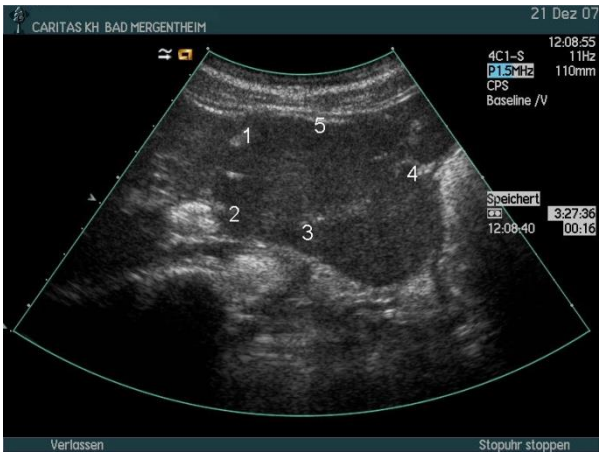

b

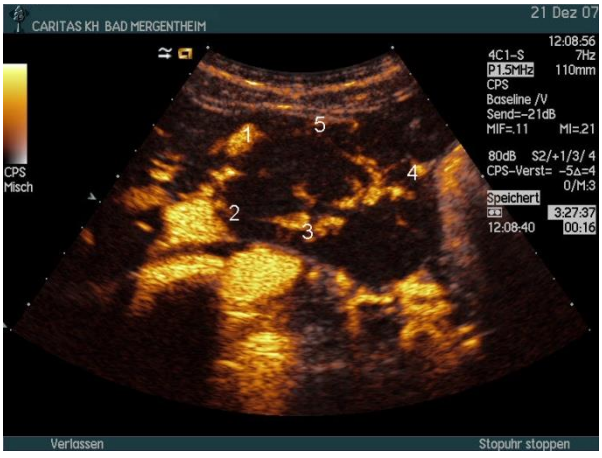

c

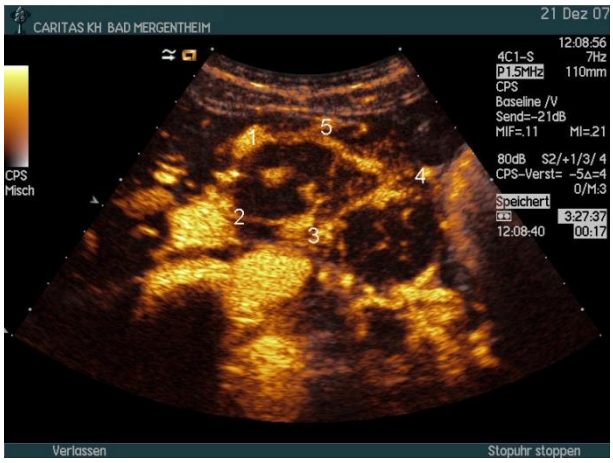
CARITAS KH BAD MERGENTHEIM
21 Dez 07
12:08:56
4C1-S
7Hz
P1.5MHz
110mm
CPS
Baseline /V
Send=-21dB
MIF=.11
MI=.21
80dB S2/+1/3/ 4
CPS-Verst= -5Δ=4
0/M:3
Speichert
3:27:37
00:17
12:08:40
CPS
Misch
1
2
3
4
5
Verlassen
Stopuhr stoppen

d

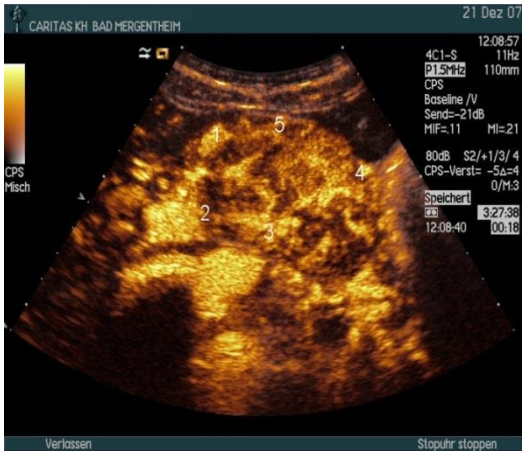
CARITAS KH BAD MERGENTHEIM
21 Dez 07
12:08:57
4C1-S
11Hz
P1.5MHz
110mm
CPS
Baseline /V
Send=-21dB
MIF=.11
MI=.21
80dB S2/+1/3/ 4
CPS-Verst= -5Δ=4
0/M:3
Speichert
3:27:38
00:18
12:08:40
CPS
Misch
1
2
3
4
5
Verlassen
Stopuhr stoppen

e

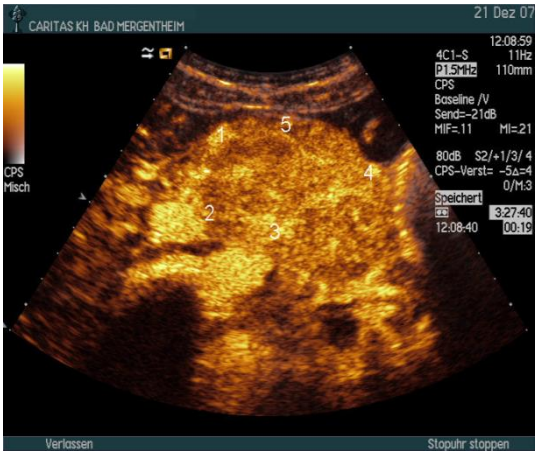
CARITAS KH BAD MERGENTHEIM
21 Dez 07
12:08:59
4C1-S
11Hz
P1.5MHz
110mm
CPS
Baseline /V
Send=-21dB
MIF=.11
MI=.21
80dB S2/+1/3/ 4
CPS-Verst= -5Δ=4
0/M:3
Speichert
3:27:40
00:19
12:08:40
CPS
Misch
1
2
3
4
5
Verlassen
Stopuhr stoppen

f

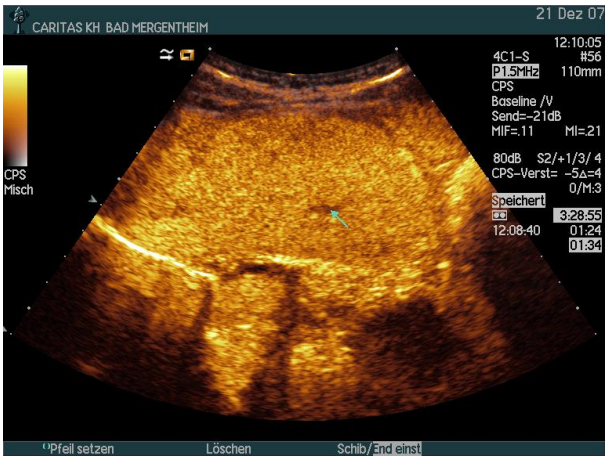

Hepatocellular adenoma

Conventional B-mode ultrasound

In B-mode ultrasound, of an otherwise normal liver, HCA is usually isoechogenic with the surrounding liver tissue. Owing to this lack of echogenicity, an adenoma can be very difficult to differentiate from the surrounding liver tissue. In a fatty liver, adenomas may be poorly echogenic, whereas in patients with storage diseases (*e.g.* glycogenosis or Niemann-Pick disease) adenomas may give stronger echoes (hyperechoic) [(152)]. A rounded contour or a vascular impression may indicate a tumour poorly discernable from liver parenchyma. There are no other typical criteria in B-mode ultrasound.

Colour Doppler imaging

HCA exhibit predominantly marginal arterial hypervascularity, which can be shown by CDI and CEUS. However, this vascular pattern can also be encountered in HCC and hyperperfused metastases, and is therefore not pathognomonic. Calcifications and other regressive changes are observed depending on the size of the lesion.

Contrast enhanced ultrasound

Histologically no portal veins (and in addition, no bile ducts) are present in adenomas, therefore, CEUS demonstrates only homogeneous enhancement during hepatic arterial

phase (8 to 25 s after injection) but no portal venous enhancement (Figure 35) resulting in slightly hypoenhancing (hypoechoic) appearance in comparison with the surrounding liver parenchyma since some overlap of the arterial and capillary phase (continuing over some minutes) may be observed [(140)].

Figure 35 Hepatocellular adenoma (HCA). (a) B-mode ultrasound shows an unspecific slightly hyperechoic focal liver lesion. (b, c) Contrast enhanced ultrasound (CEUS) revealed only arterial phase enhancement after administration of SonoVue®. (d) At the end of the arterial phase (<30 s after administration of SonoVue®) a hypoechoic liver tumour was detected on CEUS, which is the typical enhancement pattern of HCA in comparison with focal nodular hyperplasia (FNH), which showed more portal venous enhancement than the surrounding liver parenchyma in 96% of patients with FNH [(153, 154)].

a

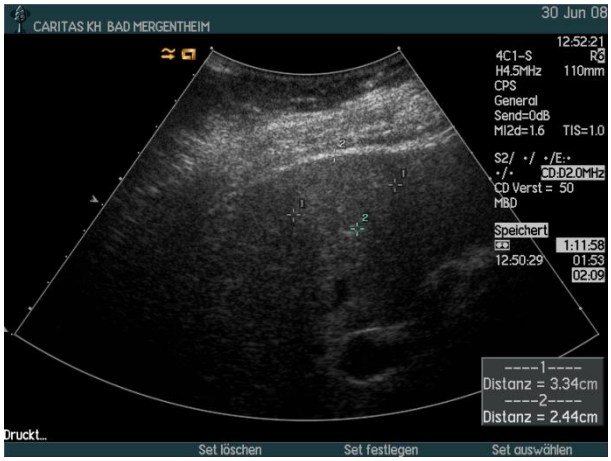

b

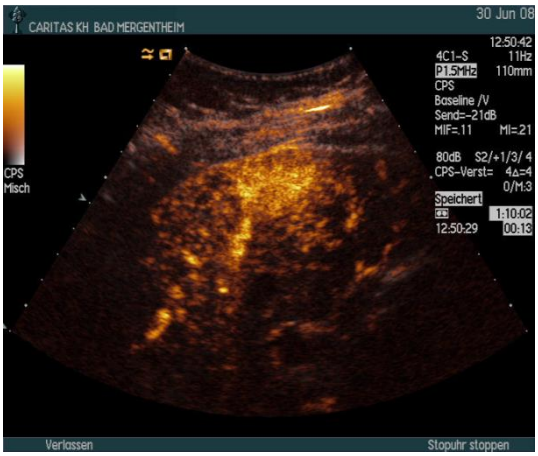
CARITAS KH BAD MERGENTHEIM
30 Jun 08
12:50:42
4C1-S 11Hz
P1.5MHz 110mm
CPS
Baseline /V
Send=-21dB
MIF=.11 MI=.21
80dB S2/+1/3/ 4
CPS-Verst= 4Δ=4
0/M:3
Speichert
1:10:02
12:50:29 00:13
CPS
Misch
Verlassen
Stopuhr stoppen

c

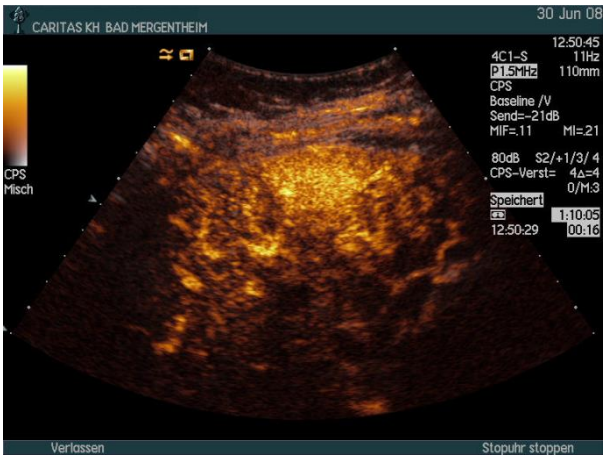
CARITAS KH BAD MERGENTHEIM
30 Jun 08
12:50:45
4C1-S 11Hz
P1.5MHz 110mm
CPS
Baseline /V
Send=-21dB
MIF=.11 MI=.21
80dB S2/+1/3/ 4
CPS-Verst= 4Δ=4
0/M:3
Speichert
1:10:05
12:50:29 00:16
CPS
Misch
Verlassen
Stopuhr stoppen

d

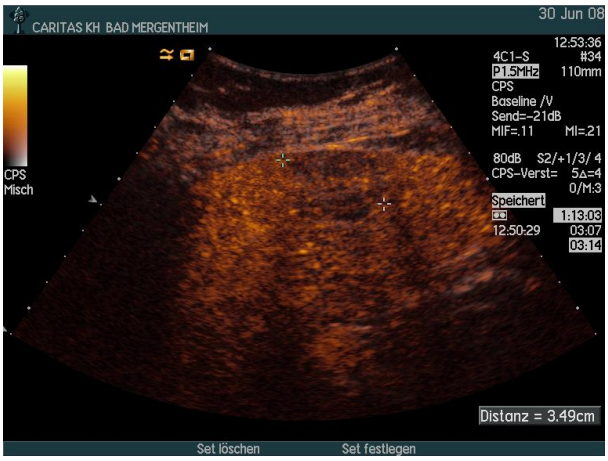
CARITAS KH BAD MERGENTHEIM
30 Jun 08
12:53:36
4C1-S #34
P1.5MHz 110mm
CPS
Baseline /V
Send=-21dB
MIF=.11 MI=.21
80dB S2/+1/3/ 4
CPS-Verst= 5Δ=4
0/M:3
Speichert
1:13:03
12:50:29 03:07
03:14
CPS
Misch
Distanz = 3.49cm
Set löschen
Set festlegen

Differential diagnosis

Hepatic adenomas are frequently seen in patients with glycogen storage disease (GSD 1), but their pathogenesis is not understood. Glucagon/insulin imbalance, cellular glycogen overload and proto-oncogene activation have been suggested as possible mechanisms.

Hamartoma of the liver

Conventional B-mode ultrasound

In grey-scale ultrasound hamartomas may have different appearances depending on their histopathology and size. They may be single or multiple. Hamartomas are described as hyperechoic (when mostly solid) or presenting mixed echogenicity with cystic components or purely anechoic (cystic). In a fatty liver they can be hypoechoic. In most reported cases hamartomas are small (< 5 mm in diameter) hyperechoic lesions, some presenting the "comet tail" artefact. However in children where they are usually large and fast growing lesions are easily detected. Because of their non-specific image appearances they can mimic a wide range of focal liver lesions from haemangiomas, cysts to metastases or HCC in cirrhotic liver.

Colour Doppler imaging

In most cases hamartomas do not exhibit any flow signal but in rare cases one vessel can be spotted. Large lesions often displace surrounding structures, thus modelling of the liver parenchymal vessels may be visible. In fast growing hamartomas exceeding 10 cm in diameter disturbances of venous flow is observed, including the signs of portal hypertension.

Contrast enhanced ultrasound

There is no consistent CEUS enhancement pattern. Some lesions show no enhancement in either of vascular phases, some enhance like surrounding liver parenchyma and occasionally some of them show bright and early enhancement in the arterial phase with gradual decrease of intensity consistent with liver parenchyma. In the single article authors

described one feeding vessel visible in arterial phase. Concerning the pattern of hamartoma enhancement malignancy may be excluded in most cases.

Focal fatty lesion (regional focal fatty infiltration)

Fatty infiltration was generally considered to be a diffuse process involving the entire liver. Since Brawer and Scott identified focal hepatic fatty infiltration at autopsy and in imaging studies in 1980, focal hepatic fatty infiltration has been widely discussed [(45)]. Bright focal areas in the liver hilum occur in >40% of inflammatory bowel disease patients while taking corticosteroid medication. The histological nature of these corticosteroid derived lesions is not yet clear. Different amounts or types (large, small vacuoles) of fat deposition are likely, because a change of appearance over time can be observed. Changes in arterioportal venous perfusion have been suggested. Haemangiomas may mimic such lesions; however, not all bright lesions in the liver are haemangiomas. It is well known that the vascular supply of the hilar region in liver segment IV differs from the perfusion of liver tissue adjacent to the gallbladder. This could give a possible explanation for different reactions of liver parenchyma to fatty infiltration. In patients with focal fatty lesions, depending on the quality of the equipment used, we observed centrally located arterial blood supply and direct venous drainage into the liver hilum.

Conventional B-mode ultrasound

Fatty infiltration may affect the liver diffusely or focally, but it does not usually cause any mass effect or displace vessels. Sonographically, hepatic fatty infiltration appears as segmental or lobular areas of brighter echogenicity, in contrast with the echogenicity of the normal liver parenchyma. A central, perihilar location in segment IV or V is typical, other locations are rarely involved.

An oval shaped hypoechoic lesion in the liver hilum is always related to a fatty liver and could represent normal liver tissue surrounded by diffuse fatty infiltration of the liver. A hypoechoic lesion in the liver hilum without signs of expansion seem to be a relevant sign of fatty liver and should not be confused with mass lesions. The typical relationship to fatty liver, location and shape are all helpful in differential diagnosis [(37, 45)].

Colour Doppler imaging

In colour Doppler ultrasound, both focal fatty degeneration and its focal absence appear normal; neither hyper- nor hypoenhancement is apparent, since the liver tissue is normal. Typically, central feeding and draining vessels may be detected in a high percentage of patients demonstrating the pathogenetic mechanism of different vascularisation of the liver hilum.

Contrast enhanced ultrasound

CEUS is helpful to rule out malignant infiltration. In the arterial and venous phase the supplying and draining vessels of the liver hilum can be imaged. In the enhanced echo-signal sequence, different fatty degeneration regions are imaged in the same way as normal liver tissue in the portal venous phase. Therefore, in the portal venous phase these lesions are indistinguishable from the background. Enhancement in the arterial phase might be slightly delayed in comparison with the surrounding liver parenchyma.

Hepatocellular carcinoma

Conventional B-mode ultrasound

There are no typical criteria in B-mode ultrasound in small HCC (<30 mm). Sonographic recognition of HCCs in liver cirrhosis can be difficult if the echo-texture is very inhomogeneous [(27, 155)]. Echogenicity of the lesion depends on its size and the surrounding liver tissue (cirrhotic *vs* non-cirrhotic) (Figure 36-37). HCC in an otherwise normal liver parenchyma is usually iso- or slightly hypoechoic compared with the surrounding liver tissue. HCC can be very difficult to identify in patients with liver cirrhosis and tumour morphology can be iso-, hypo- or hyperechoic. Dysplastic nodules are sometimes difficult to differentiate.

Colour Doppler imaging

HCC are, in most cases (80–90%), distinctly hypervascularised using conventional CDI (Figure 36) and are mainly peripherally located. In such cases, it is possible to confuse them with

other hyperperfused liver tumours; however, these are rarely observed in a cirrhotic liver [(57)]. From a differential diagnostic point of view it is then necessary to consider metastases of hyperperfused tumours, *e.g.* a hypernephroma, breast carcinoma, lung cancer or more typical neuroendocrine metastases. Metastases of primary extrahepatic tumours are, however, rare in a cirrhotic liver except of neuroendocrine origin.

Figure 36 More common, hypoechoic hepatocellular carcinoma with typically peripheral located hypervascularity using colour Doppler imaging.

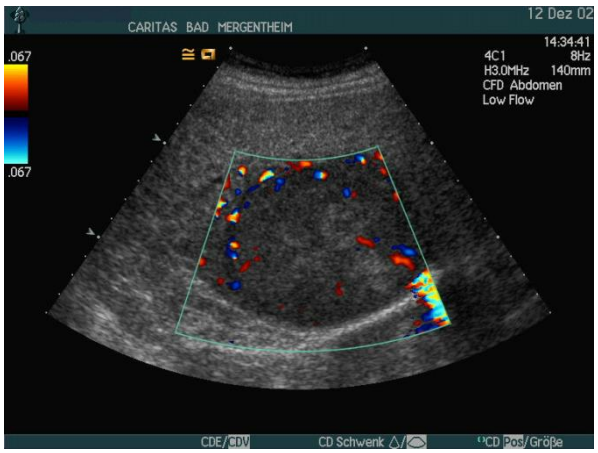

Contrast enhanced ultrasound

HCC typically exhibits arterial hyperenhancement of the tumour compared with the surrounding liver tissue and mild and late portal venous wash out. In the HCC a typically chaotic vascular pattern is observed, which is a sign of neovascularisation of the tumour. Regenerative and dysplastic nodules may also exhibit arterial enhancement. Analysis of the portal venous phase makes it often possible to differentiate these isoenhancing nodules from the weakly contrasting HCC.

LI-RADS categorization

The American College of Radiology (ACR) endorsed the Liver Imaging Reporting and Data System (LI-RADS) for standardized reporting and data collection of computed tomography

(CT) and magnetic resonance (MR) imaging for hepatocellular carcinoma (HCC) in high-risk patients (liver cirrhosis). The LI-RADS imaging criteria are used to classify ‘observations’ from 'definitely benign' (LR-1) to 'definitely HCC' (LR-5) based on imaging criteria [(156-159)].

The following CEUS diagnostic criteria are used for LI-RADS characterization [(156, 157, 159-161)]:

- *Size*. The largest dimension of the liver nodule detected on B-mode ultrasound.
- *Arterial phase enhancement.* The arterial phase enhancement of a liver nodule assessed by comparing the intensity of the signal from a liver nodule with the signal intensity from adjacent liver at the same depth during the peak of arterial phase enhancement (20-40 sec after contrast injection).
    - The type of arterial phase enhancement should be characterized using one of four possible descriptors:
        - *Hyperenhancement:* higher contrast agent signal intensity in the liver nodule or observation as compared with the intensity in the adjacent liver.
        - *Isoenhancement:* equivalent contrast agent signal intensity in the liver nodule as compared with the adjacent liver.
        - *Hypoenhancement:* less contrast agent signal intensity in the liver nodule as compared with the adjacent liver.
        - *No-enhancement:* lack of contrast agent signal in the liver nodule.
- *Washout*: Visually assessed reduction in contrast agent signal intensity in a nodule relative to the adjacent liver over time, following initial enhancement, resulting in hypoenhancement. The characterization of the timing and degree of washout should be assessed.
    - *Timing of washout onset*. Timing of the first observation of unequivocal washout, reported in seconds after contrast bolus injection.
    - *Washout degree*:
        - *Mild washout* used when a liver nodule becomes hypoechoic relative to the liver but continues to show some contrast enhancement.
        - *Marked washout* used when a focal liver nodule appears virtually devoid of contrast agent signal (“punched out”) at a time when the surrounding parenchyma is overtly enhanced. It will look black on CEUS imaging.

The key feature of CEUS in the diagnosis of HCC in liver cirrhosis is the detection of hyperenhancement of the nodule in comparison to the surrounding parenchyma in the arterial phase (whole or in part, not globular or rim-like), followed by washout in the late phase (late in onset ≥ 60 sec and mild in degree), when the nodule becomes hypoenhanced in comparison to the surrounding parenchyma. This pattern is categorized as LR-5 and is considered diagnostic for HCC. LR-4 indicates a high probability of HCC, whereas LR-3 suggests an intermediate probability of HCC. Thus patients are managed accordingly to the LR category, keeping in mind that in both cases of LR4 and LR3 there is a substantial probability that the lesion is actually an HCC and hence, if the diagnosis is not solved by alternative imaging modalities, histological confirmation may be considered [(156, 157, 159-161)].

CEUS LR-1 (definitely benign)

A liver nodule categorized as LR-1 has imaging features diagnostic of a definitely benign entity. There should be 100% certainty that the observation is benign. LR-1 applies to simple cysts, classic haemangiomas, and some cases of focal fat deposition or sparing; also a previously seen observation that demonstrates definite spontaneous disappearance at follow up may be categorized as LR-1. Observations interpreted as focal hepatic fat deposition or focal hepatic fat sparing can only be categorized as LR-1 if the CEUS features are unequivocal and/or if the diagnosis was previously confirmed at CT or MR. If there is any uncertainty in the diagnosis, it should be categorized as LR ≥2 according to the approved algorithm.

CEUS LR-2 (probably benign)

A liver observation categorized as LR-2 has imaging features that are probably benign, with high likelihood that nodule is benign. When in doubt it is recommended to categorize a lesion as LR3 rather than LR2.

Examples of LR-2 lesions include:

- Distinct solid nodules < 10 mm with isoenhancement in all phases.
- Not a distinct solid nodule of any dimension with isoenhancement in all phases.

- Nodules previously categorized as CEUS LR-3, and stable dimension for 2 years or longer.

CEUS LR-3 (intermediate probability for HCC)

A liver observation categorized as LR-3 demonstrates imaging features with intermediate probability for HCC. Both HCC and benign entities may be considered as intermediate probability.

Examples include

- ≥ 10 mm distinct solid nodule with arterial phase isoenhancement without washout of any type.
- Any size distinct solid nodule with arterial phase hypoenhancement without washout of any type.
- < 20 mm distinct solid nodule with arterial phase iso- or hypoenhancement and mild/late washout.
- < 10 mm distinct solid nodule with arterial phase hyperenhancement (in whole or in part, not rim or peripheral discontinuous globular enhancement) and without washout of any type.

CEUS LR-4 (probably HCC)

A liver observation categorized as LR-4 demonstrates imaging features probably indicating HCC (nodule is probably HCC but there is not 100% certainty of malignancy).

- ≥ 20 mm distinct solid nodule with arterial phase hypo- or isoenhancement with mild and late washout.
- < 10 mm distinct solid nodule with arterial phase hyperenhancement (in whole or in part, not rim or globular peripheral enhancement) with mild and late washout.
- ≥ 10 mm distinct solid nodule with arterial phase hyperenhancement (in whole or in part, not rim or peripheral discontinuous globular enhancement) without washout of any type.

CEUS LR-5 (definitely HCC)

A liver observation categorized as LR-5 has imaging features indicating it is definitely HCC (100% certainty nodule is HCC). The criteria are a distinct solid nodule ≥ 10 mm with arterial phase hyperenhancement (in whole or in part, not rim or peripheral discontinuous globular enhancement) with mild and late washout (Figure 37).

Figure 37 Typical HCC in liver cirrhosis with hyperenhancement of the nodule in comparison to the surrounding parenchyma in the arterial phase (a-d, 26 (a), 30 (b), 40 (c), and followed by mild washout 95 seconds after injection (d) [LR-5]. Non-enhancing areas, likely reflecting necrotic zones, are also present [(160)].

a

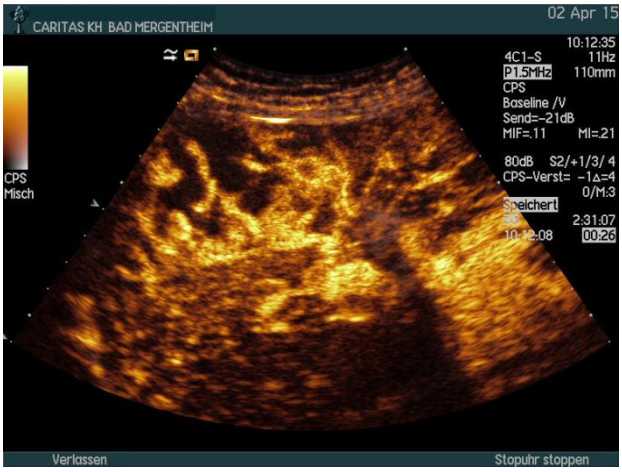

b

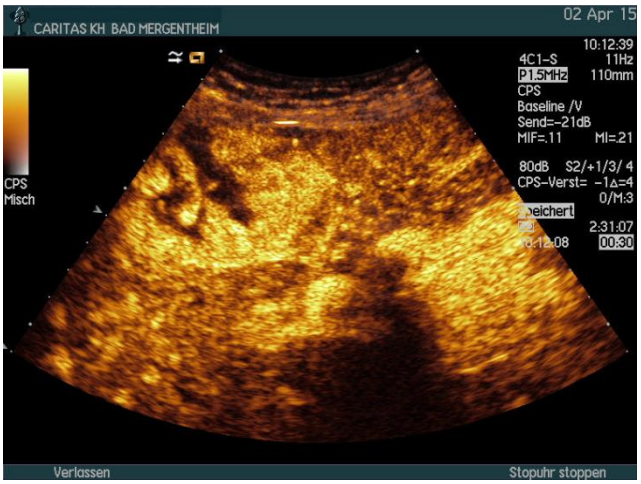

c

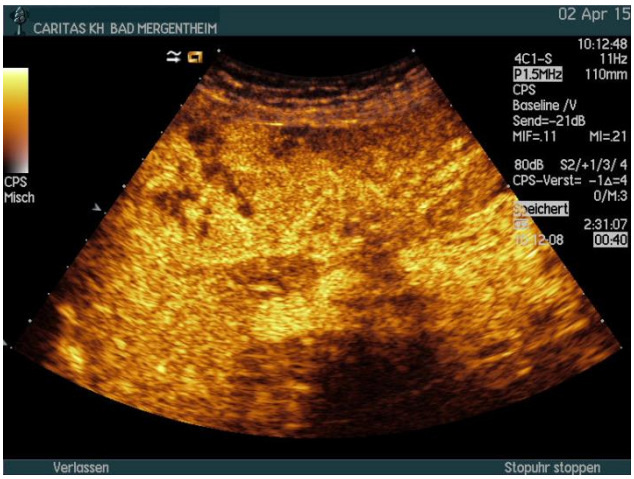

d

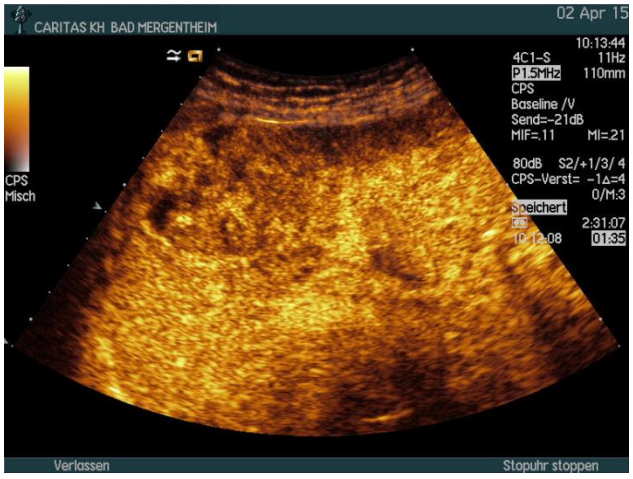

LR-5V (definite tumour in vein)

Liver observation categorized as LR-5V have imaging features indicating there is definite tumour in vein (100% certainty there is tumor within the vein). The criteria are definite enhancing soft tissue in vein regardless of visualization of parenchymal mass/nodule. Late wash-out is often seen as well. Conventional B-mode features often observed in tumour in vein instance are disruption of portal vein walls by the tumour and mass forming aspect of the thrombus (Figure 38) [(160)].

Figure 38 Typical HCC in liver cirrhosis with definite tumor in vein (a) and arterial phase enhancement of the portal vein thrombosis (b, PVT) followed by wash-out in the late phase (c).

a

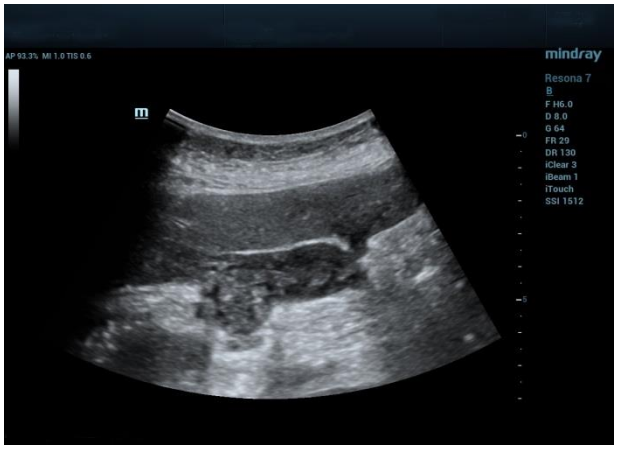

b

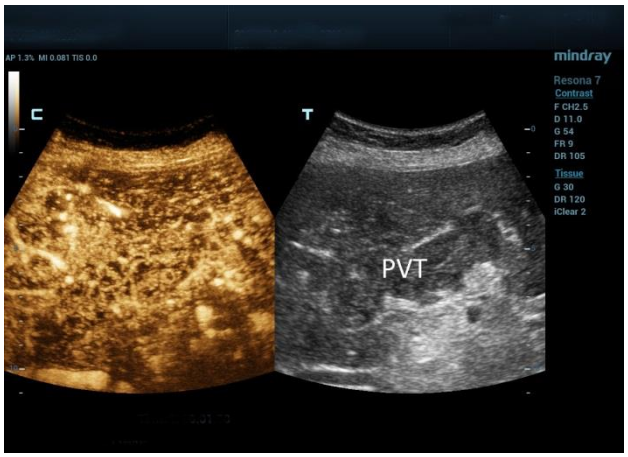

c

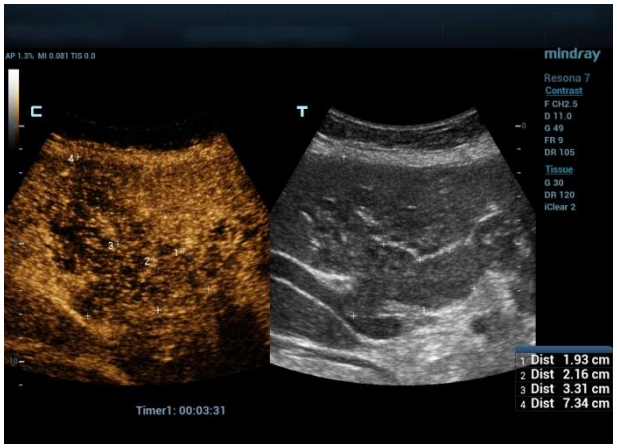

LR- M (nodule is malignant, but not specific for HCC)

Liver observations categorized as LR-M have malignant imaging features not specific for HCC (nodule is malignant, but not specific for HCC). The criteria are a distinct solid nodule with at least some enhancement in the arterial phase (regardless of morphological pattern or degree) with either or both of the following:

- Early washout relative to the liver parenchyma within 60 seconds of contrast injection.
- Marked washout resulting in a “punched out” appearance.

LR-M is defined by variable arterial phase enhancement including diffuse hyperenhancement, diffuse hypoenhancement, and most often rim enhancement (in the case of metastases and cholangiocarcinoma). The most important characteristic, however, is the washout pattern, showing early onset at <60 s and/or reaching marked or punched out appearance.

Cholangiocellular carcinoma

Conventional B-mode ultrasound

CCC can occur along the bile duct in the liver hilum as so-called Klatskin tumours (the hilar CCC is the most common) (Figure 39), but they may also appear as primary solid tumours in the liver (peripheral CCC). For the peripheral type there are no typical sonographic characteristics, and the diagnosis is usually made incidentally within the framework of a biopsy of a mass found in the liver. Ultrasound examination shows a solid mass, which can have any form echogenicity and exhibits signs of a malignant growth. The liver metastases of a peripheral CCC are often situated like satellites around the primary focus.

Colour Doppler imaging

The majority of circumscribed CCCs are slightly hypervascular in the conventional colour Doppler imaging, but CDI findings vary widely.

Contrast enhanced ultrasound

In the arterial phase the enhancement picture is variable but mainly hyperenhancing. In the late portal venous phase CCCs are early (< 60 sec) contrasted as punched-out defects [(162-165)]. This behaviour is not always easy to demonstrate in the case of the Klatskin tumours, which often exhibit an appreciable pericholangitic component. As far as differential diagnoses are concerned, in the case of the hilar type of CCC, inflammatory bile duct alterations should be considered *e.g.* cholangitis. However, stratification of the bile ducts is then reserved, and may actually be accentuated in the sonographic image [(13)].

For the detection of CCCs, the examination technique in the liver specific late phase has also proved to be diagnostically useful in patients, resulting in normal CT, MRI and magnetic resonance cholangio-pancreaticography (MRCP), but to date there have been no conclusive studies on differential diagnosis of PSC and CCCs.

Figure 39 Cholangiocellular carcinoma (CCC) (between callipers, +) can occur along the bile duct as so-called Klatskin tumours (hilar CCC is the most common), but they may also appear as primary solid tumours in the liver (peripheral CCC [(166)]). There are an abundance of different morphological patterns of CCC. B-mode (a) and contrast enhanced ultrasound (b-d) are shown [EFSUMB cases of the month 2008, www.efsumb.org].

a

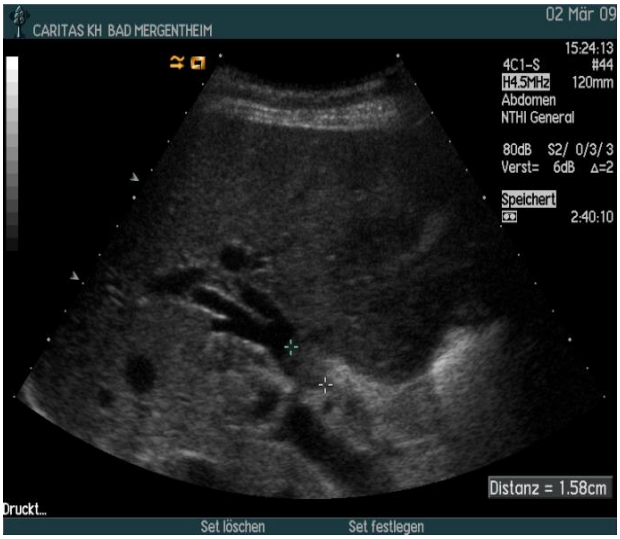

b

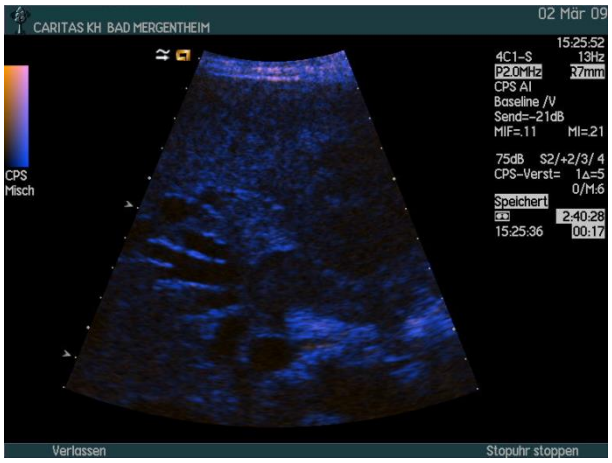
CARITAS KH BAD MERGENTHEIM
02 Mär 09
15:25:52
4C1-S
13Hz
P2.0MHz
37mm
CPS AI
Baseline /V
Send=-21dB
MIF=.11
MI=21
75dB S2/+2/3/ 4
CPS-Verst= 1Δ=5
0/M:6
Speichert
2:40:28
15:25:36
00:17
CPS
Misch
Verlassen
Stopuhr stoppen

c

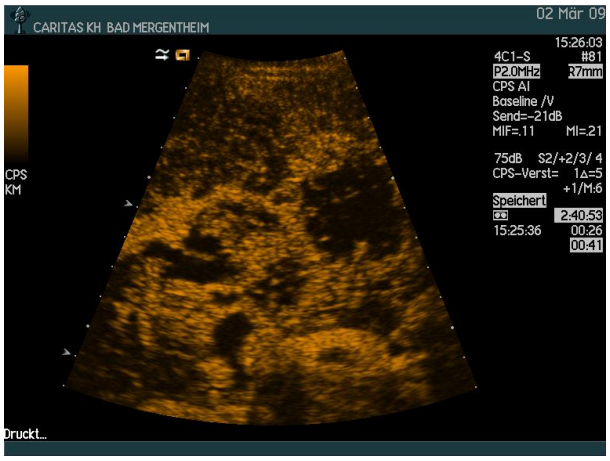
CARITAS KH BAD MERGENTHEIM
02 Mär 09
15:26:03
4C1-S
#81
P2.0MHz
37mm
CPS AI
Baseline /V
Send=-21dB
MIF=.11
MI=21
75dB S2/+2/3/ 4
CPS-Verst= 1Δ=5
+1/M:6
Speichert
2:40:53
15:25:36
00:26
00:41
CPS
KM
Druckt...

d

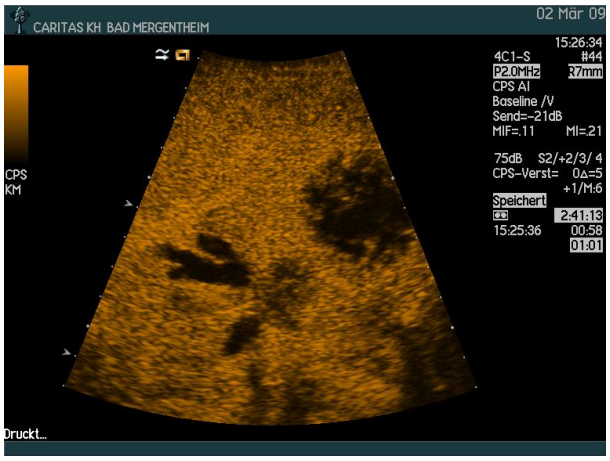
CARITAS KH BAD MERGENTHEIM
02 Mär 09
15:26:34
4C1-S
#44
P2.0MHz
37mm
CPS AI
Baseline /V
Send=-21dB
MIF=.11
MI=21
75dB S2/+2/3/ 4
CPS-Verst= 0Δ=5
+1/M:6
Speichert
2:41:13
15:25:36
00:58
01:01
CPS
KM
Druckt...

Other tumours of extrahepatic bile ducts

Other tumours of extrahepatic bile ducts are sometimes mistaken as intrahepatic FLL. CCC represents only 10% of the incidence of carcinoma and much more common in the gallbladder than the extrahepatic biliary tree. Other forms of benign tumours are rare, *e.g.* carcinoid of the extrahepatic bile ducts. Cholangiocellular carcinoma in the Klatskin position (liver hilum) arise at the confluence of the right and left hepatic ducts at the liver hilum. They are slow growing and, from a surgical point of view, features to note are the degree of obstruction, bile duct wall thickness (as a sign of infection), stones, tumour location and size, depth of invasion, tumour extension to adjacent structures and regional lymph nodes. Details of these are described in the hepatobiliary chapter.

Metastases

The liver is the parenchymatous organ in which metastases of extrahepatic tumours are usually encountered. The special features of portal vein circulation favour haematogenic metastasisation in the liver.

Conventional B-mode ultrasound

Size of the metastases can be anywhere between only microscopically detectable (cellular) infiltration and giant masses measuring more than 20 cm; the echogenicity varies widely. Intraoperative ultrasound (IOUS) may be helpful during surgery in certain cases.

Colour Doppler imaging

Metastases are, as a rule, poorly vascularised and their essential characteristic is a predominantly arterial blood supply (with little or no portal venous blood supply). Like echogenicity (most often hypoechoic), the vascularisation depends on the size, biological behaviour and nature of the primary tumour. Irregular vascularisation is often observed with broken-off vessels and peripherally situated arterio (porto-) venous shunt formation. The metastases of neuroendocrine tumours (*e.g.* metastases of renal cell carcinomas) may be more richly vascularised than other metastases. However, no conclusions are possible about the primary tumour on the basis of the echo-texture and vascularisation pattern observed.

Contrast enhanced ultrasound in metastatic disease

CEUS has markedly improved the detection rate of liver metastases. Liver metastases can be reliably diagnosed as hypoenhancing lesions during the liver specific portal venous sinusoidal phase. False-negative findings are rarely encountered whereas false-positive findings have to be ruled out by puncture and histological examination, *e.g.* abscess, necrosis, fibrous tissue and others [(26)].

Metastases may be already contrasted in the arterial phase, even though early arterial enhancement (in less than 15 s) is not typical and often the only observation is a degree of signal enhancement with a marginal emphasis (“halo sign” or “rim sign”). Contrast of the vessels proceeds from the periphery towards the centre and the vascular pattern is irregular. In poorly vascularised metastases contrast enhanced colour Doppler ultrasound often reveals only small blood vessels situated at the edges (or within the lesion), and in many patients vascularisation cannot be imaged at all. In the portal venous phase metastases are contrasted increasingly as signal “black spots” against the background of uniformly enhanced normal liver tissue (Figure 40). Contrast enhanced IOUS might be helpful in certain cases to detect lesions during surgery.

Figure 40 (a) Metastases have a wide variety of B-mode ultrasound appearance and can be confused with any kind of liver lesion. Colour Doppler imaging is helpful in only few patients. (b-f) Hypervascular metastases reveal the typical peripheral rim sign using contrast enhanced ultrasound in the arterial phase, which can also be encountered in hepatocellular adenoma and hepatocellular carcinoma, and is, therefore, not pathognomonic. (g) Metastases typically exhibit a sharp contrast to normal liver tissue in the liver specific portal venous (sinusoidal) phase.

a

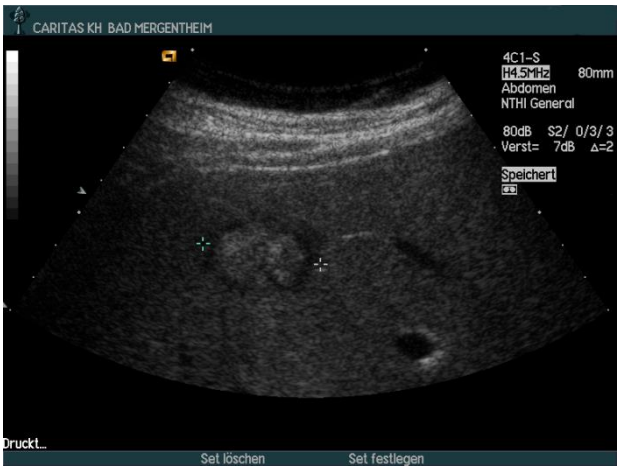
CARITAS KH BAD MERGENTHEIM
4C1-S
H4.5MHz 80mm
Abdomen
NTHI General
80dB S2/ 0/3/ 3
Verst= 7dB Δ=2
Speichert
Druckt...
Set löschen
Set festlegen

b

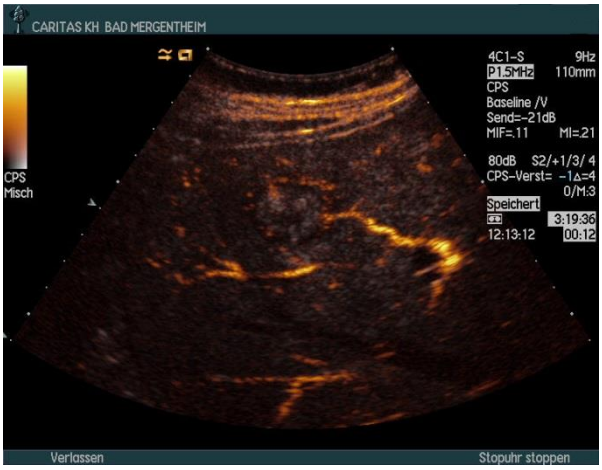
CARITAS KH BAD MERGENTHEIM
4C1-S 9Hz
P1.5MHz 110mm
CPS
Baseline /V
Send=-21dB
MIF=.11 MI=.21
80dB S2/+1/3/ 4
CPS-Verst= -1Δ=4
0/M:3
Speichert
3:19:36
12:13:12 00:12
CPS
Misch
Verlassen
Stopuhr stoppen

c

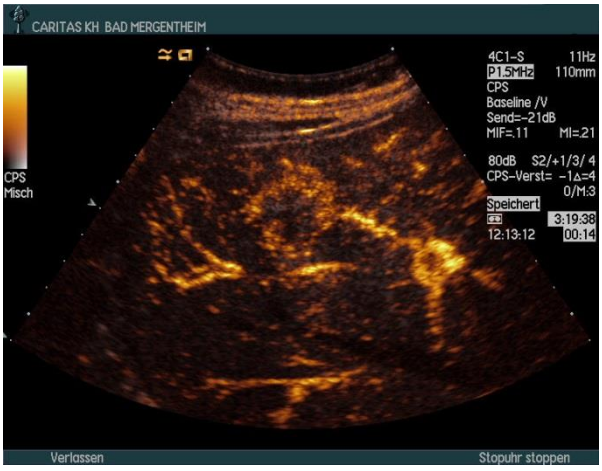
CARITAS KH BAD MERGENTHEIM
4C1-S 11Hz
P1.5MHz 110mm
CPS
Baseline /V
Send=-21dB
MIF=.11 MI=.21
80dB S2/+1/3/ 4
CPS-Verst= -1Δ=4
0/M:3
Speichert
3:19:38
12:13:12 00:14
CPS
Misch
Verlassen
Stopuhr stoppen

d

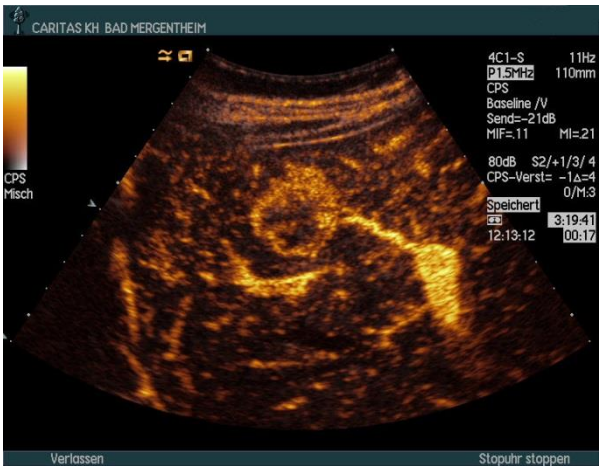
CARITAS KH BAD MERGENTHEIM
4C1-S 11Hz
P1.5MHz 110mm
CPS
Baseline /V
Send=-21dB
MIF=.11 MI=.21
80dB S2/+1/3/4
CPS-Verst= -1Δ=4
0/M:3
Speichert
3:19:41
12:13:12 00:17
CPS
Misch
Verlassen
Stopuhr stoppen

e

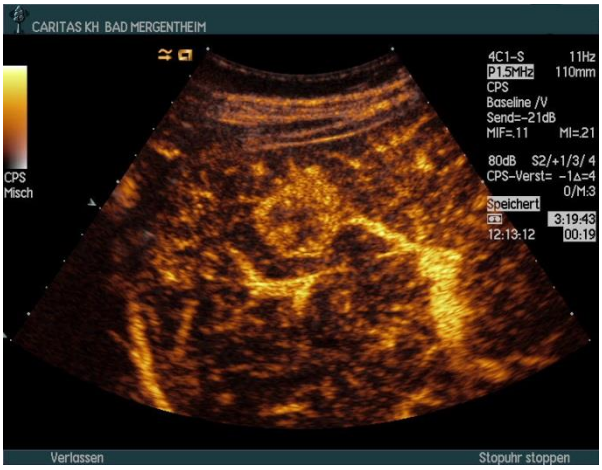
CARITAS KH BAD MERGENTHEIM
4C1-S 11Hz
P1.5MHz 110mm
CPS
Baseline /V
Send=-21dB
MIF=.11 MI=.21
80dB S2/+1/3/4
CPS-Verst= -1Δ=4
0/M:3
Speichert
3:19:43
12:13:12 00:19
CPS
Misch
Verlassen
Stopuhr stoppen

f

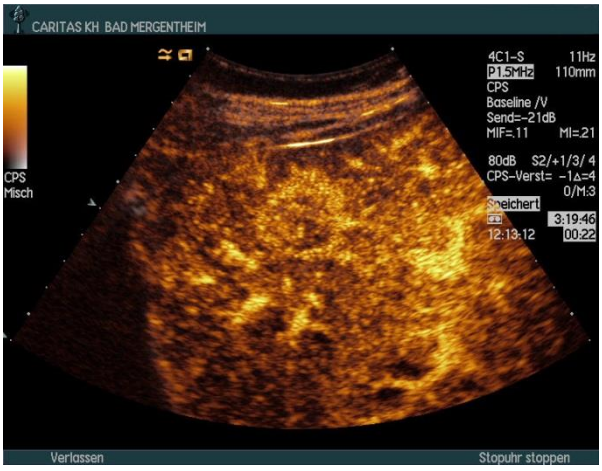
CARITAS KH BAD MERGENTHEIM
4C1-S 11Hz
P1.5MHz 110mm
CPS
Baseline /V
Send=-21dB
MIF=.11 MI=.21
80dB S2/+1/3/4
CPS-Verst= -1Δ=4
0/M:3
Speichert
3:19:46
12:13:12 00:22
CPS
Misch
Verlassen
Stopuhr stoppen

g

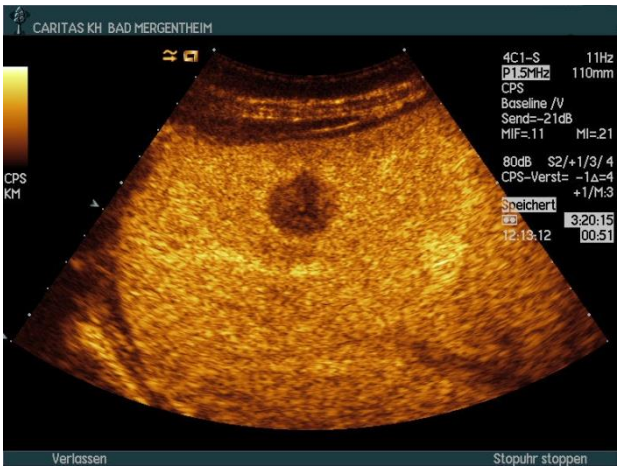

Unlike the portal venous “black spot” effect of metastases, as a rule large haemangiomas show a decrease in the unenhanced signal area (the iris diaphragm phenomenon). Any differential diagnosis must take into account complications of the underlying disease, and complications of therapy (*e.g.* neutropenia with bacterial and/or mycotic abscesses). Benign liver lesions are found with the same frequency (5–20%) in patients with metastases as in a healthy population (*e.g.* liver cysts, calcifications, haemangiomas, FNH and adenomas).

Neuro-endocrine tumour (NET)

Metastases of neuroendocrine tumours (NET) are often small and hyperechoic and therefore mimic haemangioma and occasionally metastases of other origins (*e.g.* gastrointestinal). With increasing size of NET, a combined hyperechoic and centrally echo-poor texture is observed as a typical sonomorphological characteristic, owing to frequent central necrosis, intra-tumoural haemorrhage, necrosis, fibrous tissue or calcifications. Therefore, visual diagnosis by B-mode ultrasound may be possible in approximately 50% of cases. NET are often hypervascularised, with a strong arterial and capillary blood supply similar to shunt haemangioma, small HCA or hypervascular tumours of other origin [(167-169)].

Lymphoma

Conventional B-mode ultrasound

Unlike the often diffuse infiltration of the liver by extranodal Hodgkin's, and in particular non-Hodgkin's lymphomas (approximately 50%), circumscribed alterations are only detected relatively rarely by ultrasound (in less than 10–20% of cases).

Circumscribed lymphomas can infiltrate the liver in small or large nodules or over an extended area, and depending on their rate of growth, are often very hypoechoic compared with the surrounding liver tissue (Figure 41). In individual cases they may in fact give no echoes at all. Characteristically, amplification of the echo distally is then observed. Depending on the regressive changes taking place (*e.g.* an inward flow of blood or necroses), hyperechoic lymphomas are also not uncommon. In our experience, lymphoma infiltrations of the liver are accompanied by sonographically detectable, but often only moderate, enlargement of the perihepatic lymph nodes (the normal lymph node size is up to 17 mm (median value plus two standard deviations) and 19 mm (maximum)). From a differential diagnosis perspective, inflammatory liver conditions should be considered (*e.g.* viral hepatitis B or C, PBC, PSC, etc.), as well as lymph node metastases.

Colour Doppler imaging

The vascularisation of circumscribed lymphomas is often, although not always, more sparse than in healthy liver tissue. Broken-off vessel shunts are typically observed, which in Doppler wave spectral analysis can lead to the disappearance of the diastolic flow component.

Contrast enhanced ultrasound

In contrast to variable arterial enhancement, characteristic lymphomas reveal reduced contrast enhancement in the portal venous phase in comparison with the surrounding liver tissue owing to the relative absence of portal veins in the lymphoma region. By differentiation, in the liver specific late phase, inflammatory lymph nodes can be distinguished from lymph nodes with malignant infiltration because, in the early stage at least, the latter exhibit sharply demarcated malignant infiltrated areas; however, this hypothesis still needs to be tested in prospective studies. The conditions that should be

considered as differential diagnoses are complications of the underlying lymphoma (*e.g.* extramedullary haematopoiesis and a higher frequency of sub-capsular haematomas in the presence of coagulation disturbances) and complications of therapy (*e.g.* neutropenia with bacterial and/or mycotic abscesses), as well as haemophagocytosis syndrome.

Figure 41 Lymphoma. Correct diagnosis of hepatic lymphoma infiltration may be improved by also analysing the perihepatic lymph nodes. Generalised lymphoma often shows (a) intrahepatic mass lesions and (b) perihepatic lymphadenopathy.

a

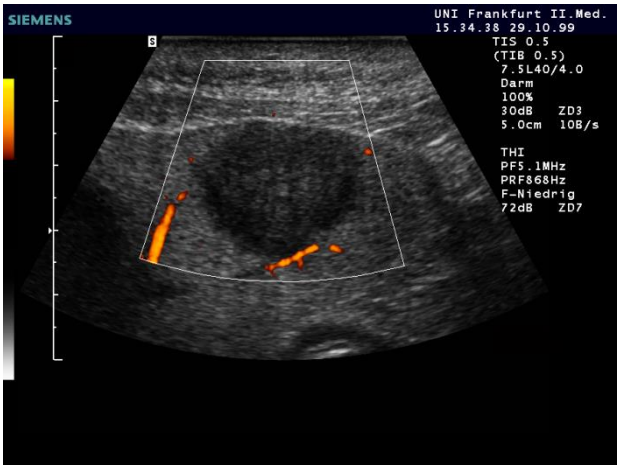

b

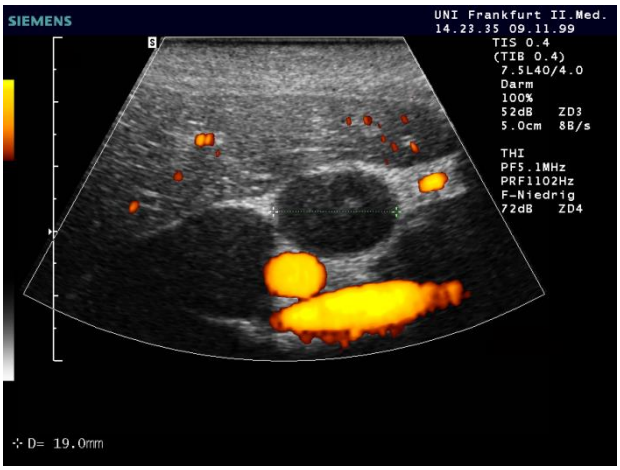

Abscess

The patient medical history and occasionally the physical examination (febrile temperature or signs of sepsis) are the most helpful in differentiating abscesses from necrotic metastases [(144, 145, 170, 171)]. Phlegmonous inflammation and abscesses demonstrate the variable and sometimes confusing change in B-mode ultrasound image over time. The initial phlegmonous inflammation is often isoechoic in comparison with the surrounding liver parenchyma and is sometimes difficult to recognise. In older (chronic) abscesses hypervascularitiy of the nodule border might be confused with a pseudotumour of the liver, even histologically. Small disseminate candida abscesses might be confused with lymphoma or circumscribed haemophagocytosis syndrome (especially in young patients). Puncture and drainage (if necessary) are the diagnostic and therapeutic interventions. Abscesses of up to 5 cm can be drained in one procedure; however, larger abscesses need to be treated over a number of days. The initial phlegmonous inflammation is often hypervascular in comparison with the surrounding liver parenchyma, but is difficult to recognise. In older (chronic) abscesses hypervascularitiy of the nodule border is typical (Figure 42). In typical cases CEUS shows sharply delineated hypervascularity (demonstrating the pseudocapsule) and no gas bubbles inside the lesion. We also refer to the EFSUMB INVUS guidelines (interventional ultrasound guidelines) [(130-133, 172-180)] and comment papers [(134, 135, 181, 182)].
See also cases of the month [http://www.efsumb-archive.org/asp/detail06.asp?ref=373&url=/case-month/cm-archive.asp?ref=1].

Figure 42 Liver abscess. (a) Typical liver abscesses demonstrating gas inside the lesion (arrow). (b-c) In CEUS, there will be no central signal at all, but a pronounced hyperenhancement at the abscess border. The underlying cause in this patient, choledocholithiasis, is detectable (not shown).

a

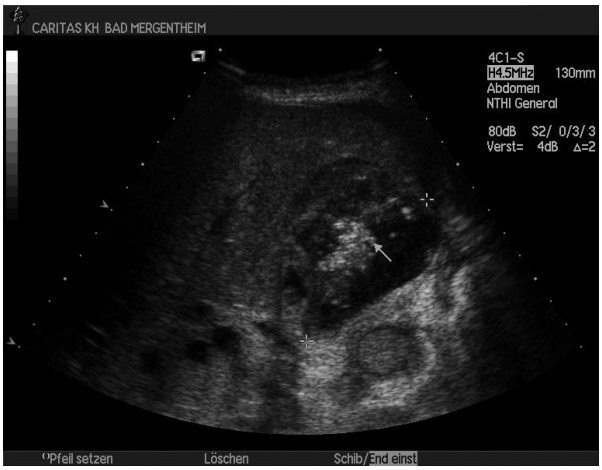
CARITAS KH BAD MERGENTHEIM
4C1-S
H4.5MHz 130mm
Abdomen
NTHI General
80dB S2/ 0/3/ 3
Verst= 4dB Δ=2
Pfeil setzen
Löschen
Schib/End einst

b

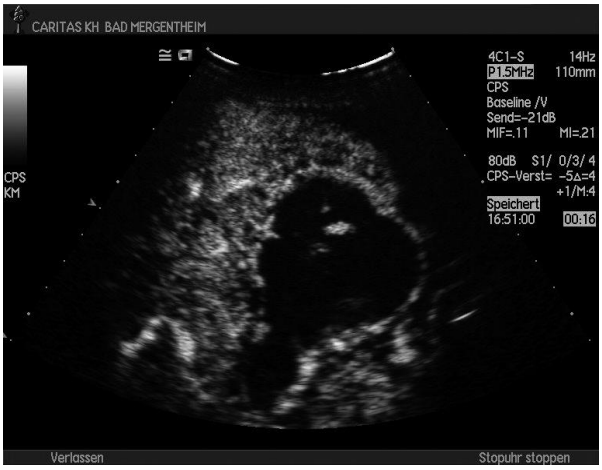
CARITAS KH BAD MERGENTHEIM
4C1-S 14Hz
P1.5MHz 110mm
CPS
Baseline /V
Send=-21dB
MIF=.11 MI=.21
80dB S1/ 0/3/ 4
CPS-Verst= -5Δ=4
+1/M:4
Speichert
16:51:00 00:16
CPS
KM
Verlassen
Stopuhr stoppen

c

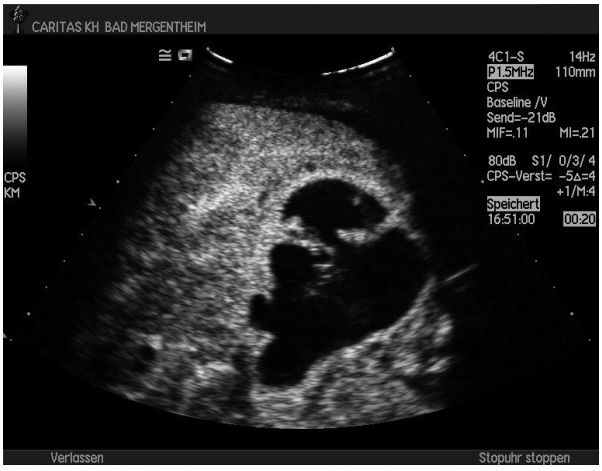
CARITAS KH BAD MERGENTHEIM
4C1-S 14Hz
P1.5MHz 110mm
CPS
Baseline /V
Send=-21dB
MIF=.11 MI=.21
80dB S1/ 0/3/ 4
CPS-Verst= -5Δ=4
+1/M:4
Speichert
16:51:00 00:20
CPS
KM
Verlassen
Stopuhr stoppen

Haematoma

Haematoma can be clinically diagnosed in most cases. The spontaneously evolving and painful haematoma is typical for amyloidosis of the liver (Figure 43) [(47, 183-186)].

Figure 43 Spontaneously evolving and painful haematoma is typical for amyloidosis of the liver [(47, 183-186)].

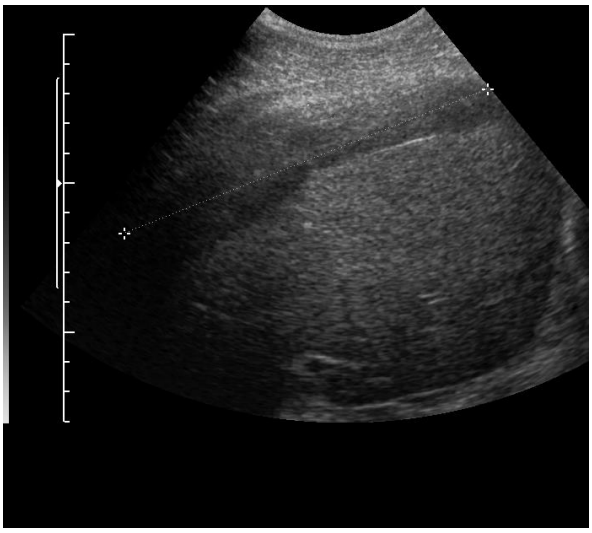

B-mode ultrasound image appearance depends on the stage of the haematoma. Very early haematomas are hyperechoic, and later stages are iso- or mostly hypoechoic. Therefore, a change in morphology is typical for haematomas. CDI demonstrates no flow pattern as there is no vascularity. CEUS is helpful in defining circumscribed *vs* diffuse infiltrating haematoma. CEUS might be helpful in clinically uncertain cases with similar results to those shown for CT (Figure 44).

Figure 44 Perihepatic haematoma using (a) B-mode ultrasound is stage dependent hypoechoic. (b) Contrast enhanced ultrasound demonstrates early vessel invasion.

a

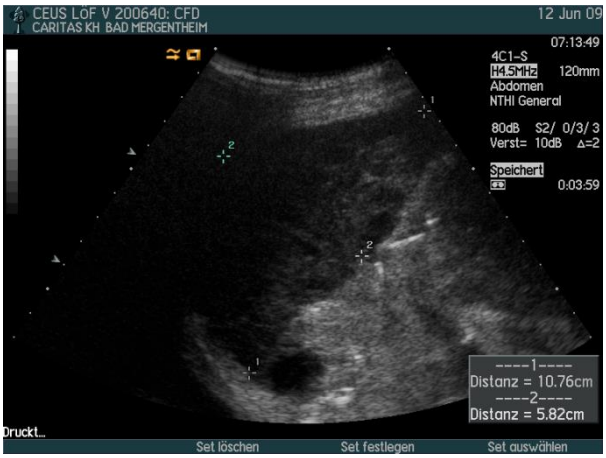

b

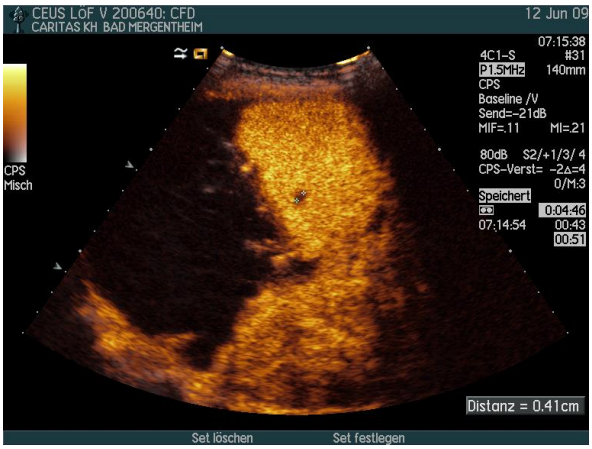

Rare focal liver lesions and other entities

Nodular regenerative hyperplasia

Nodular regenerative hyperplasia (NRH) of the liver is a rare pathological finding, which is typically associated with haematological or autoimmune disease. The main clinical symptom is portal hypertension without underlying liver cirrhosis. NRH of the liver consists of multiple hepatic nodules resulting from periportal hepatocyte regeneration with surrounding atrophy. Typically, fibrous septa between the nodules are missing. Ultrasound typically shows multiple unspecific hepatic nodules, which are suggestive of multilocular HCC or metastatic disease of the liver. Signs of portal hypertension, and the rarer Budd-Chiari syndrome, should be carefully sought. CEUS is helpful in defining circumscribed *vs* diffuse

infiltrating NRH [(187)]. Histological assessment of the liver is necessary for diagnosis because the nodular appearance of the hepatic surface may otherwise be difficult to differentiate from cirrhosis or hepatic metastases.

Haemangioendothelioma

Hepatic epithelioid hemangioendothelioma (HEHE) is a rare primary vascular neoplasm of the liver of endothelial origin. HEHE is characterized by the presence of epithelioid endothelial cells and carries intermediate malignant potential. CEUS imaging allows differentiation of HEHE from other FLL including liver haemangioma and focal nodular hyperplasia. Most HEHE present as multiple FLL with heterogenous peripheral hyperenhancement in the arterial phase and hypoenhancement also of the periphery in the PVLP, which might be useful in determining whether a biopsy is necessary for suspected malignant lesions [(188-191)].

Inflammatory pseudotumour

Inflammatory pseudotumour is a rare disease that can present with fever, abdominal pain, vomiting and weight loss, which indicates, and sonographically mimics, malignancy or abscess. The definite diagnosis is often only achieved by surgery. CEUS may reveal hypoechoic contrast enhancement falsely indicating malignant disease [(26, 192)].

Clinical importance of liver ultrasound in clinical practice

Ultrasound is the first and most important imaging method in suspected liver disease, both for proving (*e.g.* metastatic disease) and excluding pathology. It is the single best tool in the evaluation of FLL. It is unrivalled by any other imaging modality owing to its real-time, dynamic nature, high-resolution and good safety record [(109, 110, 112, 113)]. It is invaluable in the differential diagnosis of jaundice, in describing liver cirrhosis complications and in any form of ultrasound guided intervention [(130-134, 136, 137, 173-179, 193)]. In summary ultrasound is an indispensable tool in clinical hepatology.

Ultrasound of the liver:

- is the first and most important imaging method in suspected liver disease;
- is first line indication for the evaluation of elevated liver functions tests and cholestasis indicating enzymes; differential diagnosis of icterus (diagnosis/exclusion of cholestasis); monitoring of complications of liver cirrhosis (ascites, portal hypertension, HCC); and tumour detection, exclusion and follow-up;
- CEUS is especially helpful for tumour detection and characterisation and prevents unnecessary further imaging.
- is essential for guidance of liver/biliary tree interventions such as biopsy;
- is the most important imaging method for oncological follow-up;
- limitations include the exact measurement of the size of the liver (which is of limited value in clinical practice); and the diagnosis of early cirrhotic stages and in the differential diagnosis of diffuse parenchymal diseases.

References

1. Dietrich CF, Lee JH, Herrmann G, Teuber G, Roth WK, Caspary WF, Zeuzem S. Enlargement of perihepatic lymph nodes in relation to liver histology and viremia in patients with chronic hepatitis C. Hepatology 1997;26:467-472.
2. Dietrich CF, Gottschalk R, Herrmann G, Caspary WF, Zeuzem S. [Sonographic detection of lymph nodes in the hepatoduodenal ligament]. Dtsch.Med.Wochenschr. 1997;122:1269-1274.
3. Dietrich CF, Leuschner MS, Zeuzem S, Herrmann G, Sarrazin C, Caspary WF, Leuschner UF. Peri-hepatic lymphadenopathy in primary biliary cirrhosis reflects progression of the disease. Eur.J.Gastroenterol.Hepatol. 1999;11:747-753.
4. Dietrich CF, Viel K, Braden B, Caspary WF, Zeuzem S. [Mediastinal lymphadenopathy: an extrahepatic manifestation of chronic hepatitis C?]. Z.Gastroenterol. 2000;38:143-152.
5. Dietrich CF, Stryjek-Kaminska D, Teuber G, Lee JH, Caspary WF, Zeuzem S. Perihepatic lymph nodes as a marker of antiviral response in patients with chronic hepatitis C infection. AJR Am.J.Roentgenol. 2000;174:699-704.
6. Braden B, Faust D, Ignee A, Schreiber D, Hirche T, Dietrich CF. Clinical relevance of perihepatic lymphadenopathy in acute and chronic liver disease. J.Clin.Gastroenterol. 2008;42:931-936.
7. Wolf H, Gross F, Merz A, Schuler A. [Liver segment anatomy in ultrasound--examinations to define the frontier between segment II/III and literature review]. Z Gastroenterol 2013;51:271-277.
8. Couinaud C. The parabiliary venous system. Surg Radiol. Anat 1988;10:311-316.
9. Couinaud C. The anatomy of the liver. In: Ann. Ital. Chir; 1992. p. 693-697.
10. Bismuth H. Surgical anatomy and anatomical surgery of the liver. World J Surg 1982;6:3-9.

11. Bismuth H, Houssin D, Castaing D. Major and minor segmentectomies "reglees" in liver surgery. World J Surg 1982;6:10-24.
12. Ehrenstein BP, Froh S, Schlottmann K, Scholmerich J, Schacherer D. To eat or not to eat? Effect of fasting prior to abdominal sonography examinations on the quality of imaging under routine conditions: A randomized, examiner-blinded trial. Scand J Gastroenterol 2009;44:1048-1054.
13. Sabba C, Ferraioli G, Buonamico P, Mahl T, Taylor KJ, Lerner E, Albano O, et al. A randomized study of propranolol on postprandial portal hyperemia in cirrhotic patients. Gastroenterology 1992;102:1009-1016.
14. Lock G, Kammerl M, Schlottmann K, Bregenzer N, Holstege A, Scholmerich J. Gallbladder motility in healthy volunteers: effects of age, gender, body mass index, and hair color. Hepatogastroenterology 2003;50:1232-1235.
15. Dietrich CF, Goudie A, Chiorean L, Cui XW, Gilja OH, Dong Y, Abramowicz JS, et al. Point of Care Ultrasound: A WFUMB Position Paper. Ultrasound Med Biol 2017;43:49-58.
16. Sienz M, Ignee A, Dietrich CF. [Reference values in abdominal ultrasound - liver and liver vessels]. Z.Gastroenterol. 2010;48:1141-1152.
17. Borchert D, Schuler A, Muche R, Haenle MM, Akinli AS, Arnold F, Kratzer W, et al. Comparison of panorama ultrasonography, conventional B-mode ultrasonography, and computed tomography for measuring liver size. Ultraschall Med 2010;31:31-36.
18. Bonhof JA. [Written documentation of ultrasound findings. A contribution to rationalization and standardization: how should a report of ultrasound findings be organized?]. Ultraschall Med 1992;13:283-288.
19. Frey H, Hetzel G, Greis C, Dietrich CF: Grundlagen. In: Dietrich CF, ed. Ultraschall-Kurs. Köln: Deutscher Ärzteverlag, 2006; 1-38.
20. Dietrich CF, Wehrmann T, Zeuzem S, Braden B, Caspary WF, Lembcke B. [Analysis of hepatic echo patterns in chronic hepatitis C]. Ultraschall Med. 1999;20:9-14.
21. Schreiber-Dietrich D, Pohl M, Cui XW, Braden B, Dietrich CF, Chiorean L. Perihepatic lymphadenopathy in children with chronic viral hepatitis. J Ultrason 2015;15:137-150.
22. Dietrich CF, Lee JH, Gottschalk R, Herrmann G, Sarrazin C, Caspary WF, Zeuzem S. Hepatic and portal vein flow pattern in correlation with intrahepatic fat deposition and liver histology in patients with chronic hepatitis C. AJR Am.J.Roentgenol. 1998;171:437-443.
23. Dietrich CF. Sonographische Diagnostik und Differentialdiagnostik von perihepatischen Lymphknoten bei diffusen Leberkrankheiten sowie der Leberbeteiligung bei Systemkrankheiten (Habilitationsschrift). Eigendruck 1999.
24. Schacherer D, Wrede C, Obermeier F, Scholmerich J, Schlottmann K, Klebl F. Comparison of low and high frequency transducers in the detection of liver metastases. Dig Liver Dis 2006;38:677-682.
25. Schacherer D, Schuh C, Strauch U, Ehrenstein B, Wiest R, Scholmerich J, Schlottmann K, et al. Improvement in the routine diagnostic assessment of the liver by high-resolution sonography: an analysis of 999 cases. Scand J Gastroenterol 2007;42:366-373.
26. Dietrich CF, Ignee A, Trojan J, Fellbaum C, Schuessler G. Improved characterisation of histologically proven liver tumours by contrast enhanced ultrasonography during the portal venous and specific late phase of SHU 508A. Gut 2004;53:401-405.
27. Wang WP, Dong Y, Cao J, Mao F, Xu Y, Si Q, Dietrich CF. Detection and characterization of small superficially located focal liver lesions by contrast-enhanced ultrasound with high frequency transducers. Med Ultrason 2017;19:349-356.

28. Zoli M, Magalotti D, Bianchi G, Gueli C, Orlandini C, Grimaldi M, Marchesini G. Total and functional hepatic blood flow decrease in parallel with ageing. Age Ageing 1999;28:29-33.
29. Zoli M, Iervese T, Merkel C, Bianchi G, Magalotti D, Marchesini G, Gatta A, et al. Prognostic significance of portal hemodynamics in patients with compensated cirrhosis. J. Hepatol 1993;17:56-61.
30. Wermke W. Examination technique and findings of ultrasound procedures in portal hypertension. Z. Arztl. Fortbild. (Jena) 1994;88:763-772.
31. Teichgraber UK, Gebel M, Benter T, Manns MP. [Duplex ultrasound characterization of hepatic vein blood flow in healthy probands]. Ultraschall Med 1997;18:267-271.
32. Piscaglia F, Zironi G, Gaiani S, Ferlito M, Rapezzi C, Siringo S, Gaia C, et al. Relationship between splanchnic, peripheral and cardiac haemodynamics in liver cirrhosis of different degrees of severity. Eur. J. Gastroenterol. Hepatol 1997;9:799-804.
33. Piscaglia F, Valgimigli M, Serra C, Donati G, Gramantieri L, Bolondi L. Duplex Doppler findings in splenic arteriovenous fistula. J. Clin. Ultrasound 1998;26:103-105.
34. Piscaglia F, Gaiani S, Gramantieri L, Zironi G, Siringo S, Bolondi L. Superior mesenteric artery impedance in chronic liver diseases: relationship with disease severity and portal circulation [see comments]. Am. J. Gastroenterol 1998;93:1925-1930.
35. Seitz K. [Duplex sonographic findings in the portal system]. Verh. Dtsch. Ges. Inn. Med 1988;94:560-568.
36. Ignee A, Boerner N, Bruening A, Dirks K, von Herbay A, Jenssen C, Kubale R, et al. Duplex sonography of the mesenteric vessels--a critical evaluation of inter-observer variability. Z Gastroenterol 2016;54:304-311.
37. Hirche TO, Ignee A, Hirche H, Schneider A, Dietrich CF. Evaluation of hepatic steatosis by ultrasound in patients with chronic hepatitis C virus infection. Liver Int. 2007;27:748-757.
38. Abu-Yousef MM, Milam SG, Farner RM. Pulsatile portal vein flow: a sign of tricuspid regurgitation on duplex Doppler sonography. AJR Am. J. Roentgenol 1990;155:785-788.
39. Ignee A, Gebel M, Caspary WF, Dietrich CF. [Doppler imaging of hepatic vessels - review]. Z.Gastroenterol. 2002;40:21-32.
40. Aubin B, Denys A, LaFortune M, Dery R, Breton G. Focal sparing of liver parenchyma in steatosis: role of the gallbladder and its vessels. J Ultrasound Med 1995;14:77-80.
41. Wernecke K, Heckemann R, Rehwald U. [Ultrasound-guided thin-needle biopsy in focal liver diseases. II. Benign focal liver diseases]. Ultraschall Med 1984;5:303-311.
42. Kratzer W, Akinli AS, Bommer M, Arnold F, Eggink S, Imhof A, Mason RA, et al. Prevalence and risk factors of focal sparing in hepatic steatosis. Ultraschall Med 2010;31:37-42.
43. Dietrich CF. Letter to the editor: Kratzer W et al. Prevalence and risk factors of focal sparing in hepatic steatosis. Ultraschall in Med 2010; 31: 37 - 42. Ultraschall Med. 2010;31:417-419.
44. Sienz M, Ignee A, Dietrich CF. [Reference values in abdominal ultrasound - biliopancreatic system and spleen]. Z.Gastroenterol. 2011;49:845-870.
45. Dietrich CF, Schall H, Kirchner J, Seifert H, Herrmann G, Caspary WF, Lembcke B. Sonographic detection of focal changes in the liver hilus in patients receiving corticosteroid therapy. Z.Gastroenterol. 1997;35:1051-1057.
46. Dietrich CF, Mertens JC, Braden B, Schuessler G, Ott M, Ignee A. Contrast-enhanced ultrasound of histologically proven liver hemangiomas. Hepatology 2007;45:1139-1145.

47. Barreiros AP, Chiorean L, Braden B, Dietrich CF. Ultrasound in rare diffuse liver disease. Z Gastroenterol 2014;52:1247-1256.
48. Dietrich CF, Bamber J, Berzigotti A, Bota S, Cantisani V, Castera L, Cosgrove D, et al. EFSUMB Guidelines and Recommendations on the Clinical Use of Liver Ultrasound Elastography, Update 2017 (Short Version). Ultraschall Med 2017;38:377-394.
49. Dietrich CF, Bamber J, Berzigotti A, Bota S, Cantisani V, Castera L, Cosgrove D, et al. EFSUMB Guidelines and Recommendations on the Clinical Use of Liver Ultrasound Elastography, Update 2017 (Long Version). Ultraschall Med 2017;38:e16-e47.
50. Berzigotti A, Piscaglia F. Ultrasound in portal hypertension--part 1. Ultraschall Med 2011;32:548-568; quiz 569-571.
51. Berzigotti A, Piscaglia F, Education E, Professional Standards C. Ultrasound in portal hypertension--part 2--and EFSUMB recommendations for the performance and reporting of ultrasound examinations in portal hypertension. Ultraschall Med 2012;33:8-32; quiz 30-31.
52. Berzigotti A, Merkel C, Magalotti D, Tiani C, Gaiani S, Sacerdoti D, Zoli M. New abdominal collaterals at ultrasound: a clue of progression of portal hypertension. Dig Liver Dis 2008;40:62-67.
53. Lyttkens K, Hannesson P, Prytz H, Wallengren NO, Forsberg L. Lymph nodes in the hepato-duodenal ligament. A comparison between ultrasound and low-field MR imaging. Acta Radiol 1996;37:521-523.
54. Metreweli C, Ward SC. Ultrasound demonstration of lymph nodes in the hepatoduodenal ligament ('Daisy Chain nodes') in normal subjects. Clin Radiol 1995;50:99-101.
55. Sharma M, Rameshbabu CS, Dietrich CF, Rai P, Bansal R. Endoscopic ultrasound of the hepatoduodenal ligament and liver hilum. Endosc Ultrasound 2016.
56. Hirche TO, Russler J, Braden B, Schuessler G, Zeuzem S, Wehrmann T, Seifert H, et al. Sonographic detection of perihepatic lymphadenopathy is an indicator for primary sclerosing cholangitis in patients with inflammatory bowel disease. Int.J.Colorectal Dis. 2004;19:586-594.
57. Ignee A, Weiper D, Schuessler G, Teuber G, Faust D, Dietrich CF. Sonographic characterisation of hepatocellular carcinoma at time of diagnosis. Z.Gastroenterol. 2005;43:289-294.
58. Lyttkens K, Prytz H, Forsberg L, Hagerstrand I. Hepatic lymph nodes as follow-up factor in primary biliary cirrhosis. An ultrasound study. Scand. J. Gastroenterol 1995;30:1036-1040.
59. Tana C, Dietrich CF, Schiavone C. Hepatosplenic sarcoidosis: contrast-enhanced ultrasound findings and implications for clinical practice. Biomed Res Int 2014;2014:926203.
60. Tana C, Silingardi M, Dietrich CF. New trends in ultrasound of hepatosplenic sarcoidosis. Z Gastroenterol 2015;53:283-284.
61. Dietrich CF, Annema JT, Clementsen P, Cui XW, Borst MM, Jenssen C. Ultrasound techniques in the evaluation of the mediastinum, part I: endoscopic ultrasound (EUS), endobronchial ultrasound (EBUS) and transcutaneous mediastinal ultrasound (TMUS), introduction into ultrasound techniques. J Thorac Dis 2015;7:E311-325.
62. Jenssen C, Annema JT, Clementsen P, Cui XW, Borst MM, Dietrich CF. Ultrasound techniques in the evaluation of the mediastinum, part 2: mediastinal lymph node anatomy and diagnostic reach of ultrasound techniques, clinical work up of neoplastic and inflammatory mediastinal lymphadenopathy using ultrasound techniques and how to learn mediastinal endosonography. J Thorac Dis 2015;7:E439-458.

63. Dietrich CF, Chichakli M, Hirche TO, Bargon J, Leitzmann P, Wagner TO, Lembcke B. Sonographic findings of the hepatobiliary-pancreatic system in adult patients with cystic fibrosis. J.Ultrasound Med. 2002;21:409-416.
64. Bargon J, Stein J, Dietrich CF, Muller U, Caspary WF, Wagner TO. [Gastrointestinal complications of adult patients with cystic fibrosis]. Z.Gastroenterol. 1999;37:739-749.
65. Braden B, Helm B, Fabian T, Dietrich CF. [Bacillary angiomatosis of the liver, a suspected ultrasound diagnosis?]. Z.Gastroenterol. 2000;38:785-789.
66. Dietrich CF, Sharma M, Chaubal N, Dong Y, Cui XW, Schindler-Piontek M, Richter J, et al. Ascariasis imaging: pictorial essay. Z Gastroenterol 2017;55:479-489.
67. Dietrich CF, Kabaalioglu A, Brunetti E, Richter J. Fasciolosis. Z Gastroenterol 2015;53:285-290.
68. Richter J, Azoulay D, Dong Y, Holtfreter MC, Akpata R, Calderaro J, El-Scheich T, et al. Ultrasonography of gallbladder abnormalities due to schistosomiasis. Parasitol Res 2016;115:2917-2924.
69. Richter J, Botelho MC, Holtfreter MC, Akpata R, El Scheich T, Neumayr A, Brunetti E, et al. Ultrasound assessment of schistosomiasis. Z Gastroenterol 2016;54:653-660.
70. Colli A, Cocciolo M, Riva C, Martinez E, Prisco A, Pirola M, Bratina G. Abnormalities of Doppler waveform of the hepatic veins in patients with chronic liver disease: correlation with histologic findings. AJR Am. J. Roentgenol 1994;162:833-837.
71. Abu-Yousef MM. Duplex Doppler sonography of the hepatic vein in tricuspid regurgitation. AJR Am. J. Roentgenol 1991;156:79-83.
72. Gaiani S, Bolondi L, Li BS, Zironi G, Siringo S, Barbara L. Prevalence of spontaneous hepatofugal portal flow in liver cirrhosis. Clinical and endoscopic correlation in 228 patients [see comments]. Gastroenterology 1991;100:160-167.
73. Seitz K, Wermke W. Portal hypertension--current status of ultrasound diagnosis. Z. Gastroenterol 1995;33:349-361.
74. Sabba C, Merkel C, Zoli M, Ferraioli G, Gaiani S, Sacerdoti D, Bolondi L. Interobserver and interequipment variability of echo-Doppler examination of the portal vein: effect of a cooperative training program. Hepatology 1995;21:428-433.
75. Roobottom CA, Hunter JD, Weston MJ, Dubbins PA. Hepatic venous Doppler waveforms: changes in pregnancy. J Clin Ultrasound 1995;23:477-482.
76. Abu-Yousef MM. Normal and respiratory variations of the hepatic and portal venous duplex Doppler waveforms with simultaneous electrocardiographic correlation. J. Ultrasound Med 1992;11:263-268.
77. Teichgraber UK, Gebel M, Benter T, Manns MP. Effect of respiration, exercise, and food intake on hepatic vein circulation. J. Ultrasound Med 1997;16:549-554.
78. Piscaglia F, Gaiani S, Zironi G, Gramantieri L, Casali A, Siringo S, Serra C, et al. Intra- and extrahepatic arterial resistances in chronic hepatitis and liver cirrhosis. Ultrasound Med. Biol 1997;23:675-682.
79. Leen E, Anderson JR, Robertson J, O'Gorman P, Cooke TG, McArdle CS. Doppler index perfusion in the detection of hepatic metastases secondary to gastric carcinoma. Am. J. Surg 1997;173:99-102.
80. Strunk H, von Falkenhausen M, Hofer U, Remig J, Konig R, Wilhelm K, Textor J. [Variants of the hepatic artery: detection with color--coded sonography pre and post levovist injection]. Ultraschall Med 1999;20:26-30.
81. Dietrich CF, Ignee A, Seitz KH, Caspary WF. [Duplex sonography of visceral arteries]. Ultraschall Med 2001;22:247-257.

82. Jenssen C, Tuma J, Moller K, Cui XW, Kinkel H, Uebel S, Dietrich CF. [Ultrasound artifacts and their diagnostic significance in internal medicine and gastroenterology - part 2: color and spectral Doppler artifacts]. Z Gastroenterol 2016;54:569-578.
83. Colli A, Cocciolo M, Mumoli N, Cattalini N, Fraquelli M, Conte D. Hepatic artery resistance in alcoholic liver disease. Hepatology 1998;28:1182-1186.
84. Leen E, Goldberg JA, Angerson WJ, McArdle CS. Potential role of doppler perfusion index in selection of patients with colorectal cancer for adjuvant chemotherapy [see comments]. Lancet 2000;355:34-37.
85. Kirchner J, Zipf A, Dietrich CF, Hohmann A, Heyd R, Berkefeld J. [Universal organ involvement in Rendu-Osler-Weber disease: interdisciplinary diagnosis and interventional therapy]. Z.Gastroenterol. 1996;34:747-752.
86. Caselitz M, Wagner S, Chavan A, Gebel M, Bleck JS, Wu A, Schlitt HJ, et al. Clinical outcome of transfemoral embolisation in patients with arteriovenous malformations of the liver in hereditary haemorrhagic telangiectasia (Weber-Rendu-Osler disease). Gut 1998;42:123-126.
87. Becker D, Dietrich CF: M. Osler. In: Dietrich CF, Becker D, eds. Farbduplexsonographie des Abdomens. Konstanz: Schnetztor Verlag, 2002; 77-79.
88. Abraldes JG, Gilabert R, Turnes J, Nicolau C, Berzigotti A, Aponte J, Bru C, et al. Utility of color Doppler ultrasonography predicting tips dysfunction. Am J Gastroenterol 2005;100:2696-2701.
89. Gaiani S, Gramantieri L, Venturoli N, Piscaglia F, Siringo S, d'Errico A, Zironi G, et al. What is the criterion for differentiating chronic hepatitis from compensated cirrhosis? A prospective study comparing ultrasonography and percutaneous liver biopsy [see comments]. J. Hepatol 1997;27:979-985.
90. Gebel M, Caselitz M, Bowen-Davies PE, Weber S. A multicenter, prospective, open label, randomized, controlled phase IIIb study of SH U 508 a (Levovist) for Doppler signal enhancement in the portal vascular system. Ultraschall Med 1998;19:148-156.
91. Ochs A. Transjugular intrahepatic portosystemic shunt. Dig Dis 2005;23:56-64.
92. Piscaglia F, Donati G, Serra C, Muratori R, Solmi L, Gaiani S, Gramantieri L, et al. Value of splanchnic Doppler ultrasound in the diagnosis of portal hypertension. Ultrasound Med. Biol 2001;27:893-899.
93. Rossle M, Haag K, Ochs A, Sellinger M, Noldge G, Perarnau JM, Berger E, et al. The transjugular intrahepatic portosystemic stent-shunt procedure for variceal bleeding. N. Engl. J Med 1994;330:165-171.
94. Sabba C, Ferraioli G, Buonamico P, Berardi E, Antonica G, Taylor KJ, Albano O. Echo-Doppler evaluation of acute flow changes in portal hypertensive patients: flow velocity as a reliable parameter. J. Hepatol 1992;15:356-360.
95. Wanless IR. Micronodular transformation (nodular regenerative hyperplasia) of the liver: a report of 64 cases among 2,500 autopsies and a new classification of benign hepatocellular nodules. Hepatology 1990;11:787-797.
96. Wermke W. Etiopathogenesis, morphology and hemodynamics of portal hypertension. Z. Arztl. Fortbild. (Jena) 1993;87:961-967.
97. Berzigotti A, Castaldini N, Rossi V, Magalotti D, Tiani C, Zappoli P, Zoli M. Age dependency of regional impedance indices regardless of clinical stage in patients with cirrhosis of the liver. Ultraschall Med 2009;30:277-285.
98. Lassau N, Leclere J, Auperin A, Bourhis JH, Hartmann O, Valteau-Couanet D, Benhamou E, et al. Hepatic veno-occlusive disease after myeloablative treatment and bone marrow

transplantation: value of gray-scale and Doppler US in 100 patients. Radiology 1997;204:545-552.
99. Dietrich CF, Schreiber-Dietrich D: Veno-occlusive disease (VOD). In: Dietrich CF, Becker D, eds. Farbduplexsonographie des Abdomens. Konstanz: Schnetztor Verlag, 2002; 91-95.
100. Lassau N, Auperin A, Leclere J, Bennaceur A, Valteau-Couanet D, Hartmann O. Prognostic value of doppler-ultrasonography in hepatic veno-occlusive disease. Transplantation 2002;74:60-66.
101. Becker D, Dietrich CF: Transjugulärer portosystemischer Shunt (TIPS). In: Dietrich CF, Becker D, eds. Farbduplexsonographie des Abdomens. Konstanz: Schnetztor Verlag, 2002; 73-77.
102. Piscaglia F, Zironi G, Gaiani S, Mazziotti A, Cavallari A, Gramantieri L, Valgimigli M, et al. Systemic and splanchnic hemodynamic changes after liver transplantation for cirrhosis: a long-term prospective study. Hepatology 1999;30:58-64.
103. Piscaglia F, Cecilioni L, Gaiani S, Rossi C, Losinno F, Cescon M, Camaggi V, et al. Use of perfusional angiosonography in liver transplantation and conservative management of post-transplant intra-hepatic pseudo-aneurysm. Transpl. Int 2004;17:634-638.
104. Garcia-Criado A, Gilabert R, Berzigotti A, Bru C. Doppler ultrasound findings in the hepatic artery shortly after liver transplantation. AJR Am J Roentgenol 2009;193:128-135.
105. Leen E, Angerson WG, Cooke TG, McArdle CS. Prognostic power of Doppler perfusion index in colorectal cancer. Correlation with survival. Ann. Surg 1996;223:199-203.
106. Becker D, Dietrich CF: Doppler-Perfusions-Index (DPI)). In: Dietrich CF, Becker D, eds. Farbduplexsonographie des Abdomens. Konstanz: Schnetztor Verlag, 2002; 76-77.
107. Berzigotti A, Seijo S, Reverter E, Bosch J. Assessing portal hypertension in liver diseases. Expert Rev Gastroenterol Hepatol 2013;7:141-155.
108. Berzigotti A, Reverter E, Garcia-Criado A, Abraldes JG, Cerini F, Garcia-Pagan JC, Bosch J. Reliability of the estimation of total hepatic blood flow by Doppler ultrasound in patients with cirrhotic portal hypertension. J Hepatol 2013;59:717-722.
109. Claudon M, Dietrich CF, Choi BI, Cosgrove DO, Kudo M, Nolsoe CP, Piscaglia F, et al. Guidelines and good clinical practice recommendations for contrast enhanced ultrasound (CEUS) in the liver--update 2012: a WFUMB-EFSUMB initiative in cooperation with representatives of AFSUMB, AIUM, ASUM, FLAUS and ICUS. Ultraschall Med 2013;34:11-29.
110. Claudon M, Dietrich CF, Choi BI, Cosgrove DO, Kudo M, Nolsoe CP, Piscaglia F, et al. Guidelines and good clinical practice recommendations for Contrast Enhanced Ultrasound (CEUS) in the liver - update 2012: A WFUMB-EFSUMB initiative in cooperation with representatives of AFSUMB, AIUM, ASUM, FLAUS and ICUS. Ultrasound Med Biol 2013;39:187-210.
111. Piscaglia F, Nolsoe C, Dietrich CF, Cosgrove DO, Gilja OH, Bachmann NM, Albrecht T, et al. The EFSUMB Guidelines and Recommendations on the Clinical Practice of Contrast Enhanced Ultrasound (CEUS): update 2011 on non-hepatic applications. Ultraschall Med. 2012;33:33-59.
112. Claudon M, Cosgrove D, Albrecht T, Bolondi L, Bosio M, Calliada F, Correas JM, et al. Guidelines and good clinical practice recommendations for contrast enhanced ultrasound (CEUS) - update 2008. Ultraschall Med 2008;29:28-44.
113. Albrecht T, Blomley M, Bolondi L, Claudon M, Correas JM, Cosgrove D, Greiner L, et al. Guidelines for the use of contrast agents in ultrasound. January 2004. Ultraschall Med 2004;25:249-256.

114. Dietrich CF, Becker D: Budd-Chiari-Syndrom (BCS). In: Dietrich CF, Becker D, eds. Farbduplexsonographie des Abdomens. Konstanz: Schnetztor Verlag, 2002; 84-91.
115. Rickes S, Csepregi A. Images of interest. Hepatobiliary and pancreatic: Budd-Chiari syndrome. J. Gastroenterol. Hepatol 2004;19:828.
116. Martin-Llahi M, Albillos A, Banares R, Berzigotti A, Garcia-Criado MA, Genesca J, Hernandez-Gea V, et al. Vascular diseases of the liver. Clinical Guidelines from the Catalan Society of Digestology and the Spanish Association for the Study of the Liver. Gastroenterol Hepatol 2017;40:538-580.
117. Ignee A, Atkinson NS, Schuessler G, Dietrich CF. Ultrasound contrast agents. Endosc Ultrasound 2016.
118. Dietrich CF, Kratzer W, Strobe D, Danse E, Fessl R, Bunk A, Vossas U, et al. Assessment of metastatic liver disease in patients with primary extrahepatic tumors by contrast-enhanced sonography versus CT and MRI. World J.Gastroenterol. 2006;12:1699-1705.
119. Hohmann J, Muller A, Skrok J, Wolf KJ, Martegani A, Dietrich CF, Albrecht T. Detection of hepatocellular carcinoma and liver metastases with BR14: a multicenter phase IIA study. Ultrasound Med Biol 2012;38:377-382.
120. Bernatik T, Schuler A, Kunze G, Mauch M, Dietrich CF, Dirks K, Pachmann C, et al. Benefit of Contrast-Enhanced Ultrasound (CEUS) in the Follow-Up Care of Patients with Colon Cancer: A Prospective Multicenter Study. Ultraschall Med 2015;36:590-593.
121. Seitz K, Strobel D, Bernatik T, Blank W, Friedrich-Rust M, Herbay A, Dietrich CF, et al. Contrast-Enhanced Ultrasound (CEUS) for the characterization of focal liver lesions - prospective comparison in clinical practice: CEUS vs. CT (DEGUM multicenter trial). Parts of this manuscript were presented at the Ultrasound Dreilandertreffen 2008, Davos. Ultraschall Med. 2009;30:383-389.
122. Strobel D, Seitz K, Blank W, Schuler A, Dietrich C, von Herbay A, Friedrich-Rust M, et al. Contrast-enhanced ultrasound for the characterization of focal liver lesions--diagnostic accuracy in clinical practice (DEGUM multicenter trial). Ultraschall Med 2008;29:499-505.
123. Strobel D, Bernatik T, Blank W, Schuler A, Greis C, Dietrich CF, Seitz K. Diagnostic accuracy of CEUS in the differential diagnosis of small (</= 20 mm) and subcentimetric (</= 10 mm) focal liver lesions in comparison with histology. Results of the DEGUM multicenter trial. Ultraschall Med. 2011;32:593-597.
124. Seitz K, Greis C, Schuler A, Bernatik T, Blank W, Dietrich CF, Strobel D. Frequency of tumor entities among liver tumors of unclear etiology initially detected by sonography in the noncirrhotic or cirrhotic livers of 1349 patients. Results of the DEGUM multicenter study. Ultraschall Med. 2011;32:598-603.
125. Bernatik T, Seitz K, Blank W, Schuler A, Dietrich CF, Strobel D. Unclear focal liver lesions in contrast-enhanced ultrasonography--lessons to be learned from the DEGUM multicenter study for the characterization of liver tumors. Ultraschall Med. 2010;31:577-581.
126. Sporea I, Badea R, Popescu A, Sparchez Z, Sirli RL, Danila M, Sandulescu L, et al. Contrast-enhanced ultrasound (CEUS) for the evaluation of focal liver lesions - a prospective multicenter study of its usefulness in clinical practice. Ultraschall Med 2014;35:259-266.
127. Trillaud H, Bruel JM, Valette PJ, Vilgrain V, Schmutz G, Oyen R, Jakubowski W, et al. Characterization of focal liver lesions with SonoVue-enhanced sonography: international multicenter-study in comparison to CT and MRI. World J Gastroenterol 2009;15:3748-3756.
128. von Herbay A, Vogt C, Haussinger D. Pulse inversion sonography in the early phase of the sonographic contrast agent Levovist: differentiation between benign and malignant focal liver lesions. J. Ultrasound Med 2002;21:1191-1200.

129. von Herbay A, Vogt C, Willers R, Haussinger D. Real-time imaging with the sonographic contrast agent SonoVue: differentiation between benign and malignant hepatic lesions. J. Ultrasound Med 2004;23:1557-1568.
130. Sidhu PS, Brabrand K, Cantisani V, Correas JM, Cui XW, D'Onofrio M, Essig M, et al. EFSUMB Guidelines on Interventional Ultrasound (INVUS), Part II. Diagnostic Ultrasound-Guided Interventional Procedures (Long Version). Ultraschall Med 2015;36:E15-35.
131. Sidhu PS, Brabrand K, Cantisani V, Correas JM, Cui XW, D'Onofrio M, Essig M, et al. EFSUMB Guidelines on Interventional Ultrasound (INVUS), Part II. Diagnostic Ultrasound-Guided Interventional Procedures (Short Version). Ultraschall Med 2015;36:566-580.
132. Dietrich CF, Lorentzen T, Appelbaum L, Buscarini E, Cantisani V, Correas JM, Cui XW, et al. EFSUMB Guidelines on Interventional Ultrasound (INVUS), Part III - Abdominal Treatment Procedures (Long Version). Ultraschall Med 2016;37:E1-E32.
133. Dietrich CF, Lorentzen T, Appelbaum L, Buscarini E, Cantisani V, Correas JM, Cui XW, et al. EFSUMB Guidelines on Interventional Ultrasound (INVUS), Part III - Abdominal Treatment Procedures (Short Version). Ultraschall Med 2016;37:27-45.
134. Dietrich CF, Cui XW, Chiorean L, Appelbaum L, Leen E, Ignee A. Local ablative procedures of the liver. Z Gastroenterol 2015;53:579-590.
135. Dietrich CF, Chiorean L, Potthoff A, Ignee A, Cui X, Sparchez Z. Percutaneous sclerotherapy of liver and renal cysts, comments on the EFSUMB guidelines. Z Gastroenterol 2016;54:155-166.
136. Meloni MF, Chiang J, Laeseke PF, Dietrich CF, Sannino A, Solbiati M, Nocerino E, et al. Microwave ablation in primary and secondary liver tumours: technical and clinical approaches. Int J Hyperthermia 2017;33:15-24.
137. Meloni MF, Galimberti S, Dietrich CF, Lazzaroni S, Goldberg SN, Abate A, Sironi S, et al. Microwave ablation of hepatic tumors with a third generation system: locoregional efficacy in a prospective cohort study with intermediate term follow-up. Z Gastroenterol 2016;54:541-547.
138. Dietrich CF, Averkiou MA, Correas JM, Lassau N, Leen E, Piscaglia F. An EFSUMB introduction into Dynamic Contrast-Enhanced Ultrasound (DCE-US) for quantification of tumour perfusion. Ultraschall Med 2012;33:344-351.
139. Frohlich E, Muller R, Cui XW, Schreiber-Dietrich D, Dietrich CF. Dynamic contrast-enhanced ultrasound for quantification of tissue perfusion. J Ultrasound Med 2015;34:179-196.
140. Dietrich CF, Schuessler G, Trojan J, Fellbaum C, Ignee A. Differentiation of focal nodular hyperplasia and hepatocellular adenoma by contrast-enhanced ultrasound. Br.J.Radiol. 2005;78:704-707.
141. Dong Y, Wang WP, Mao F, Fan M, Ignee A, Serra C, Sparchez Z, et al. Contrast enhanced ultrasound features of hepatic cystadenoma and hepatic cystadenocarcinoma. Scand J Gastroenterol 2017;52:365-372.
142. International classification of ultrasound images in cystic echinococcosis for application in clinical and field epidemiological settings. Acta Trop 2003;85:253-261.
143. Dietrich CF, Mueller G, Beyer-Enke S. Cysts in the cyst pattern. Z.Gastroenterol. 2009;47:1203-1207.
144. Dietrich CF, Nuernberg D. Interventional ultrasound. A practical guide and atlas: Thieme, 2014.
145. Dietrich CF, Nuernberg D. Interventioneller Ultraschall. Lehrbuch und Atlas für die interventionelle Sonographie: Thieme Verlag, 2011.

146. Tuma J, Jenssen C, Moller K, Cui XW, Kinkel H, Uebel S, Dietrich CF. [Ultrasound artifacts and their diagnostic significance in internal medicine and gastroenterology - Part 1: B-mode artifacts]. Z Gastroenterol 2016;54:433-450.
147. Bonhof JA. Ultrasound Artifacts - Part 1. Ultraschall Med 2016;37:140-153; quiz 154-145.
148. Bonhof JA. Ultrasound Artifacts - Part 2. Ultraschall Med 2017;38:130-148.
149. Dietrich CF, Mathis G, Blaivas M, Volpicelli G, Seibel A, Atkinson NS, Cui XW, et al. Lung artefacts and their use. Med Ultrason 2016;18:488-499.
150. Dietrich CF, Mathis G, Blaivas M, Volpicelli G, Seibel A, Wastl D, Atkinson NS, et al. Lung B-line artefacts and their use. J Thorac Dis 2016;8:1356-1365.
151. Nguyen BN, Flejou JF, Terris B, Belghiti J, Degott C. Focal nodular hyperplasia of the liver: a comprehensive pathologic study of 305 lesions and recognition of new histologic forms. Am. J. Surg. Pathol 1999;23:1441-1454.
152. Gossmann J, Scheuermann EH, Frilling A, Geiger H, Dietrich CF. Multiple adenomas and hepatocellular carcinoma in a renal transplant patient with glycogen storage disease type 1a (von Gierke disease). Transplantation 2001;72:343-344.
153. Dietrich CF, Schreiber-Dietrich D, Hocke M. [Comments on the EFSUMB non-liver Guidelines 2011]. Praxis.(Bern.1994.) 2012;101:1175-1181.
154. Dietrich CF, Cui XW, Schreiber-Dietrich DG, Ignee A. EFSUMB guidelines 2011: comments and illustrations. Ultraschall Med 2012;33 Suppl 1:S11-21.
155. Dong Y, Wang WP, Mao F, Dietrich C. Contrast-enhanced ultrasound features of hepatocellular carcinoma not detected during the screening procedure. Z Gastroenterol 2017;55:748-753.
156. Wilson SR, Lyshchik A, Piscaglia F, Cosgrove D, Jang HJ, Sirlin C, Dietrich CF, et al. CEUS LI-RADS: algorithm, implementation, and key differences from CT/MRI. Abdom Radiol (NY) 2017.
157. Tang A, Bashir MR, Corwin MT, Cruite I, Dietrich CF, Do RKG, Ehman EC, et al. Evidence Supporting LI-RADS Major Features for CT- and MR Imaging-based Diagnosis of Hepatocellular Carcinoma: A Systematic Review. Radiology 2017:170554.
158. Lyshchik A, Kono Y, Dietrich CF, Jang HJ, Kim TK, Piscaglia F, Vezeridis A, et al. Contrast-enhanced ultrasound of the liver: technical and lexicon recommendations from the ACR CEUS LI-RADS working group. Abdom Radiol (NY) 2017.
159. Kim TK, Noh SY, Wilson SR, Kono Y, Piscaglia F, Jang HJ, Lyshchik A, et al. Contrast-enhanced ultrasound (CEUS) liver imaging reporting and data system (LI-RADS) 2017 - a review of important differences compared to the CT/MRI system. Clin Mol Hepatol 2017.
160. Dietrich CF, Kono Y, Cosgrove D, Jang HY, Kim TK, Piscaglia F, Sirlin CB, et al. Contrast-Enhanced Ultrasound: Liver Imaging Reporting and Data System (CEUS LI-RADS). In: Solutions in contrast imaging.
http://www.solutionsincontrastimaging.com/upload/pdf_riviste/32016.pdf: Solutions in CONTRAST IMAGING; 2016.
161. Piscaglia F, Wilson SR, Lyshchik A, Cosgrove D, Dietrich CF, Jang HJ, Kim TK, et al. American College of Radiology Contrast Enhanced Ultrasound Liver Imaging Reporting and Data System (CEUS LI-RADS) for the diagnosis of Hepatocellular Carcinoma: a pictorial essay. Ultraschall Med 2017;38:320-324.
162. Barreiros AP, Piscaglia F, Dietrich CF. Contrast enhanced ultrasound for the diagnosis of hepatocellular carcinoma (HCC): Comments on AASLD guidelines. J.Hepatol. 2012;57:930-932.

163. Schellhaas B, Waldner MJ, Gortz RS, Vitali F, Kielisch C, Pfeifer L, Strobel D, et al. Diagnostic accuracy and interobserver variability of Dynamic Vascular Pattern (DVP) in primary liver malignancies - A simple semiquantitative tool for the analysis of contrast enhancement patterns. Clin Hemorheol Microcirc 2017;66:317-331.
164. Wildner D, Bernatik T, Greis C, Seitz K, Neurath MF, Strobel D. CEUS in hepatocellular carcinoma and intrahepatic cholangiocellular carcinoma in 320 patients - early or late washout matters: a subanalysis of the DEGUM multicenter trial. Ultraschall Med 2015;36:132-139.
165. Dietrich CF, Maddalena ME, Cui XW, Schreiber-Dietrich D, Ignee A. Liver tumor characterization--review of the literature. Ultraschall Med 2012;33 Suppl 1:S3-10.
166. Bleck JS, Gebel M, Witt B, Schmitt KJ, Breitkopf P, Westhoff-Bleck M, Wagner S, et al. Sonography under Daylight Conditions. Ultraschall Med 1998;19:259-264.
167. Mork H, Ignee A, Schuessler G, Ott M, Dietrich CF. Analysis of neuroendocrine tumour metastases in the liver using contrast enhanced ultrasonography. Scand.J.Gastroenterol. 2007;42:652-662.
168. Rickes S, Ocran KW, Gerstenhauer G, Neye H, Wermke W. Evaluation of diagnostic criteria for liver metastases of adenocarcinomas and neuroendocrine tumours at conventional ultrasound, unenhanced power Doppler sonography and echo-enhanced ultrasound. Dig. Dis 2004;22:81-86.
169. Dorffel Y, Wermke W. Neuroendocrine tumors: characterization with contrast-enhanced ultrasonography. Ultraschall Med 2008;29:506-514.
170. Gottschalk U, Ignee A, Dietrich CF. [Ultrasound guided interventions, part 1, diagnostic procedures]. Z.Gastroenterol. 2009;47:682-690.
171. Gottschalk U, Ignee A, Dietrich CF. [Ultrasound-guided interventions and description of the equipment]. Z.Gastroenterol. 2010;48:1305-1316.
172. Dietrich CF, Lorentzen T, Sidhu PS, Jenssen C, Gilja OH, Piscaglia F. An Introduction to the EFSUMB Guidelines on Interventional Ultrasound (INVUS). Ultraschall Med 2015;36:460-463.
173. Lorentzen T, Nolsoe CP, Ewertsen C, Nielsen MB, Leen E, Havre RF, Gritzmann N, et al. EFSUMB Guidelines on Interventional Ultrasound (INVUS), Part I. General Aspects (long Version). Ultraschall Med 2015;36:E1-14.
174. Lorentzen T, Nolsoe CP, Ewertsen C, Nielsen MB, Leen E, Havre RF, Gritzmann N, et al. EFSUMB Guidelines on Interventional Ultrasound (INVUS), Part I. General Aspects (Short Version). Ultraschall Med 2015;36:464-472.
175. Jenssen C, Hocke M, Fusaroli P, Gilja OH, Buscarini E, Havre RF, Ignee A, et al. EFSUMB Guidelines on Interventional Ultrasound (INVUS), Part IV - EUS-guided Interventions: General aspects and EUS-guided sampling (Long Version). Ultraschall Med 2016;37:E33-76.
176. Jenssen C, Hocke M, Fusaroli P, Gilja OH, Buscarini E, Havre RF, Ignee A, et al. EFSUMB Guidelines on Interventional Ultrasound (INVUS), Part IV - EUS-guided interventions: General Aspects and EUS-guided Sampling (Short Version). Ultraschall Med 2016;37:157-169.
177. Fusaroli P, Jenssen C, Hocke M, Burmester E, Buscarini E, Havre RF, Ignee A, et al. EFSUMB Guidelines on Interventional Ultrasound (INVUS), Part V. Ultraschall Med 2016;37:77-99.
178. Fusaroli P, Jenssen C, Hocke M, Burmester E, Buscarini E, Havre RF, Ignee A, et al. EFSUMB Guidelines on Interventional Ultrasound (INVUS), Part V - EUS-Guided Therapeutic Interventions (short version). Ultraschall Med 2016;37:412-420.

179. Jenssen C, Brkljacic B, Hocke M, Ignee A, Piscaglia F, Radzina M, Sidhu PS, et al. EFSUMB Guidelines on Interventional Ultrasound (INVUS), Part VI - Ultrasound-Guided Vascular Interventions. Ultraschall Med 2016;37:473-476.
180. Dietrich CF. EFSUMB guidelines 2015 on interventional ultrasound. Med Ultrason 2015;17:521-527.
181. Mohaupt MG, Arampatzis S, Atkinson N, Yi D, Cui XW, Ignee A, Dietrich CF. Comments and extensions to EFSUMB guidelines on renal interventional ultrasound (INVUS). Med Ultrason 2016;18:351-361.
182. Dietrich CF, Muller T, Bojunga J, Dong Y, Mauri G, Radzina M, Dighe M, et al. Statement and Recommendations on Interventional Ultrasound as a Thyroid Diagnostic and Treatment Procedure. Ultrasound Med Biol 2018;44:14-36.
183. Dietrich CF, Brunner V, Lembcke B. [Intestinal ultrasound in rare small and large intestinal diseases]. Z.Gastroenterol. 1998;36:955-970.
184. Barreiros AP, Otto G, Ignee A, Galle P, Dietrich CF. Sonographic signs of amyloidosis. Z.Gastroenterol. 2009;47:731-739.
185. Dietrich CF, Lembcke B, Jenssen C, Hocke M, Ignee A, Hollerweger A. Intestinal ultrasound in rare gastrointestinal diseases, update, part 1. Ultraschall Med 2014;35:400-421.
186. Dietrich CF, Lembcke B, Jenssen C, Hocke M, Ignee A, Hollerweger A. Intestinal Ultrasound in Rare Gastrointestinal Diseases, Update, Part 2. Ultraschall Med 2015;36:428-456.
187. Faust D, Fellbaum C, Zeuzem S, Dietrich CF. Nodular regenerative hyperplasia of the liver: a rare differential diagnosis of cholestasis with response to ursodeoxycholic acid. Z.Gastroenterol. 2003;41:255-258.
188. Dong Y, Wang WP, Cantisani V, D'Onofrio M, Ignee A, Mulazzani L, Saftoiu A, et al. Contrast-enhanced ultrasound of histologically proven hepatic epithelioid hemangioendothelioma. World J Gastroenterol 2016;22:4741-4749.
189. Ishak KG. Primary hepatic tumors in childhood. Prog. Liver Dis 1976;5:636-667.
190. Ishak KG, Sesterhenn IA, Goodman ZD, Rabin L, Stromeyer FW. Epithelioid hemangioendothelioma of the liver: a clinicopathologic and follow-up study of 32 cases. Hum. Pathol 1984;15:839-852.
191. Chiorean L, Cui XW, Tannapfel A, Franke D, Stenzel M, Kosiak W, Schreiber-Dietrich D, et al. Benign liver tumors in pediatric patients - Review with emphasis on imaging features. World J Gastroenterol 2015;21:8541-8561.
192. Schuessler G, Fellbaum C, Fauth F, Jacobi V, Schmidt-Matthiesen A, Ignee A, Dietrich CF. [The infammatory pseudotumour -- an unusual liver tumour]. Ultraschall Med. 2006;27:273-279.
193. Dietrich CF, Lorentzen T, Sidhu PS, Jenssen C, Gilja OH, Piscaglia F, Efsumb. An Introduction to the EFSUMB Guidelines on Interventional Ultrasound (INVUS). Ultraschall Med 2015;36:460-463.